European Cells and Materials Vol. 9. Suppl. 1, 2005 (pages 1-2) ISSN 1473-2262

Stress Distribution In Abutment Teeth Involved In The Treatment With Removable Partial Dentures – A Finite Elements Analysis

Lavinia Ardelean[1], Liliana Sandu[1], Cristina Borţun[1] & Nicolae Faur[2]

[1] *"Victor Babeş" University of Medicine and Pharmacy, University Dental College, Spl. T. Vladimirescu nr. 14, Timişoara, România*

[2] *Politehnica University, Timisoara, Department Strength of Materials, B-dul M. Viteazul nr. 1, Timişoara, România*

INTRODUCTION: The finite element method represents a technique of numerical analysis performed by means of computers. It appeared as a result of the necessity to study complex structures which did not allow for classical methods of calculus [1]. This method was used to assess the stress distribution in the abutment teeth of patients treated with removable partial dentures [2,3].

METHODS: The study was conducted on a Kennedy class I edentation, characteristic for removable dentures. The the abutment teeth are represented by the upper premolars on both hemi-arches [4].

The study was conducted on two distinct cases. In the first case the elements of maintaining, support and stabilization of the denture are represented by dental open Akers clasps applied on the second premolars, while in the second case, by biactive Bonwill clasps, applied on the two upper premolars on each hemi-arch.

The geometrical models for these teeth were made taking into account the morphology and average size of the respective teeth. The pattern of calculus focused on revealing the stress distribution in abutment teeth under the action of occlusal forces. We used tetra-type finite elements, with four knots on each element. The resistance structures of the teeth detailed into 10416 finite elements.

Considering the biomechanics of the removable partial denture, whose tipping after setting can not be wholly compensated, the lever effect of terminal saddles on abutment teeth was simulated. The finite element analysis method made possible the assessment of stress distribution in these teeth under the action of occlusal forces [1].

RESULTS: The computer programme made possible the assessment of stress distribution, characterized by the equivalent stress $\sigma_{\text{von Mises}}$. The distribution of the equivalent stress was represented as coloured spectra, each colour standing for a certain value of the equivalent stress. Figure 1 shows the way in which stress is distributed in case 1, namely in the upper second premolar, on which the dental open Ackers clasp was placed.

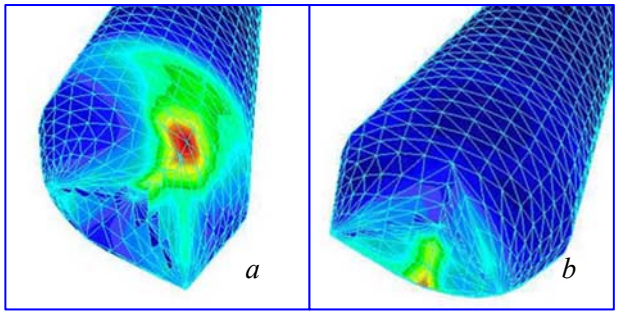

Fig. 1: Detail showing the distribution of the equivalent stress in the right upper second premolar in the first case: a. distal aspect; b. mezial aspect

The results show that the maximum equivalent stress recorded in the first case was 11.697 MPa in the second premolar, with a concentration of stress near the support area, i.e. the distal part of the denture.

Figure 2 shows the distribution of the equivalent stress in case 2, namely in the two upper premolars, where the biactive Bonwill clasp was placed.

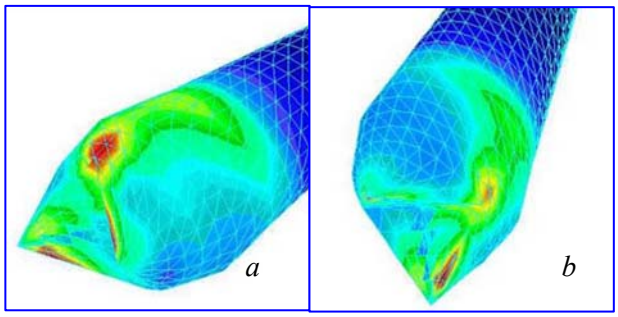

Fig. 2: Detail showing the distribution of stress in the right upper premolars in the second case: a. palatine aspect; b. distal aspect of the first premolar

In the second case, the maximum equivalent stress had much lower values and were approximately equal in all abutment teeth (4.481 MPa in the

second premolars and 4.392 MPa in the first premolars). In this case, stress is distributed throughout the entire denture, and the values are slightly higher in the area of the second premolar and distally in the first premolar, near the point of occlusal support, but without any massive stress concentration.

DISCUSSION & CONCLUSIONS: The analysis of the results reveal the following:

1. professional analysis programmes with finite elements make possible the simulation of the interaction between dentures and abutment teeth;
2. the finite element analysis makes possible the comparative assessment of different conception projects of the removable partial denture adapted to a specific clinical situation;
3. the anterior movement of the rotation axis in the case of dentures with terminal saddles and the more rigid denture significantly reduce stress in abutment teeth.

REFERENCES: [1] N. Faur (2002) *Elemente finite – fundamente*, Ed. Politehnica, Timisoara. [2] Liliana Sandu, N. Faur, Cristina Bortun (2003) *Finite Element Analysis of Stress in the Abutment Teeth Involved in the Treatment with Removable Partial Dentures*, Proceedings of the 6th International Conference on Boundary and Finite elements, Ed. Politehnica. [3] Liliana Sandu, N. Faur, Cristina Bortun (2003) *Investigarea unor probleme biomecanice implicate in terapia cu proteze partiale mobilizabile – analiza cu metoda elementelor finite*, Al V-lea Simpozion International inerii si cercetarea multidisciplinara, Timisoara. [4] Cristina Bortun, M. Leretter, Liliana Sandu (2002) *Tehnologia protezelor partiale*, vol I si II, Ed. Eurobit, Timisoara.

Finite Element Analysis Of Stress Distribution Induced By Thermal Variations On Cast Clasps

Liliana Sandu[1], Cristina Borţun[1], Lavinia Ardelean[1] & Nicolae Faur[2]

[1] *"Victor Babeş" University of Medicine and Pharmacy, University Dental College, Spl. T. Vladimirescu nr. 14, Timişoara, România*

[2] *Politehnica University, Timisoara, Department Strength of Materials, B-dul M. Viteazul nr. 1, Timişoara, România*

INTRODUCTION: The mouth is subject on a daily basis to thermal aggressions resulted from the ingestion of food and liquids at various temperatures. In the case of patients with removable partial dentures, these thermal variations induce alterations both at the level of the teeth and oral mucosa, and at the level of the dentures themselves, as a result of heat transfer. The result of these thermal variations at the level of the dentures is the occurrence of stress, which can be analysed using the finite element method [1].

METHODS: The finite element analysis carried out on removable partial dentures revealed that the parts that are the most affected are the cast clasps. Consequently, the study focused on these elements [2-4].

The study method used was the finite element method (Cosmos/M software, version 2.5).

The object of study was represented by real clasps of removable partial dentures. In what follows we are going to exemplify the analysis carried out for a type of circular clasp, namely the back action clasp or the "G" clasp.

The geometrical models were made by the manual measurement of tri-dimensional co-ordinates of the clasp surfaces. Their resistance structure was detailed in 1772 finite elements, connected to a number of 1263 knots. SHELL 3 type finite elements were used (Triangular Thin Shell). At the same time, the calculus system was provided with data on the mechanical, elastic and thermal characteristics of the material the framework is made of, an Co-Cr alloy.

The finite element analysis programme was used for the first time in order to assess stress distribution resulting the simulation of a static charge (average force 20 N). The thermal analysis was conducted with stimuli of extreme temperatures of 0°C, respectively 60°C.

At the end, the static and thermal charges were cumulated and the stress induced in clasps was assessed.

RESULTS: Fig. 1 shows the equivalent stress distribution in case of thermal charge by variation from 37°C to 0°C (Fig. 1a) and induced by the thermal gradient of 37 °C - 60 °C (Fig. 1b).

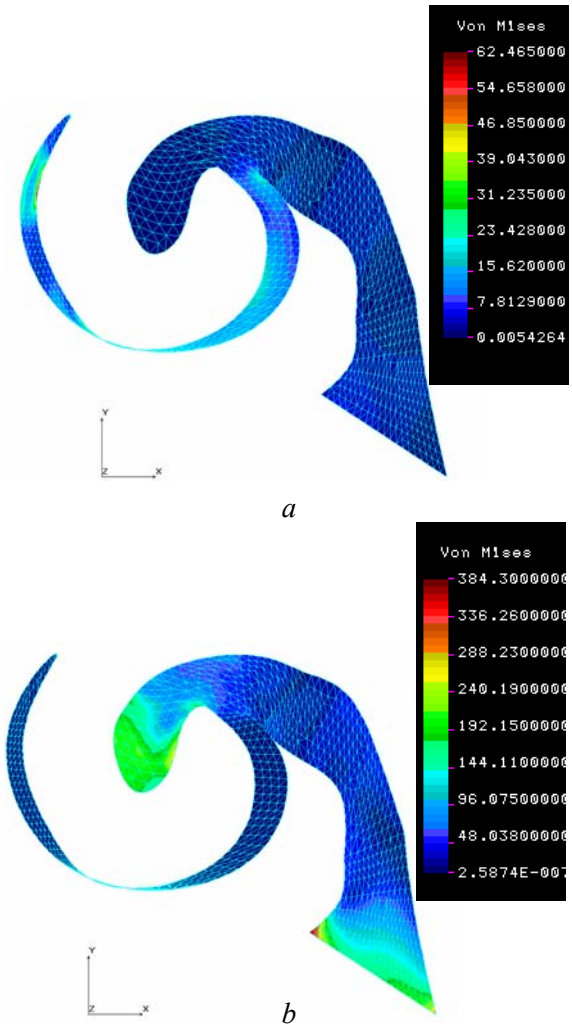

Fig. 1: Representation of equivalent stress distribution under thermal charge – occlusal aspect: a. variation from 37 °C to 0 °C and b. variation from 37°C to 60°C

The analysis of stress induced by ingestion of cold liquids revealed the development of stress in the clasp arm, with a maximum value of 62.46 MPa. The ingestion of warm liquids resulted in a much higher maximum value of equivalent stress (451.15 MPa), and the stress is concentrated in the occlusal

rest and at the point where the minor connector converges with the major one.
Further on we assessed a complex situation, i.e. the ingestion of food at different temperatures, when both mechanical and thermal aggression occur (Fig. 2)

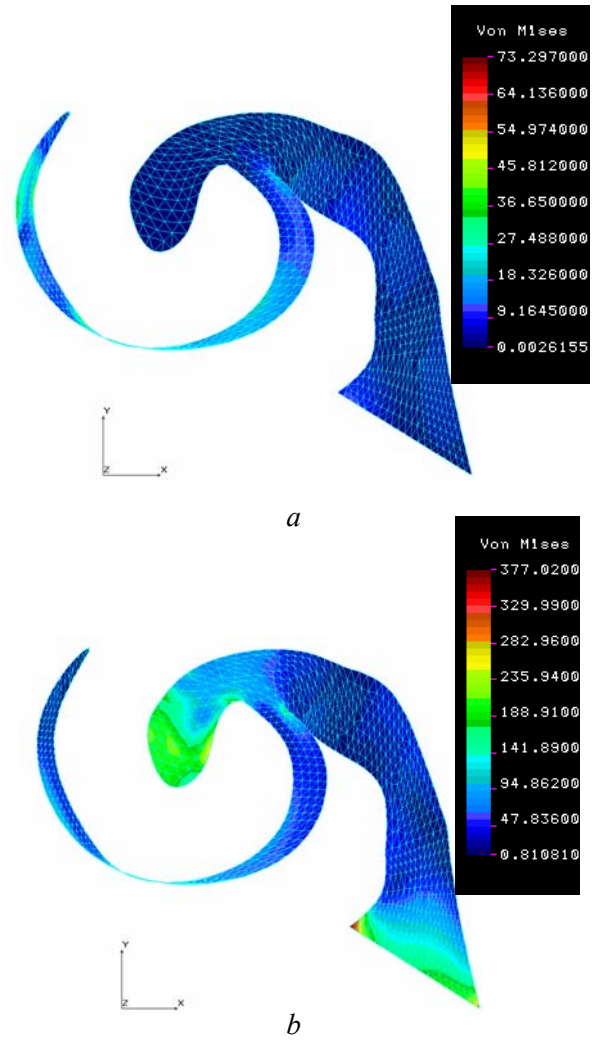

Fig. 2: Representation of equivalent stress distribution when thermal charge is associated with mechanical charge: a. thermal stimulus of 0 °C and charge of 20 N and b. thermal stimulus of 60 °C and charge of 20N.

The association of the thermal gradient from 37 °C to 0 °C under mechanical charge also alters the distribution of stress and the value of the maximum equivalent stress (217.08 MPa versus 73.29 MPa). The association of the thermal gradient from 37 °C to 60 °C under mechanical charge significantly increases the maximum equivalent stress from 217.08 MPa to 377.02 Mpa, and induces the development of stress in the body of the clasp and in the occlusal rest.

DISCUSSION & CONCLUSIONS:

1. Thermal variations induce stress in dental clasps, high temperatures having a more aggressive effect than lower ones.
2. Associating the thermal gradient with functional stress alters both the stress spectrum and the values of maximum equivalent stress.
3. Consequently, the effect of thermal variations in the mouth should not be overlooked when assessing stress distribution in dental clasps.

REFERENCES: [1] N.Faur (2002) *Elemente finite - fundamente*, Ed. Politehnica, Timişoara. [2] Cristina Borţun, M. Leretter, Liliana Sandu (2002) *Tehnologia protezelor parţiale, vol I şi II*, Ed. Eurobit,Timişoara. [3] Liliana Sandu, Cristina Borţun, N.Faur, M. Leretter (2002) *Studiul stărilor de tensiune şi deformaţie ale elementelor componente ale protezelor scheletate printr-o analiză cu elemente finite*, Revista Naţională de Stomatologie, volumul V, nr. 1: 17 - 21. [4] Liliana Sandu, N.Faur, Cristina Borţun (2003) *The Finite Element Analysis – A Method for the Study of the States of Tension and Deformation of a Removable Partial Denture. Trends in Romanian Health. Proceedings of MEDINF 2002* (Editors: Gh. Mihalaş, Diana Lungeanu), Ed Eurobit, Timişoara, pp 25 – 28.

European Cells and Materials Vol. 9. Suppl. 1, 2005 (pages 5-6) ISSN 1473-2262

Clinical Assessment Of Marginal Closure Tightness In Restoring Class II Cavities With Fuji IX GP

L Ardelean[1]

[1] *"Victor Babes" University of Medicine and Pharmacy, Timisoara, College of Dental Technique, 2, Eftimie Murgu Square, 300041 Timisoara , Romania*

INTRODUCTION: Fuji IX GP is a self-curing packable glass-ionomer cement indicated in restoring class II cavities. The material can also be found in a fast setting type: Fuji IX GP Fast. Among the qualities that make Fuji IX GP an ideal material for posterior restorations, we could mention: high wear resistance, intrinsec adhesion to dentine and enamel: no need for etching and bonding, can be used with metal matrices, easy contouring in the cavity, good radiopacity facilitating post-operative diagnosis, ease of use: no need for rubber dam, tooth-conserving preparation technique, single step placement: no need for layering technique, releases fluoride and acts as a deposit for fluoride ions coming from exogenic sources, such as: tooth pastes, mouth washes, etc., excellent biocompatibility. Moreover, it is suitable for application on cement when the cavity floor is situated subgingival. Fuji IX GP is also recommended in deep cavities, with excellent results. As an extra Fuji IX GP Fast offers: shorter setting time, final finishing being possible after only 3 minutes from start of mix, thicker consistency for easy packing, strength for improved longevity [1,4].

METHODS: We have used Fuji IX GP in restoring more than 200 class II cavities over a two-year period. We assessed the tightness of the marginal closure in fifty of these cases, by inspection, palpation and X-ray [3]. On inspection we also assessed the condition of the contact point with the adjoining tooth. Assessment was made at intervals of six months, one year and two years. All the assessed teeth were vital teeth, condition that was clinically confirmed by palpation, vitality tests and X-ray. The caries was X-rayed and photographed pre-operatively. The cavities were prepared by using a tooth-conserving preparation technique with the help of pear-shaped diamond burs. We tried to preserve as much as possible of the hard dental tissue, removing only the layer of infected dentine. In deep cavities dentin was removed by using excavators. In order to improve enamel adhesion we polished the margins of the cavity with a low granulation diamond bur. During the restoration process, the cavities were isolated by using cotton rolls and a saliva ejector, and conditioned with GC Cavity Conditioner for 10 seconds. We applied a single layer of Fuji IX GC and we performed occlusal packing. After setting, finishing and polishing were carried out. The restored surface was protected by applying GC Fuji Varnish. All restorations had occlusal contacts with antagonists and they re-established contact points with adjoining teeth. Photographs were taken after treatment. Tightness was assessed clinically, by inspection and probing, as well as radiographically, at intervals of six months, one year and two years. Photographing was also repeated at the same intervals, accompanied with X-ray examination.

RESULTS: All the restorations were considered successful. None of the subjects developed secondary marginal caries. For two years, no secondary caries was revealed at X-ray.

Fig.1:Carious lesion (left); *Prepared cavity (right)*

Fig.2:Restoration with Fuji IX GP (left); Same restoration after 2 years (right)

DISCUSSION & CONCLUSIONS: Fuji IX GP is a material specially designed for use in wet environment. Chemical self-adherence to the cavity walls is strong, long-lasting and ensures safe clinical protection against marginal infiltrations,

the material being practically insoluble in oral fluids. Marginal closure is tight, both at the level of the enamel and to that of the dentine and cement, minimizing the risk of subsequent damage. In day-to-day practice Fuji IX GP can be successfully used even in extremely difficult clinical cases, both as far as the extent and the depth of the damage are concerned, Fuji IX GP contributing to the remineralization of advanced damage [2]. The packable non-sticky consistency of Fuji IX GP makes it ideal to be used in Class II restorations. The genuine glass-ionomer properties in combination with the ease of use ensures that GC Fuji IX GP matches all the demands of a modern restorative material.

REFERENCES: [1]J.F.McCabe, A.W.G Walls (2003) *Applied Dental Materials, 8th Edition,* Blackwell Publishing. [2]J.W.McLean (1992*) Dent. Clin. North. Am.* **36**: 693. [3]M.Ferrari, C.L. Davidson (2001) *Romania Dental Update* **10**:10. [4]T.P.Croll (2001) *Compendium* **22**: 442-448

Filler Systems, Interface, Radiopacity of some New Light-Curing Composite Materials

M.Moldovan[1], C.Prejmerean [1], D.Borzea[2], C.Nicola[2], A.Colceriu[1], G.Furtos[1] & S. Sava [2]

[1] "Raluca Ripan" Chemistry Research Institute, 30 Fantanele Street, 400294, Cluj-Napoca, RO

[2] "Iuliu Hatieganu" University of Medicine and Pharmacy, Faculty of Dentistry, Department of Propaedeutics and Dental Materials, 13 Emil Isac street, Cluj-Napoca, RO

INTRODUCTION: The studies of literatures are based on finding some ways of improvement to the properties of composites by changing the chemical nature the size of particles, the ratio between the base components[1-3] The properties of composites depend of: the composition of the inorganic phase and organic phase; the way the two components are coupled; the mechanism of the polymerization reaction. The purpose of this study is the obtaining and characterization of three inorganic fillers; the evidencing of the silane agent posed on these fillers; the study of the radiopacity of five composites.

MATERIALS & METHODS: ***The Inorganic Phase*** The experiments were based on obtaining two (G_2,G_3) vitreous masses through the conventional melting method. The G_1 filler was obtained through the sol-gel method. The conditon for synthesized and the chemical composition is shown in table 1.

Table 1.The chemical composition of glasses [%wt]

Oxides /Glass	G_1	G_2	G_3
SiO_2	72,8	26,8	40
Al_2O_3	-	12,4	5
ZrO_2	-	-	-
ZnO	27,2	-	30
BaF_2	-	49,6	
AlF_3; CaF_2; NaF	-	-	15
Melting temp. [^{0}C]	1000	1150	1350
Surface area [m^2/g]	75,20	9,5	8,5

The Organic Phase consist of **65%Bis-GMA$_n$**4-(2-hydroxy-3-methacryloyloxy propoxy)-phenyl]-propane, **35%** triethyleneglycol dimethacrylate (TEGDMA), 0.5% camphorquinone (CQ), 1% N,N,-dimethylaminoethyl methacrylate (DMAEM) and the polymerization inhibitor 3.5-ditertbutyl-4-hydroxytoluene(BHT). The chemical bond between the organic and inorganic phases, was provided by silanation of fillers from an acidulated ethanol-water with 3-methacryloyloxypropyl-1-trimethoxysilane(A-174). The compositions of the light-curing composite resins are shown in table 2.

Table 2. The compositions of the light-curing composite resins [wt%]

Composite	Organic phase	Inorganic phase
$CF_{(Ba)}$	20 %	G_2 - 80 %
$CF_{(Zn)}$	20 %	G_3 - 80 %
$CF_{(Zr)}$	30 %	G_1 – 70 %
$CF_{(Zn)}$	25 %	$G_3$50%+25%SiO_2colloidal
$CF_{(Zn+Ba)}$	22 %	G_3 40% + G_2 38 %

Characterization of the filler. The **IR spectra** were registered on a FTIR Spectrophotometer, JASCO– 610 mark. Information upon the **silane-coupling agent** is obtained from the KBr pills in domain analysis 400-2000cm^{-1}. The **X – ray** scattering patterns were obtained by means of standard DRON-3M powder diffractometer, working at 40 kV and 30 mA The CuK_α (λ=1.54178 Å) radiation, Ni filtered, was collimated with Soller slits. X-ray scattering patterns were recorded on the 2θ=2-120 degrees angular domain in a step-scanning mode with $\Delta 2\theta = 0.10^0$ steps.

Characterization of the composite resins. The **relative radiopacity (ISO-4049)** (aluminium [Al]-equivalent values) was densitometrically determined for these composite resins and for the dentine and enamel. The optical density of each radiographic image was measured with a 100 Microdensitometer. To compare the composite sample radiopacity with the enamel and dentin, slices of teeth were sectioned and they were X-rayed in the same conditions as the experimental composite samples. The readings in fraction units, I transmitted, were calculated and expressed in optical density OD according to the formula:

$$OD=\log I_0/I$$

where **I** is the light intensity transmitted through the sample, $\mathbf{I_0}$ is the light intensity which crosses the sample associated to the aluminum small plates having 10mm in thickness and being equal to 1000 divisions.

RESULTS & DISCUSSION: In figure 1 the spectra of absorption in IR on the G_1, G_2 filler silanised and unsilanised is presented. Bands that show the presence of the organic rest, can be observed by the band's presence because of the deformation vibration in plan from 1453 cm^{-1}. The band from 1638 cm^{-1} correspondent to the link ν(C=C) from the methacrylic group, and absorption band intense from 1720 cm^{-1} is

attributed to the link ν(C=O) from the methacrylic group that enters in the silane's structure. The bands from the 2800-3000 cm^{-1} field are because of the asymmetrical and symmetrical vibrations of the CH_3 and CH_2 groups. Important modifications in the 1000-1200 cm^{-1} domain show the formation of some new types of links Si-O after the filler's silanation.

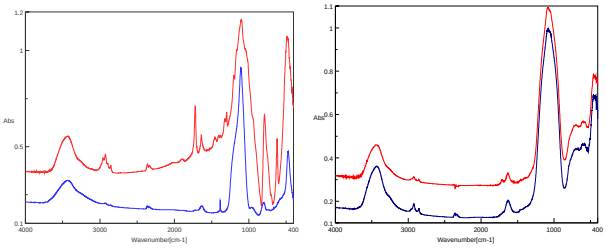

Figure 1: IR spectra of the G_1, G_2 red –silanised, blue- unsilanised

The intensity of the δ(Si-O-Si) 470 cm^{-1} band from the unsilanised powder shows a growth of the number of units Si_2O_5 and SiO_3 chains with oxygen that isn't in the bridge. The presence of the silane on the probes for the vitreous filler and through very weak bands in the 2800-3000 cm^{-1} domain absorption drops are present because of the ν(C-H) and ν(C=C) from A-174 silane.

The structure of the synthesized inorganic phase were investigated by the atomic radial distribution function obtained from X ray scattering data using a PEDX program [4].

Table 3.Atom pairs, ccoordination number and distances for G_3, glasses

Layer	Atom pairs	Coordination number	Distances [Å]
I	B – O	4	1.39
	Si – O	4	1.62
	Al – O		1.62
	Al – O(t)		1.75
	Zn – O		1.96
II	O – O	6	2.38
	Ca – O	3	2.65
	O – O		2.38
III	Si – Ca	4	3.10
	O – O	3	3.12
	Si – Si	3	3.15
IV	Si – Ca	6	3.56
V	Ca – Ca	8	3.63
	O – O	7	3.65
	Si – O	6	3.77
	Ca – O	3	3.80

The atom pairs correlation function g(r) shows maxims and their position, width of the area determined by the distribution of atom pairs in the structural disordered sample. In the ZnO system (table3) the 1.94 Å distance maximum's positioning from the correlation function g(r) is because of the presence in this system of the tetrahedra made out of Zn^{2+} cations with a average distance between the pairs cation-oxygen of 1.96 Å [6]. The tetrahedra symmetry of the zinc cations are formed from Zn^{2+} cations surrounded by 4 oxygens, that present a high disordering degree. For the peaks corresponding to the interatomic distance of about 3.6 – 3.9 Å both possible contributions of the Zn-O distances and of 4 Zn-Ca pairs with distances of 3.824 Å and 3.863 Å [4] can be taken into consideration. Researches made by severals [3,4] on borosilicate glasses with zinc addition showed that the ZnO addition in borosilicate glasses determines the linkage of ZnO tetrahedras. The *radiopacity* values for the five composite series was presented in table 4. The highest radiopacity (5.15) has the CF_{Ba} composite, that contains 32, 24%BaF_2 followed by the CF_{zn} composition (4.16) with 21% ZnO. Comparative with the values obtained for email and dentine it can be observed that the composites based on radiopaque elements like Ba, Zn, Zr has a bigger radiopacity than the email.

Table 4. The radiopacity values of the composites

Code	**adiopac element**	**Optical density**	**Radiopacity in Al mm equivalents**
CF_{Ba}	Ba	0	5.15
CF_{Zn}	Zn	0,22	4.16
CF_{Zn+Ba}	Sr	0,408	3.31
CF_{Zn}	Zn	0,515	2.83
CF_1	Zr	0,638	2.27
Email		0.732	2.2
Dentin		0.838	1.09

CONCLUSIONS: The filler systems G_1, G_2, G_3 was evaluated. The presence of silane A-174 on the filler system is shown. The G_1 (non-vitreous) powder has the specific surface (75,20 m^2/g) much bigger than the vitreous powder (9.5; 8.5 m^2/g), G_2, G3 that is determining factor of the strength and stability of the link at the filler/polymer interface. For the G_3 powders, addition of ZnO in borosilicate glasses produces benefic effects regarding the resistance at solvability.

The variation of the radiopacity values of the composites depends on the nature and concentration of the radiopaque element present in the filler. The best radiopacity of the composite was obtained with filler system, which contain Ba.

REFERENCES: [1] M.R. Bouschlicher, S.C. Cobb, D.B. Boyer (1999) *Radiopacity of compomers. Flowable on Conventional resin Composite for Posterior Restoration*, Op. Dent., **24**: 20-25. [2] M. Chen, G.N. Brauer (1982) *Solvent effects on bonding organo-silane to silica surfaces*, J.Dent. Res., **61**: 1440-1443. [3] M. Okozak, W.H. Douglas (1984) *Comparasion of surface layer properties of composites resin by ESCA, SEM and X-ray diffractometry*, Biomat., **5**: 284-287. [4] V. Petkov, PEDX program for radial distribution function analysis of energy-dispersive X-ray diffraction data from disordered materials.

Study of the toxicological, biological and clinical properties for new restorative materials

S Sava [1], D Borzea [1], C Nicola[1], A Delean[2], C Prejmerean[3] & M Moldovan[3]

[1] *University "Iuliu Hatieganu", Faculty of Dentistry, Propaedeutics and Dental materials Department, 13, Emil Isac street, Cluj-Napoca, RO*

[2 1] *University "Iuliu Hatieganu", Faculty of Dentistry, Odontology and Parodontology Department, 13, Emil Isac street, Cluj-Napoca, RO*

[3]*Chemical Research Institute "Raluca Ripan", 30 Fantanele Street, 400294, Cluj-Napoca, RO*

INTRODUCTION: An important step in testing dental materials refers to their biocompatibility [1-3]. At the same time, dental materials have some characteristics that can be verified only by clinical long-term trials. The aim of this study is to determine the toxicological, biological and clinical properties of a new light-cured composite for direct fillings.

METHODS: The biological answer of the light-cured composite was evaluated using the specimen with best standard specification.Biological tests included test of acute toxicity of the material, primary irritation tests and test of tolerance by the implantation of the final product. The implantation test was conducted on two species of experimental rats using two methods: subcutaneous and intramuscular implantation.

Clinical trials were carried out on 100 patients, on a five-year study concerning the treatment of frontal and/ or posterior teeth using direct fillings with our light-cured composite resin. The restorations were applied in cavities class I, II, III, IV or V and were evaluated every six month using USPHS system.

RESULTS: All biological tests have demonstrated the biocompatibility of this material. Figure 1 shows (left) the relationship between the cured composite resin specimen and the muscular tissue of the rat, 21 days after the implantation.

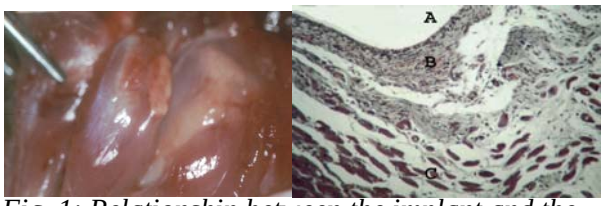

Fig. 1: Relationship between the implant and the muscular tissue at 21 post implant days. Morphological aspect (left), histological aspect (right).

Tissue fragments were processed by classic histological technique and the microscopic image (figure 1-right) confirmed the morphological results of the experiment. The composite resin doesn't contain toxic substances that could provoke reject phenomenon at a local level or the alteration of the anatomical integrity of the implant zone.

Clinical investigations have evidenced that this light-cured composite resin preserves its mechanical, aesthetic and surface properties in time like other similar materials. Because of the microhybrid inorganic filler the surface properties of these material make it suitable for aesthetic restorations especially on frontal teeth. But its mechanical properties demonstrated in our clinical study by the low wear rate indicate this material for posterior fillings as well.

DISCUSSION & CONCLUSIONS:

Biological tests lead to the conclusion that the elaborated light-cured composite resin is well tolerated by the organism without any systemic or local rejection manifestation.

The results of the clinical trials reveal that this composite resin has no irritation effects on the pulp if we use a liner. The restorations have maintained their colour and morphological aspect during the five-year study. Also the marginal adaptation is good in time because of the reduced polymerisation shrinkage and good adhesion properties leading to a small risk for microleakage.

REFERENCES: [1] R.L. Bowen, W.A. Marjenhoff (1992) *Dental composites / glass ionomers: the materials*, Adv. Dent. Res., **6**: 44-49. [2] N. Moszner, U. Salz (2001) *new developments of polymeric dental composites*, Prog. Polym. Sci., **26**: 535-576. [3] G. Goracci, G. Mori, L.C. de Martinis (1996) *Curing light intensity and marginal leakage of resin composite restorations*, Quint. Int., **27(5)**: 355-362.

European Cells and Materials Vol. 9. Suppl. 1, 2005 (pages 10-11) ISSN 1473-2262

Influence of the chemical composition upon the properties of some experimental dental indirect resin composites

C. Prejmerean[1], M. Moldovan[1], L. Vezsenyi[1], D. Borzea [2], C. Nicola[2], S. Sava[2], & A. Farcas[1]

[1] *"Raluca Ripan" Chemistry Research Institute, 30 Fantanele Street, 400294, Cluj-Napoca, RO*

[2] *"Iuliu Hatieganu"University of Medicine and Pharmacy, Faculty of Dentistry, Department of Propaedeutics and Dental Materials, 13 Emil Isac street, Cluj-Napoca, RO*

INTRODUCTION: The use of direct composite restorations seems to be very efficiently only if they are applied to class I and II cavities, due to the inadequate resistance to wear under masticatory attrition in large occlusal cavities [1]. It was demonstrated that the use of additional extra-oral post-cure of the resin composites involving heat and pressure (indirect restorations) increases the degree of conversion of the resin matrix. This is why the mechanical properties of the material are improved, leading to the possibility of using the resin composites for restoration of posterior dental cavities [2,3]. *The purpose* of the present study was focused on obtaining a series of experimental indirect resin composites based on different resin matrix and on investigating the effect of post-curing upon the degree of conversion of the resin and respectively on the mechanical properties of the cured experimental indirect composites.

MATERIAL AND METHODS: 1.Obtaining of the experimental indirect composite resins. The resins were prepared from $(Bis\text{-}GMA)_{0\text{-}2}$ aromatic dimethacrylic oligomers synthesized in our laboratory, having 39 mol % $Bis\text{-}GMA_0$ monomer - 2,2-bis[4-(2-hydroxy-3-methacryloyloxypropoxy) phenyl]-propane, 60 mol % $Bis\text{-}GMA_1$ dimer and 1 mol % $Bis\text{-}GMA_2$ trimer; and aliphatic monomers TEGDMA, EGDMA, and HEMA. The inorganic filler consisted of 90% silanized glass belonging to the oxidic system -SiO_2, Al_2O_3, CaO, SrO, P_2O_5, CaF_2- and 10% silanized colloidal silica. The powder/liquid ratio was 4/1. For the obtaining of specimens, the resin composites were light-cured by exposing to a visible radiation in the wavelength range of 400-500 nm for 40 sec (Optilux dental lamp). After initial polymerisation, the specimens were postcured by barro-thermic treatment at 135^0C temperature and 60 psi pressure, for 20 minutes, using a "belleGlass" warmer.

2. Evaluation of the degree of conversion was performed by determination of the residual double bonds (RDB) using the IR spectroscopy method. The quantity of RDB has been determined as percent of the methacrylate groups originally present in the unpolymerised material. For establishing the quantity of the unreacted methacrylate groups, the absorption band at 1635-1640 cm^{-1} caused by C=C stretching vibrations was used. As internal standard the C-C band at 1610 cm^{-1} caused by stretching vibrations of aromatic Bis-GMA molecules was used [4].

3. Determination of the mechanical properties

The compression strength (CS) was determined using specimens having the form of cylinders – 6 mm in height and 4 mm in diameter (d). The specimens were polymerized and stored in water at 37^0 C for 24 hours before measurements. The CS (in MPa) was calculated applying the formula*:*

$$CS=F / 0.785d^2$$

where F is the maximum applied load .

The tensile strength (DTS) was measured using the diametral compression test. The cylindrical specimens had 4 mm in length (T) and 8 mm in diameter (D). The specimens were subjected to compression along the cylinder generator. The DTS (in MPa) was determined applying the formula:

$$DTS=2 \times F/\pi \times D \times T.$$

The flexural strength (FS) was recorded using rectangular specimens (length 10 mm, height (a) 2 mm and width (b) 2 mm). The specimens were subjected to three-point loading with 6 mm between the supports. The FS (in MPa) was calculated applying the formula:

$$FS=9 \times F/b \times a^2$$

The measurements of CS, DTS and FS were made using an INSTRON UNIVERSAL apparatus at a 0.5 mm/min pressing speed for CS and DTS and 1 mm/min for FS.

RESULTS: The composition of the resin matrix are presented in table 1:

Table 1

Composition of the resin matrix in the experimental indirect composites (%)

No	Bis-GMA_{0-2}	EGDMA	TEGDMA	HEMA
1.	50	-	-	50
2.	50	50	-	-
3.	50	-	50	-
4.	50	-	25	25

The quantity of residual double bonds (RDB), determined in the experimental resin composites, after initial light curing, and respectively after post-curing are presented in fig. 1.

The values of the investigated mechanical properties (CS, DTS, FS) determined for the experimental resin composites after initial light-curing and respectively after barro-thermic treatment are shown in fig. 2-4.

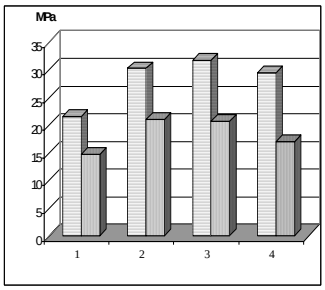

Fig. 1: The RDB values for the light-cured and post-cured resin composites

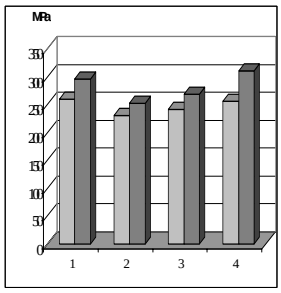

Fig. 2: The CS values for the light-cured, and post-cured resin composites

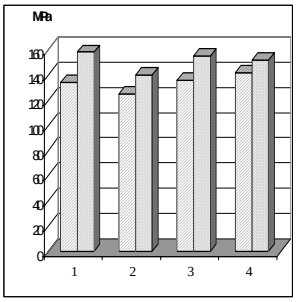

Fig. 3: The FS values for the light-cured and post-cured resin composites

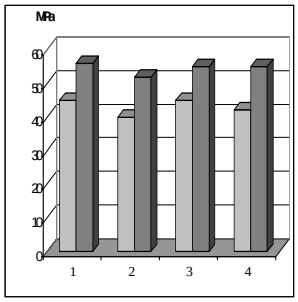

Fig. 4: The DTS values for the light-cured and post-cured resin composites

DISCUSSION & CONCLUSIONS: The RDB involves both the unreacted monomers and the pendant double bonds attached to the polymer network. All the values obtained for the RDB for the post-cured resin composites were lower than the RDB values recorded for the corresponding untreated materials. The decrease of RDB quantity was maximum for the Bis-GMA_{0-2}/HEMA/TEGDMA matrix (45% from RDB of untreated copolymer polymerized after post-curing), followed by the Bis-GMA_{0-2}/HEMA copolymer (42% RDB). The Bis-GMA/TEGDMA and Bis-GMA_{0-2}/EGDMA copolymers display lower RDB diminution after post-curing 35% respective 31%. The lowest RDB value (14,8%) was recorded for the post-cured Bis-GMA_{0-2}/HEMA based resin composite.

The values for the mechanical properties are increased in the case of resin composites subjected to the barro-thermic treatment compared to the corresponding untreated materials. The increase of CS was maximum in the case of Bis-GMA_{0-2}/HEMA/TEGDMA based composite (21,5%), DTS has a higher increase, approximately 30% in the case of the same composite, and the increase of FS was maximum in the case of of Bis-GMA_{0-2}/HEMA composite (18%).

Taking into consideration the quantity of RDB and the values obtained for the mechanical properties in the case of post-cured resins, the Bis-GMA_{0-2}/HEMA based experimental resin composite was proposed for further investigations, toxicological and clinical tests, in order to be used as restorative material in indirect techniques.

REFERENCES: [1]A. Peutzfeldt (1997) *Eur J Oral Sci* **105**:97-116. [2]J.F. Roulet and M. Degrange (1996) *J Calif Dent Assoc* **24(9)**:48-62. [3] D.A. Terry and B.Touati (2001) *Pract Proced Aesthet Dent* **13(1)**: 51-8. [4] I.E. Ruyter and S.A. Svendsen (1978) *Acta Odontol Scand* **36**: **75**-82

European Cells and Materials Vol. 9. Suppl. 1, 2005 (pages 12-13) ISSN 1473-2262

An experimental dental indirect composite resin – biological and clinical trials

C Nicola [1], S Sava [1], D Borzea [1], M Moldovan [2] & C Prejmerean [2]

[1] *University "Iuliu Hatieganu", Faculty of Dentistry, 13, Emil Isac street, Cluj-Napoca, RO*

[2] *Chemical Research Institute "Raluca Ripan", 30 Fantanele Street, 400294 , Cluj-Napoca, RO*

INTRODUCTION: Accordingly with the increasing demands of patients for aesthetic restorations, even on posterior teeth we initiated a research project with the Chemical Research Institute concerning composites for indirect restorations.

The aim of this paper is to present the biological and clinical trials conducted for this new elaborated microhybrid light-cured resin, postcured by heat and pressure, resembling belle-Glass HP.

METHODS: For the biological tests of polyglass we have chosen the specimen with best standard specifications [1-2]. Biological tests were carried out on 3 levels, as follows: systemic toxicology tests, irritational potential test, limited usage by intramuscular and subcutaneous implants.

To accomplish these objectives we used several groups of experimental animals, investigating systemic, local, morphological and histological effects that this material could have upon natural tissues. Because biological tests lead to the conclusion that the elaborated material is well tolerated by the organism we initiated the clinical trial.

Clinical trials were conducted on 70 patients, on a four-year study concerning the treatment of extremely damaged teeth using composite inlays, and coloured modified frontal teeth using full-veneers [3]. The restorations were evaluated every six months for marginal fit, interproximal contacts, static and dynamic occlusion and aesthetic. For a better interpretation of the results we conducted the clinical study comparing our material with belle-Glass HP, a well-known material on the market.

RESULTS:

Biological tests demonstrated the biocompatibility of this material. We observed good healing without mobility or sensibility problems at the implant zone. Figure 1 (left) shows the relationship between the cured polyglass (implant) and the rat's muscular tissue at 21 post implant days. Histological tests confirmed the morphological results of the experiment.

Figure 1 (right) shows the histological aspect of the implant zone, revealing a small inflammatory local reaction.

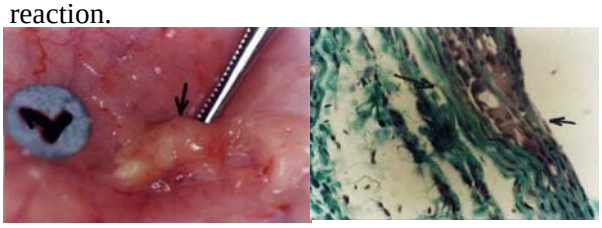

Fig. 1: Morphological (left) and histological (right) aspects of the intramuscular implant zone after 21 days.

The clinical investigations have evidenced that this material preserves its characteristics in time like other polyglass used for indirect fixed restorations (fig.2).

Fig. 2: Clinical aspects of a full veneer (left) and inlay (right) made from our polyglass.

The polymerisation shrinkage is well reduced by the high content of inorganic filler (80%), so marginal fit of these indirect restorations is better than for direct filling, reducing the risk for microleakage.

The triple curing system using light, heat and pressure will determine a high polymerisation conversion (over 90%), so the material will have a very low abrasion rate in time, suitable for posterior teeth restorations [4].

DISCUSSION & CONCLUSIONS:

The evaluation of biological tests has demonstrated that the polyglass is well tolerated by the organism without rejection.

The results of this comparing study reveal that all mechanical, aesthetic and surface properties were similar for the two materials we investigated.

The functional and aesthetic long-term results we have obtained with this material recommend it as an alternative to other composite systems used for indirect fixed restorations like inlays or full-veneers.

REFERENCES: [1] E. Asmussen, A. Peutzfeld (1998) *Influence of UDMA, BisGMA and TEGDMA on selected mechanical properties of experimental resin composites*, Dental Mat. J.,**14**:51-56. [2] R.G. Craig (1997) *Restaurative dental materials*, Tenth Edition, Mosby. [3] L.C. Howe and al (1993) *Inlays, Crowns and Bridges*, Butterworth – Heinemann Ltd., Oxford. [4] A. Peutzfeld, E. Asmussen (1992*) Effect of temperature and duration of postcure on selected mechanical properties of resin composites containing carboxylic anhydride*, Scan. J. Dent. Res., **100:** 296-298.

European Cells and Materials Vol. 9. Suppl. 1, 2005 (pages 14-16) ISSN 1473-2262

Thermal Expansion Polymerization of Composite Resins: Influence on Shrinkage Stress and Interest for The Qualitative Degree of Conversion Analysis

C. Charton[1], A. Petit, P. Colon[2], F. Pia

[1] UFR d'Odontologie, Nancy, France, [2] UFR d'Odontologie, Paris VII, France

INTRODUCTION

Since the 1970's, Brannström and Aström have shown that the loss of marginal adaptation seemed more harmful on pulpal tissues than toxicity of resin-based materials [1]. Today, it is considered that bacterial presence on the dentin/restoration interface is the basic reason for pulpal inflammation [2]. The interfacial integrity is closely related to shrinkage polymerization, but when a bonding procedure is efficient, the shrinkage takes the form of stress which is capable to separate the composite from the cavity walls. According to DAVIDSON's Dutch team [3], these strains are at the heart of the problematical interface. Most studies related to the shrinkage stress analysis of photoactived composites, reveal a recurrent phenomenology at the beginning of the recordings: all curves are generally S-shaped [4, 5]. However, nobody has carried out a thorough analysis of this part of the curve where a slowing down of the stress development occurs. In fact, this zone characterizes the thermal expansion strain in the sol/gel transition. It is linked to the effects of temperature changes due to:

- the start and stop of the light-curig device.
- the reticulation exothermy.

The thermal expansion strain is linked to both coefficients of thermal expansion and thermal conductivity of the material. It could have an influence on the degree of conversion and consequently on shrinkage stress.

OBJECTIFS

The aim of this study is firstly to set up an *in vitro* system for measuring the polymerization shrinkage stress. Then it is a question of evaluating the maximal stresses of 6 commercially available photoactivated composites: Solitaire[1], Solitaire2[1], Aelitefil[2], Tetric Ceram[3], Z100[4] et AP-X[51]. To analyze the effect of thermal expansion strain on shrinkage stress and the thermodynamic equilibrium of the products, complementary recordings were carry out on polymerized samples under identical isolation. The last investigation allows a qualitative analysis of the degree of conversion.

[1] HERAEUS KULZER (Heraeus kulzer Inc, Wehrheim, Allemagne)
[2] BISCO (Itasca, Illinois 60143, USA)
[3] VIVADENT (Vivadent Ets, FL – 9494 Schaan, Liechtenstein)
[4] 3M (Saint Paul, Minnesota 55101, USA)
[5] KURARAY (Kuraray Compagny, 530-8611 Osaka, Japon)

MATERIALS AND METHODS

A mechanical testing machine records the polymerization contraction strain (MPa) of cylindrical composite specimens (∅ = 6 mm ; h = 2 mm ; C = 1,5) over a period of 400s. The Elipar Trilight* (3M-ESPE) light-curing unit is used with 2 forms and 2 lengths of irradiation:

-- Standard 40 et 60 seconds : with power density (PD) = 800 mW/cm^{-2}.

-- Exponential 40 et 60 seconds: PD increases exponentially from 150 to 800 mW.cm^{-2} during the first 15 seconds of irradiation then beyond that it stabilises to 800 mW.cm^{-2}.

Five trials were carried out for each experimental group (n = 5/group). The following values were calculated from stress/time graphs :

- Maximum Shrinkage Stress (MSS): maximum contraction stress after 400s (MPa_{400s}).
- Maximum Thermal Expansion Strain (MTES): expansion strain related to thermal effects induced by light radiation and/or exothermal reticulation. It is recorded at the moment the lamp is switched off($T_{60/40s}$).

are calculated from the strain/time graphs of all trials). A multiple Student t-test (modified by Bonferroni) enabled the evaluation of the influence of the materials on the results ($\alpha < 0,05$). Finally, a simple correlation test ($\alpha < 0,05$) was set up to establish whether MTES has an effect on MSS.

RESULTS

- Maximum Shrinkage Strain (MSS) :

In Standard 60s mode, the highest MSS values were recorded for Aelitefil (1,45 ±0,063 MPa) and Solitaire (1,51 ±0,066 MPa) without a significant difference. AP-X and Z100 (0,92 ±0,051 MPa ; 1,03 ±0,03 MPa) showed the lowest strain values without a significant difference.

The same logic resulted from the inter-material analysis regardless of the insolation type.

- Maximum Thermal Expansion Strain (MTES) :

In Standard 60s mode, the highest MTES values were recorded for Aelitefil (-0,38 ±0,024 MPa).

AP-X and Z100 (-0,92 ±0,051 MPa ; -1,03 ±0,03 MPa) showed the lowest values without a significant difference.
The same logic resulted from the inter-material analysis regardless of the insolation type.
- The simple correlation test shows a positive MTES/MSS correlation.
- In Standard 60s mode, the products did not reach a state of thermodynamic equilibrium at the end of the test (400s). A feasibility study showed that the time required by the system to return to a state of thermodynamic equilibrium, was 600s (10 min). This time was used as a minimum resting time between the shrinkage strain measurements and thermal expansion strain measurements.
- Solitaire shows instability in its degree of conversion as from the Standard 60s mode. The same applies to all the materials as from the Standard 40s mode.

DISCUSSION

Our results show that the materials with the lowest shrinkage strain values were those which were had the highest filler particle load, were the most rigid and the most stable in terms of shrinkage volume. The most efficient way of reducing these strains and improving the interfacial impermeability of the composite resins, is to make the appropriate choice of product composition [6], especially with regard to the choice of filler particle load which should be as high as possible [7], and the chemistry of the matrix.
Its flexibility (due to the addition of thinners with a long and flexible chain such as TEGDMA) improve the visco-elastic properties of the material and thus eliminate the strain. The tetrafunctional monomers with a high molecular weight (up to-GMA and UEDMA) with a high volume skeleton and limited flexibility, increase the compactness of the structures formed and reduce the molecular mobility. They generate greater stressess due to their limited visco-elastic relaxation capacities [8].

Our study of the thermal expansion strain of the products confirms that the latter is certainly at the origin of the S-curve registered by all the authors of the recording period corresponding to the irradiation phase [4, 5, 9]. In addition to the increase in temperature, the thermal expansion introduces a temporary excess in the free volume within the network which favours the degree of conversion and therefore the strains. One can consider it to be an element just as decisive as the filler particle load quantity or the reticulation speed because it reflects the chemical composition of the matrice which in itself constitutes a factor with a great influence on the reticulation strains [3].

Our thermal expansion results simply enabled us to understand how crucial it is to respect the time required for the samples to return to a state of thermodynamic equilibrium. A feasibility study enabled us to establish this time at 10 minutes. To violate this principle is to take the risk of interpreting the completely distorted results of the inter-material or inter-mode analyses, whether they concern volume or linear shrinkage, or shrinkage strain.

Finally, it is necessary to come to a rapid consensus concerning the determination of the optimal degree of conversion for each material because our qualitative study showed that certain products [10] are obviously chemically unstable despite a classic light energy density.

BIBLIOGRAPHIE

[1] Brännström M and Aström A. The hydrodynamics of the dentin: its possible relationship to dentinal pain. Int Dent J 1972; **22**: 219-27.
[2] Camps J, Dejou J, Remusat M and About I. Factors influencing pulpal response to cavity restorations. Dent Mater 2000; **16**: 432-40.
[3] Davidson CL and Feilzer AJ. Polymerisation shrinkage and polymerisation shrinkage stress in polymer-based restoratives. J Dent 1997; **25**: 435-40.
[4] Chen HY, Manhart J, Hickel R and Kunzelmann KH. Polymerization contraction stress in light-cured packable composite resins. Dent Mater 2001; **17**: 253-9.
[5] Bouschlicher MR, Rueggeberg FA. Effect of ramped light intensity on polymerization force and conversion in a photoactived composite. Esthet Dent, 2000; **12**: 328-339.
[6] Rees JS and Jacobsen PH. The polymerisation shrinkage of composite resins. Dent Mater 1989; **5**: 41-4.
[7] Iga M, Takeshige F, Ui T, Torii M and Tsushitani M. The relationship between polymerization shrinkage measured by a modified dilatometer and the inorganic filler content of light-cure composite. Dent Mater 1991; **10**: 38-45.
[8] Peutzfeld A. Resin composites in Dentistry : the monomer systems. Eur J Oral Sci 1997; **105**: 97-106.
[9] Pearson JD and Bouschlicher MR. Polymerization contraction force of packable composites. Gen Dent 2001; **17**: 643-647.

[10] Watts DC, Cash AJ. Intrinsic "soft-start" polymerization shrinkage-kinetics in an acrylate-based resin-composite. Dent Mater 1999; **15**: 39-45.

European Cells and Materials Vol. 9. Suppl. 1, 2005 (pages 17-18) ISSN 1473-2262

Reconstruction of craniofacial bone defects with alloplastic biomaterials

S. Bran, Mihaela Baciut, G. Baciut, Lucia Hurubeanu, Al. Rotaru, R.S. Campian, H. Rotaru, C. Dinu

Clinic of Cranio-Maxillofacial Surgery, Oral Implantology and Oral Rehabilitation
"Iuliu Hatieganu" University of Medicine and Pharmacy
Str. Cardinal Iuliu Hossu 37,
3400 CLUJ-NAPOCA, ROMANIA

INTRODUCTION: Bone defects in the craniofacial region are consequent to trauma, tumor surgery or congenital malformation and require surgical reconstruction. Reconstructive surgery using autogenous bone are associated to considerable morbidity and disadvantages. Biomaterials support and integrate the physical and mechanical role of the bone tissue, inducing and accelerating the process of osteogenesis. We present a modality for reconstruction of craniofacial bone defects using an indigenous alloplastic biomaterial.

METHODS: Experimental research in order to implement the biomaterial has been conducted in cooperation with the University of Agricultural Sciences and Veterinary Medicine Cluj-Napoca on various animal species (Table 1). A composite organic and inorganic polymer biomaterial of indigenous production (polymethylmetacrylate combined with hydroxyapatite - PEMA-HA) was inserted in fracture sites in various bones in the animal group in order to study the bone healing and osteogenesis.

Table 1. Experimental research conducted on various animal species

Species	Breed	Age	Bone segment
Ovine (3)	"turcana"	3 - 4 yrs	mandible
Canine (4)	common	2 – 3 yrs	tibia
Leporide (1)	common	2 yrs	ulna
Leporide (1)	common	7 months	rib

The clinical study was performed based on the favorable results of the experimental research, on patients with odontogenic mandibular cysts and tumors, as well as patients with mandibular tumors imposing segmental bone resections.

The biomaterial was modeled using 3D reconstruction techniques. It has been used in combination with a plasmatic growth factor and with biodegradable poly-L-lactide, vicryl, or titanium membranes for reconstruction of the post-surgical bone defect.

RESULTS: Results pertaining to the healing at the bone-biomaterial interface in the animal experiment have been evaluated on a clinical, radiologic and histologic basis (Fig. 1).

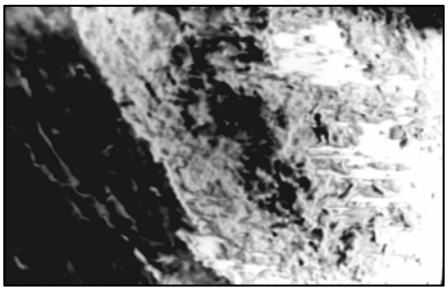

Fig. 1: Tissue healing at the bone – biomaterial interface (scanning electron microscope, X 800)

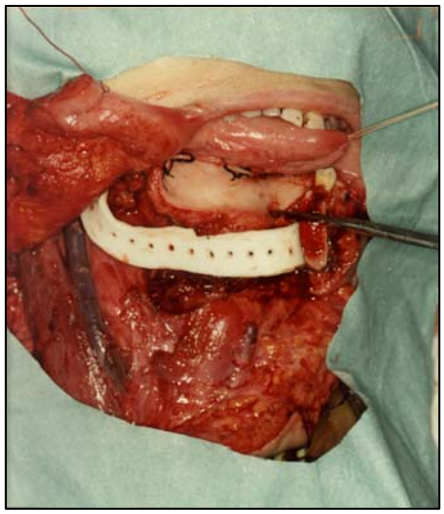

Fig. 2: Right hemimandible reconstructed with PEMA-HA bar after resection for carcinoma

All cases demonstrated good clinical, radiologic and histologic healing (Fig. 2).

DISCUSSION & CONCLUSIONS: The indigenous PEMA-HA biomaterial proved to favorize optimum quality bone healing at the interface, according to the theory of "guided bone regeneration". If used properly, the biomaterial can

offer good morphologic and functional restoration of the affected bone. The proportion of the biomaterial components used in the mixture for reconstructing craniofacial bone defects must consider the complex specific functions of the host bone – chewing, swallowing, speech, esthetics. Ongoing studies focus on its use in cranioplasty.

European Cells and Materials Vol. 9. Suppl. 1, 2005 (pages 19-20) ISSN 1473-2262

Calcium dissolution by seven self etching systems on an experimental human enamel model

K Nasr[1], G Grégoire[1], P Sharrock[2]

[1]*Laboratoire Ecosystème Buccal et Biomatériaux, UFR d'Odontologie – Toulouse III*
[2]*Laboratoire de Chimie Bioinorganique Médicale JE 2400, Université Paul Sabatier – Toulouse III*

INTRODUCTION: Self etching adhesives, like other systems, rely on micromechanical retention and chemical bonding to previously demineralized enamel and dentine surfaces. Two actions are involved in this process. The first step consists in creating surface microporosities by removing calcium phosphates from the dental material. The second step then creates hybridization. With self etching systems both steps operate simultaneously. Recognized procedures for calcium phosphate dissolution use a mineral acid, 36% orthophosphoric acid, for acid dissociation of apatites, followed by water for rinsing away the salts. Self etching products contain a solution of an organic monomer carrying one or more acid functional groups such as carboxylic or phosphoric acids. These bivalent reactants act on the dental surfaces by penetrating the mineral phase with the substituted acid groups and by preparing the hybrid layer by substituted methacrylate infiltration for copolymerization with adhesive agents and composite constituents[1]. While some authors claim that self etchants are a satisfactory alternative[2], others say that the weaker substituted acids are not as efficient in promoting adhesion as the reference orthophosphoric acid procedure[1,3-5]. We have investigated the first action of self etchants by measuring their capacity for dental apatite dissolution. This adhesion determining step was comparatively evaluated by chemical analysis of the amounts of calcium eliminated from human enamel during the use of phosphoric acid or self etchants on identical experimental specimens.

METHODS: *Experimental model*. Sound human enamel originated from third molars extracted from young patients for orthodontic reasons. Absence of trauma or carious infection was verified. 35 crowns were sectioned and dentine removed by abrasion. The enamel shells were ground and hand sieved under 400 micrometers to obtain a homogeneous powder[6]. The enamel particles were suspended in a warm 5% gelatine solution to obtain a paste which was moulded in a 7mm diameter polyolefin tube. After drying, the cylinders were embedded in epoxy resin and cut into thin slices with a low speed diamond saw. Reconstituted enamel was compared with normal enamel by **thermogravimetry** using a SETARAM (Lyon, France) CS92 thermal analyser.

Adhesive systems. Seven self etch products were used: AdheSE (VIVADENT, Schaan, Liechtenstein), Adper Prompt L-Pop (3M ESPE, Seefeld, Germany), Clearfil SE Bond (KURARAY, Osaka, Japan), iBond GI (HERAEUS KULZER, Hanau, Germany), One up Bond F (TOKUYAMA Corp, Tokyo, Japan) Optibond Solo Plus Self/etch primer (SDS KERR, Glendora, CA, USA) and Xeno III (DENTSPLY, Konstanz, Germany). Their pH was measured with a model 210 microprocessor pH meter by Hanna Instruments, Woonsoket, RI, USA.

Adhe SE	*Adper Prompt L-Pop*	*Clearfil SE Bond*	*iBond GI*	*One Up Bond F*	*Opti Bond Solo Plus/ Self-etch Primer*	*Xeno III*
Primer 1,76 Bond 6,92 Mix 1,90	0,28	Primer 2,04 Bond 1,70 Mix 2,27	1,77	Agent A 0,08 Agent B 6,22 Mix 1,16	Primer 1,12 Bond 2,29 Mix 1,64	Universal 3,04 Catalysor 0,04 Mix 0,92

Table 1. pH of the self-etching systems used (pH meter by Hanna Instruments, Woonsoket, RI, USA).

Products were applied according to the manufacturer's instructions on one side of the experimental specimens. The final photopolymerization step was replaced with rinsing by immersion and agitation in 50 ml of ultrapure demineralized water. A reference sample was obtained using 36% phosphoric acid gel during 30 seconds and rinsing in the same manner.

Chemical analysis. The rinse solutions obtained were analysed as such (no additives or dilution) by **acetylene flame atomic absorption** with a SOLAR SYSTEM 929 AA spectrometer from UNICAM, Cambridge, UK) and the calcium concentrations extrapolated from appropriate calcium standards under similar conditions.

RESULTS: *Thermal analysis*. Enamel experimental specimens were found to contain, by weight, 2,21% water, 6,91% organic matter and 90,88% mineral contents. Intact enamel contained

2,90% water, 5,50% organic matter and 91,60% minerals.

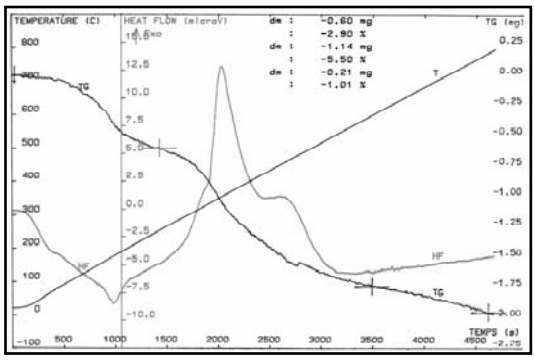

Fig. 1: Thermogram of intact human enamel.

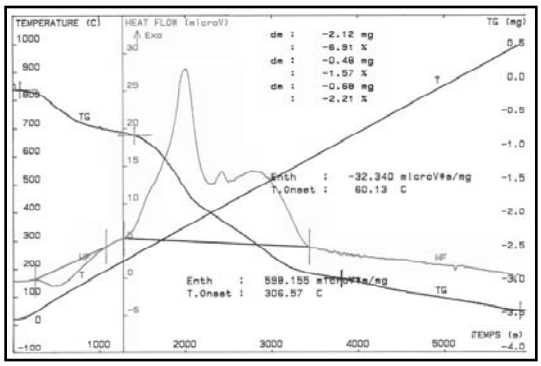

Fig. 2: Thermogram of reconstituted human enamel disk.

Flame atomic absorption analysis. Calcium concentrations found in the rinse solutions are expressed in ppm (mg/l) and vary widely.

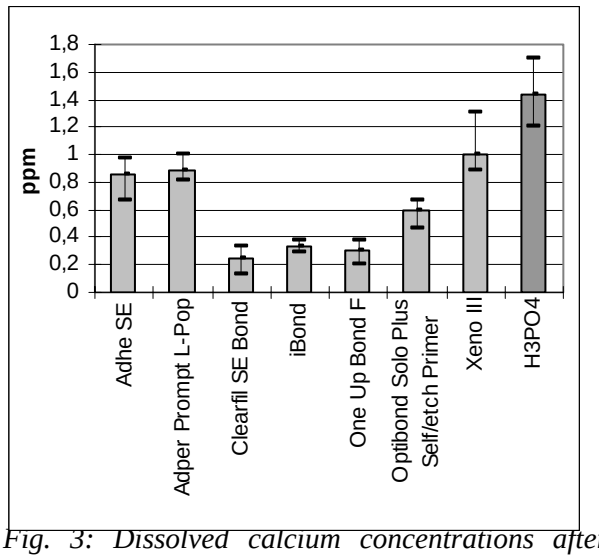

Fig. 3: Dissolved calcium concentrations after application of the different self-etching systems,analysed by flame atomic absorption.

The highest concentration, 1,44ppm is found for phosphoric acid. XenoIII (1.0ppm), Adper Prompt L-Pop (0,89ppm) and AdheSE (0,85ppm) give slightly smaller values while Optibond Solo Plus/Self-etch gives half as much (0,59ppm). Three products, iBond GI (0,33ppm), One Up Bond F (0,30ppm) and Clearfil SE Bond (0,24ppm) yield very low values of dissolved calcium.

DISCUSSION & CONCLUSIONS: The demineralizing capacity of a product depends on such factors as its pH[5,7] (for strong acids) or pKa[8] (for weaker acids), its chelating ability, of the solubility of its calcium salts and of the duration of application[9-10]. Obviously the observed calcium release is not directly related to the measured pH values of the self etchants. The strongest demineralizations are yet less than the reference value observed with phosphoric acid. The chemical compositions of the primers (phosphate esters, pyrophosphates, mono and diHEMA phosphonates, etc.) as well as their relative concentrations play a role in their mode of action[1]. It seems that in order to incorporate the dissociated minerals into the hybrid layer, manufacturers have relied on less aggressive formulations. Further research is needed to explain the fate of the dissolved calcium and phosphate ions and establish the stability of the resulting composite hybridization.

REFERENCES: [1] M. Hannig, K.J. Reinhardt, B. Bott (1999) *Oper Dent* **24**:172-180. [2] A.T.Hara, C.M. Amaral, L.A. Pimenta, M.A. Sinhoreti (1999) *Am J Dent* **12**:181-184. [3] U. Blunck, J.F. Roulet (1999) *J Adhes Dent* **1**:143-151. [4] N. Kanemura, H. Sano, J. Tagami (1999) *J Dent* **27**:523-530. [5] D.H. Pashley, F.R. Tay (2001) *Dent Mater* **17**:430-444. [6] S. Elfersi, G. Grégoire, P. Sharrock (2002) *Dent Mater* **18**:529-534. [7] B. Van Meerbeck et al. (2003) *Oper Dent* **28-3**:215-235. [8] F.R. Tay, D.H. Pashley (2001) *Dent Mater* **17**:296-308. [9] W.W. Barkmeier, S.A. Los, P.T. Triolo (1995) *Am J Dent* **7**:59-62. [10] V.V. Gordan, M.A. Vargas, G.E. Denehy (1998) *Am J Dent* **11**:13-16.

European Cells and Materials Vol. 9. Suppl. 1, 2005 (pages 21-22) ISSN 1473-2262

Effect of multiple desinfection/sterilization on surface characteristics of titanium based implants and *in vitro* bacterial adherence

F. Mabboux [1], L. Ponsonnet [2], J. J. Morrier [1], G. Benay [1], N. Jaffrezic [2] & O. Barsotti [1]

[1] *Faculté d'Odontologie UCB Lyon1, rue G.Paradin, 69372 Lyon cedex 08, France.*

[2] *CEGELY Ecole Centrale de Lyon, 36, avenue Guy de Collongue, 69134 Ecully cedex, France.*

INTRODUCTION: The characteristics of a dental implant surface have been shown to modulate the behaviour of bacteria and cells both *in vivo* and *in vitro*. For example, previous studies on dental implant materials have shown that a certain threshold roughness ($R_a \approx 0.2$ µm) is necessary to obtain a stable soft tissue scaling around titanium abutments without enhancing plaque formation [1]. Cells attachment and bacterial adherence are also sensitive to the chemical composition of the implant surfaces [1, 2]. Today, several dental clinicians re-use various implant components, including transgingival healing abutments and implant coverscrews, that can be cleaned and re-sterilized, since it is safe and cost-effective. Reports on the re-use of medical devices after sterilization are limited and concern exists about the consequences of systemic infection and host tissue reactions [3]. Until now, it appears that no works have investigated the effect of repeated cleaning and sterilization procedures of dental implant devices on bacterial adherence. Therefore, the purpose of this study was firstly to determine the surface properties of titanium and Ti-6Al-4V discs, highly polished or of an average R_a of 0.3 µm, before and after multiple cleaning and sterilization procedures. The 2nd aim of this study was to evaluate the importance of (i) surface topography of the tested surfaces (similar to that of functional dental transgingival healing abutments) and (ii) multiple sterilization procedures on bacterial adhesion. Two bacterial strains (one hydrophylic strain and one hydrophobic strain) were used and the following were evaluated: bacterial adherence, Surface Free Energy (SFE) values of the saliva-coated and uncoated substrata, as well as the Lifshitz-van-der Waals and the Lewis acid-base components of SFE, according to the Wilhelmy Plate method [2].

METHODS: The materials used as substrata are listed in *Table 1*.

Experimental salivary pellicle on the materials was prepared similarly to that described by Grivet et al. [4]. Test samples (Ø = 10 mm, e = 2 mm) were subjected to wetting measurements with and without a salivary coating according to the Wilhelmy technique. SFE (γ_S^{tot}) and its components of the different samples were calculated using the Van Oss model [2].

Table 1. Characteristics of the dental implant materials used as substrata (DSA: desinfection 1 h lysetol® and Steam Autoclaving 18 minutes at 134 °C, 5 cycles)

Material	Treatment	Topography
cp-Ti	DSA (n = 10)	R_a = 0.1 µm (n = 5)
		R_a = 0.3 µm (n = 5)
cp-Ti	No treatment (n = 10)	R_a = 0.1 µm (n = 5)
		R_a = 0.3 µm (n = 5)
Ti-6Al-4V	DSA (n = 10)	R_a = 0.1 µm (n = 5)
		R_a = 0.3 µm (n = 5)
Ti-6Al-4V	No treatment (n = 10)	R_a = 0.1 µm (n = 5)
		R_a = 0.3 µm (n = 5)

The 2 bacterial strains used were: *S. sanguinis* ATCC 10556 and *S. constellatus* CIP 103247. Their hydrophobicity (*S. sanguinis*) and hydrophilicity (*S. constellatus*) had been controlled according to the MATS test [2]. *In vitro* experiments of bacterial adherence and numeration were conducted according to the method described by Grivet et al. [4]. For each strain, 3 experiments were done, with 5 discs of each type of material. The average number of adherent cells per mm^2 was calculated. All the statistical analysis was carried out using Stat-View 4.51.1 software. Non-paired and paired groups were respectively compared, using one way analysis of variance (ANOVA 1), and paired Student's t-test at a significance level of $p = 0.05$.

RESULTS:

Metal surface analysis: i) non-sterilized surfaces: in the absence of salivary coating, the γ_S^{tot} of polimirror and rough cp-Ti and TA6V are similar ($\approx$ 48.00 mJ/m^2), with a polar component quite negligible ($\gamma^+ \leq 0.48$ mJ/m^2). With saliva, the γ_S^{tot} of the 4 types of substrata are slightly higher, and they all exhibit a strong increase in basic properties. The 4 kinds of surfaces, even covered with saliva, remain moderately wettable and slightly hydrophobic ($\gamma_S^{tot} \approx$ 51.00 mJ/m^2); ii) sterilized surfaces: without saliva, DSA significantly increases the γ_S^{tot} (and its different components) of all the surfaces. These variations are more marked for polimirror samples ($\gamma_S^{tot} \approx$

77.00 mJ/m^2 for smooth DSA cp-Ti and TA6V) than for rough substrata ($\gamma_S^{tot} \approx$ 54.00 mJ/m^2 for rough cp-Ti and TA6V). Also, although for polimirror samples, DSA markedly increases the acid/base component (tenfold higher), for rough substrata, DSA decreases the basic polar component (twofold lower), and does not change the acid/base component. With saliva, the 4 types of surfaces display fairly more uniform γ_S^{tot} (and its different components) values, being still moderately wettable and slightly hydrophobic ($\gamma_S^{tot} \approx$ 51.00 mJ/m^2), and display stronger basic character.

Bacterial adherence: Adherent bacteria counts are shown in *Fig. 1*.

Fig. 1. Bacterial adherence (bacteria/mm^2 – S: Smooth; R: Rough).

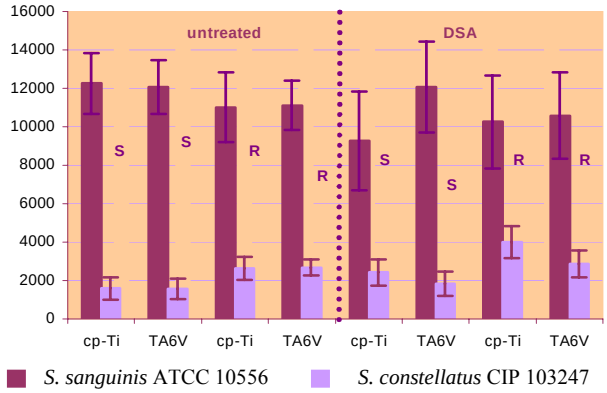

DISCUSSION & CONCLUSIONS: In this study, we used the Wilhelmy plate method to detect any modification of the physico-chemical properties of the samples because it is very sensitive. DSA significantly changes the wettability of smooth cp-Ti and TA6V surfaces which demonstrated more hydrophilic characters. The wettability of uncoated cp-Ti and TA6V appears to be much more sensitive to chemical changes, induced by DSA, than surface geometrical disorders, induced by roughening. These results are quite surprising since it has been shown in other studies that SA can seriously affect cp-Ti and TA6V surfaces by alteration of the oxide layer and deposition of surface hydrophobic contaminants, lowering their SFE and increasing their hydrophobicity [3]. Since the chemical surface components of cp-Ti and TA6V prepared with different surface roughness and repeatedly sterilized were not caracterized, it is difficult to explain this behaviour. One may suggest that the lysetol used as the desinfectant agent between two stages of SA, counteracts the decrease in surface energetics induced by SA by eliminating the hydrophobic contaminants and cleaning the surfaces. In the above mentioned studies, contact angle measurements were done on surface which had been submitted only to multiple SA. Therefore our study is closer to the reality of clinical re-use of cp-Ti and TA6V dental implants. However, our results show that saliva coating has a dramatic effect on the final SFE of all the substrata by masking the effects of geometrical and chemical changes, with a convergence of the SFE values to a moderate wettability of the surfaces, with a stronger basic character in accordance with previous studies.

All the cp-Ti and TA6V surfaces show very similar properties in terms of bacterial colonization by oral strains tested. One explanation is that the surface properties of these 2 saliva-coated biomaterials are similar as showed by the similar surface physico-chemical properties analysis. Therefore, multiple cycles of DSA on cp-Ti and TA6V samples induce different *in vitro* microbiologic and biologic responses. Whereas several studies showed that the significant surface alterations following SA led to decreased *in vitro* fibroblast cell attachment and could therefore inhibit *in vivo* tissue integration [3], our results show that DSA doesn't increase bacterial adherence. Thus, re-using transgingival healing abutments after repeated SA procedures seems to have no effects on further bacterial infection. But since the adhesion of hydrophobic *S. sanguinis* was more important than hydrophilic *S. constellatus*, a pathogenic bacterial strain, we confirm that physico-chemical surface properties of oral bacterial strains determine adhesion to implant materials in the presence of adsorbed salivary proteins. Our results underline the necessary rigorous oral hygiene required for people wearing dental implants in order to avoid plaque accumulation around cp-Ti and TA6V based implant surfaces.

REFERENCES: [1] M. Quirynen, M. Marechal, H.J; Busscher, A.H. Weerkamp, P.L. Dariius and D. van Steenberghe (1990) *J. Clin. Periodontol.* **17**: 138-144. [2] R. Bos, H.C. Van der Mei and H.J. Busscher (1999) *FEMS Microbiol. Rev*. **23**: 179-230. [3] P.J. Vezeau, J.C. Keller, J.P. Wightman (2000) *Implant Dent.* **9**: 236-246. [4] M. Grivet, J.J. Morrier, C. Souchier and O. Barsotti (1999) *J. Microbiol. Methods* **38**: 33-42.

ACKNOWLEDGEMENTS: We thank F. Gourbière for the statistical analysis (Laboratoire d'Ecologie Microbienne du Sol, UCB Lyon 1).

European Cells and Materials Vol. 9. Suppl. 1, 2005 (pages 23-24) ISSN 1473-2262

Biocorrosion and biocompatibility of NiTi alloys

P. Rocher [1], L. El Medawar [1], J.-C. Hornez [1], M. Traisnel [2], J. Breme [3] & H.F. Hildebrand [1]

[1] *GRB, UPRES EA 1049, Faculté de Médecine, F-59045 Lille cedex, France*

[2] *PERF, UPRES EA 2698, ENSCL, F-59652 Villeneuve d'Ascq, France*

[3] *Inst. Materialwissensch. -Metalle, Universitât Saarland, D-66041 Saarbrücken, Germany*

INTRODUCTION: The aim of this work is to determine possible *in vitro* biological side effect of nickel-titanium alloys, containing a high rate of nickel; the toxicity, allergenicity and carcinogenicity of which are generally recognised. This work consists in assessing the NiTi-alloy electrochemical characteristics under biological conditions in relation to its components nickel and titanium. Therefore, corrosion assays were conducted with conventional artificial saliva and especially with a culture medium with or without a human lymphoid cell line in suspension culture. The biological parameters were evaluated by means of the proliferation and cytotoxicity assessments with relevant human cell lines in direct contact with NiTi. They were completed with a test of inflammatory effects.

METHODS: NiTi-alloy (49% Ni, 51% Ti), highly pure nickel (hp-Ni), commercially pure titanium (cp-Ti), Ti6Al4V, PdAg-alloy (60% Pd, 7% Ag), NiCrMo-alloy (59% Ni, 26% Cr, 11% Mo) and stainless steel 316L were used for this work. Specimens were automatically polished at grade 1200 using carbide silicon paper. After polishing, the samples were cleaned in an ultrasonic ethanol bath, air dried, and sterilized. All metal powders were produced by the hydrogenation dehydrogenation process (HDH). Sieving and ethanol suspensions allowed to obtain particles with a size lower than 10 µm. Roughness was characterised by LASER confocal microscopy, the Rt differences of all samples was between 1.8 and 2.46 µm.

The electrochemical device was a Bioreactor. It is based on a classical fermentator arranged specifically for multiple investigations on the corrosion behaviour of metallic biomaterials, in particular to realize simultaneously bacterial or cell cultures and electrochemical tests. A first test series was conducted with the synthetic saliva according to the NF-standard S 91-141 as reference electrolyte. The electrolyte of the second test series was the culture medium RPMI complemented with 10% foetal calf serum. All assays were performed with each alloy or metal in the culture medium with and without CEM cells, a human lymphoid cell line (CEM, ATCC TIB-195). The applied cell concentration was 10 000 cells/ml. The following sequence of measurements was used throughout the whole study: (i) determination of the open-circuit potential over a 24 h period, the value obtained after stabilisation of the curve being called the rest potential; (ii) cathodic scouring of the working electrode at -800 mV/SCE for 10 min to reduce the surface films; (iii) assessment of the global polarisation curves between -800 and +1000 mV/SCE with a scanning rate of 60 mV/min.

Human epithelial embryonic cells (L-132, ATCC CCL 5), human embryonic palatal mesenchymal cells (HEPM, ATCC CRL-1486) and NIH/3T3 mouse connective tissue fibroblasts (ATTC CRL-1658) were used for cell proliferation tests. Cell suspensions (10^5 cells/ml for L-132 and NIH/3T3, $6x10^4$ cells/ml for HEPM) were placed for 72 hours on each disk. Empty culture chambers filled only with cell suspension served as negative controls.

Viability tests were performed by using the colony forming method on human epithelial cells (L-132) in culture. Cells were exposed during 12 days to increasing concentrations (0, 25, 50, 100, 200 and 400 µg/ml) of metal and alloy powders without renewal of the growth medium during the experiments.

The test of inflammatory reactions consisted of quantifying the multinucleated giant cells (MGC) in monolayer cell cultures of L-132 in the presence of the metal or alloy powders. The concentration of NiCrMo and hp-Ni powder used for this test was the 50% lethal concentration (LC50) given by the viability tests. For cp-Ti, NiTi, Ti6Al4, PdAg and 316L the strongest concentration, which was previously used (400 µg/ml) was applied.

RESULTS: Ti6Al4V and cp-Ti, present the highest rest potentials, which significantly increase a first time in the organic electrolyte (RPMI) and further in the presence of CEM cells. A similar behaviour is observed for hp-Ni. The values of NiTi, NiCrMo and PdAg remain stable and those

of 316L decrease having significantly more anodic rest potentials (Tab. 1).

Table 1. Electrochemical results after corrosion assays under standard and biological conditions (AS: artificial saliva, CM: culture medium, CEM: human lymphoid cell line, Er: rest potential, Ec: corrosion potential, Eb: breakdown potential).

	316L	NiCrMo	hp-Ni	NiTi	cp-Ti	Ti6Al4V	PdAg
Er (mV/SCE)							
AS	-290	-277	-650	-322	-350	-328	-197
CM	-341	-260	-412	-338	-145	-274	-220
CEM	-386	-252	-347	-352	-121	-109	-216
Ec (mV/SCE)							
AS	-650	-738	-500	-730	<-800	-600	-350
CM	-450	-750	-287	-425	-416	-454	-260
CEM	-400	-500	-282	-615	-287	-454	-280
Eb (mV/SCE)							
AS	300	644	-200	>1000	>1000	>1000	>1000
CM	280	305	9	600	>1000	>1000	>1000
CEM	150	460	2	530	>1000	>1000	>1000

A remarkable influence of the organic electrolyte and living cells has been observed for hp-Ni, where the breakdown potential increased and for 316L and NiCrMo, where the breakdown potential decreased. Although the breakdown potential of NiTi decreases, this alloy still remains passive at values higher than 500 mV/SCE.

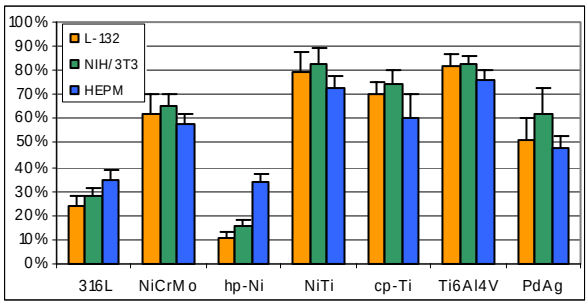

Fig. 1: Proliferation of HEPM, L-132 and NIH/3T3 cells.

NiTi and Ti6Al4V are the most cytocompatible materials (Fig. 1). hp-Ni produces very low proliferation rates with HEPM cells (34%), NIH/3T3 cells (16%) and L-132 cells (11%). Thus its toxic potency seems to depend on the cell type, i.e. hp-Ni is more toxic for L-132 cells than for HEPM cells. A similar toxic effect of hp-Ni (1 ± 0.2%) is revealed by the cell viability test performed with the various metallic powders (Fig. 2). The survival rate in the presence of NiTi and cp-Ti is 79 ± 3.9% and 81 ± 4.2% respectively for the highest concentration used (400 µg/ml).

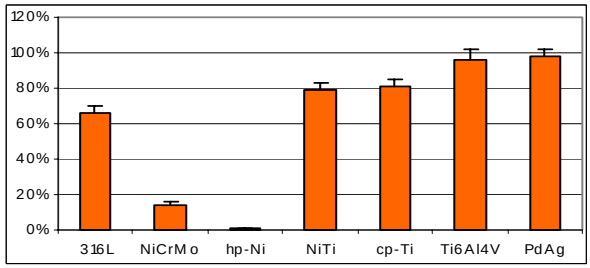

Fig. 2: Viability of L-132 cells for a concentration of powder of 400 µg/ml.

Ti6Al4V produces the best viability with a 96 ± 5.8% survival rate. 316L also induces only little cell death (76 ± 4.5%). The appearance of MGC reveals an inflammatory response to a chemical substance. The frequency of the MGC appearance is approximately 1.3% for NiTi, Ti6Al4V and cp-Ti (Fig. 3). No significant differences could be stated with respect to the control cultures (1.5%). Whereas for 316L and in particular for hp-Ni, the frequency of MGC is significantly higher: 2.9% and 5.1% respectively.

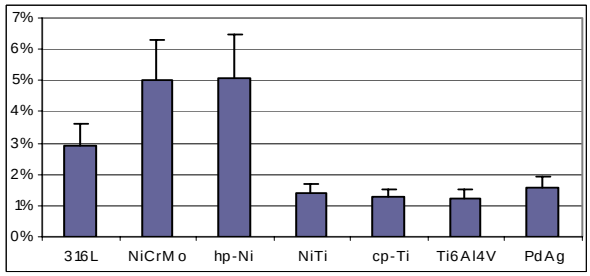

Fig. 3: Frequency of MGC induced in L-132 cells.

DISCUSSION & CONCLUSIONS: The electrochemical assays reveal a clear difference of corrosion behaviour in inorganic and organic (biological) electrolytes, and that living organisms such as cells have an additional effect on the corrosion resistance. Cytotoxicity tests have confirmed that nickel is not only a corrosive but also a cytotoxic material. cp-Ti and NiTi are biocompatible and particularly corrosion resistant. Evidence is shown here that the introduction of nickel into this alloy does not generate any cytotoxic reaction nor alters the physiological and functional behaviour of cells. In addition, it confers a very special property on this alloy which is shape memory and which provides this alloy with some important advantages in orthodontic and cardiovascular domains.

European Cells and Materials Vol. 9. Suppl. 1, 2005 (pages 25-26) ISSN 1473-2262

Finite Element Analysis Contribution for Ceramic-Titane Alloys Adhesiveness Studies.

D. Dhenain[1] , G. Labbé[1] , P.D. Rey [2] , B. Laveissière[1], M. Morenas[3]

[1]Laboratoire d 'Ingenierie des Matériaux Avancés - CUST - Université B. PASCAL(Clermont 2)

[2]Laboratoire de Prothèse Dentaire ARV - Clermont-Ferrand

[3] Laboratoire de Biomatériaux Dentaires - Université d'AUVERGNE(Clermont 1)

INTRODUCTION: Two technologies are usually suitable for providing dental prothetic substrate: casting and machining. The promotion of titanium and its alloys presents a lot of benefits. Nevertheless vitroceramic coatings are known to be difficult to perform. The measure of the ceramic/metal alloys adhesiveness was the subject of the Norm AFNOR EN NF ISO 9693 (1995). It applies on plane samples that had been submissive a mechanical test of flexion three points .The previously works shows qualitatively the capabilities of ARV process against classical process[1].
The aim of this study is to reach more precise characterisation of the mechanical behaviour of different sample configurations. Finite elements analysis allows us to quantify differently the stresses applied to the model, to understand their consequences and finally to optimise any clinical application system.

FIRST RESULTS Histograms on fig.1 show the good results obtained in term of remaining ceramic on titanium after sample folding at 90°.

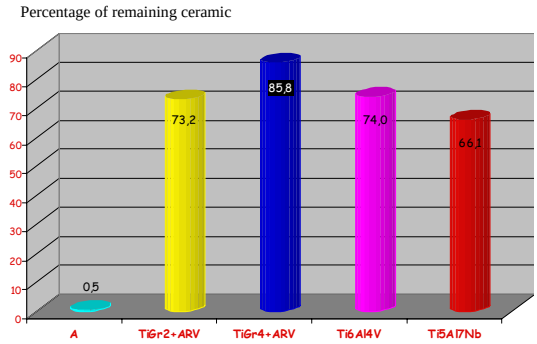

Fig. 1: the most advanced commercial ceramization product ''A'' is here compared with ''ARV process'' applied to different substrate.

The same test normalized in 2000 is largely more quantitative than the first version as seen in fig.2.

(a)

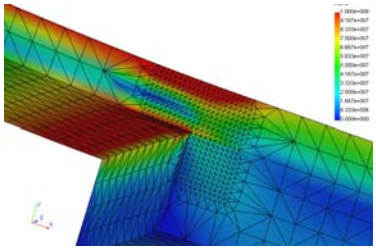

(b)

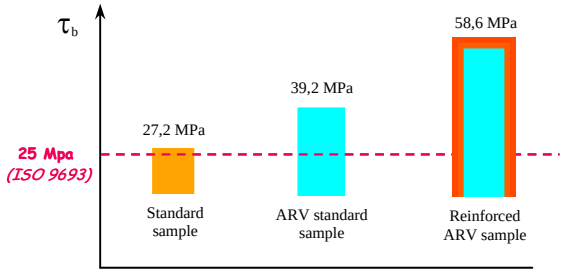

Fig. 2: the stresses distribution predicted in (a) is used to calculate the appearance of the first failure F_{fail}, (b): value obtained.

The occurrence of the first failure may be evaluated thanks to the numerical treatment of Lenz and Schwickerath[2].

$$\tau_b = k.\ F_{fail}$$

It is then possible to correlate test modelization with experimental values used as normalization.

Extensions of experiments:
Some other test configurations have been promoted to reach better understanding of the three layer compound behaviour [3]. The four points bending test would be useful as other complementary geometrical assemblies such as tensile experiments for which we are able to calculate localized stresses as seen on fig.3.

(a)

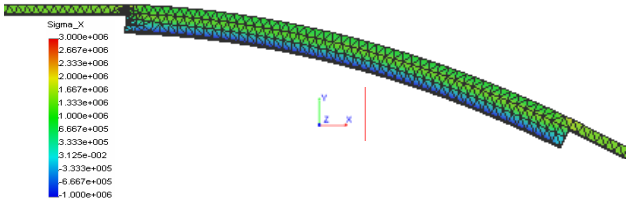

b)

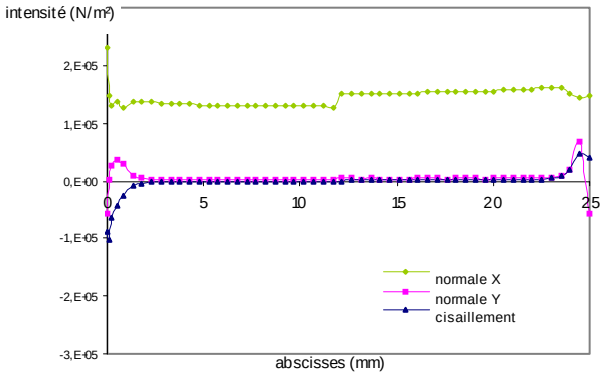

Fig. 3: (a) modelization results showing compression effort during a standard traction test, (b) stress level for the two principal directions (x, y).

Precedent modelizations are for a 1N strength. Observations will be different and more expressive with other strength values.

The only normative documents, that deal with the systems described above, concern very different applications and must be adapted to dental prothesis field.

DISCUSSION & CONCLUSION:

The bending three-point test is effective to quickly determine the behaviour of titanium/ceramic interface created by the unknown commercial products that have been recently proposed. This study deals with dental prothesis but may be extended to different kind of systems such as articulation prothesis or composites with titanium substrate that are now elaborated.

Starting from simple tests it will also be possible to specify bonding nature. When it is cohesive, in the ceramic matrix, the Lenz and Schwickerath procedure may be applied if the ceramic cohesiveness is reinforced. The modelization by finite elements is very useful to predict the experiment behaviour and quantitative correlations.

In the same way, the calculated stress maps obtained in other test configurations allow us to adapt them for better quantifications.

REFERENCES: [1] J. GACHON, P.-D. REY, M. VASCONCELOS, B. LAVEISSIERE, E. ALBUISSON et M. MORENAS (2002) -Actual. en Biomatériaux, Paris- Edit. Romillat, VII, 423-31

[2] J. LENZ, S. SCHWARZ, H. SCHWICKERATH, F. SPERNER and A. SCHÄFER (1995) Bond strenght of metal-ceramic systems in three-point flexure bond test, J App Biomater 6: 55-64

[3] R.D. ADAMS and W.C. WAKE (1986) Structural adhesive joints in engineering. Ed. ELSEVIER London

European Cells and Materials Vol. 9. Suppl. 1, 2005 (pages 27-28) ISSN 1473-2262

Chemical Composition and Surface Preparation Level Influence On Metallic Implants Biointegrability

N. Dumitru[1], D, Bunea[1], I. Patrascu[2], L.T. Ciocan[2], F. Miculescu[1]

[1] *Politehnica University of Bucharest, Bucharest, Romania*

[2] *Medicine and Pharmacy University of Bucharest, Bucharest, Romania*

INTRODUCTION: Implant behaviour in the biological environment has been an interesting major field in surgery. Although, the direct maintenance in the bone tissue, without the connective tissue forming, was not accepted as a bioinginery specific feature until the titanium implants success in dentistry prosthetics was described, using the biointegration concept.

An implant performance depends on more parameters: biomaterial structure, implant surface preparation level, implant design, and especially its biocompatibility. Beside these biomaterial dependent factors, there are also, certain clinical parameters (surgical procedures) and some biological ones (age, state of health, etc.) that interfere in the implants biointegration complex processes. In this paper we have analyzed the metallic implants biointegration way according to their chemical composition and implants surface preparation level. With this research we meant to follow the forming and maturing steps of peri-implant neo-formation bone tissue, trying to bind these transformation forces to the implanted alloy compositional type.

METHODS: We studied four types of implants, used in dental surgery, which are made out of: 99,99% purity titanium, Ti6Al4V type alloy, ASTM F75 type Co-Cr-Mo alloy and 316L type austenitic stainless steel. Equal dimensions and surfaces samples were transmedulary implanted in the tibia of the same body (rabbit), two by two bilaterally. Two months from the implant process, biological samples (the two tibias with metallic implants) by sacrificing the animal. These were subdued to imagistic investigations using XL30-ESEM electron microscope.

RESULTS: According to the implant type, these transformations happened with certain individual features. At P1000 roughness titanium implant, hiatus peri-implanted has dimensions from 5 to 8 µm, vascular plexus being still enough well developed. The thickness of the calcifying peri-implanted fibrous callus is almost 40 µm and the neo-formation bony tissue has a primary morphology (developing incipient level). P800 level surface roughness has been a growth factor for the non-bony tissue (3-5 µm), the vascular plexus being of almost 30-35 µm. The bony structure has an intermediary morphology. At a P600 roughness we observed adhesion growth at bone-implant interface by diminishing peri-implant hiatus interface, reaching 2-3 µm approaches. The vascular net has almost disappeared, according to the peri-implant fibrous tissue intense calcification.

We observed the bony tissue maximum adhesion at P320 roughness, the hiatus being the minimum (1-2 µm) from all the four different roughness prepared surfaces. Fibrous tissue has almost disappeared while the bony tissue has already begun its functional re-modeling (several haversiene channels appearance).

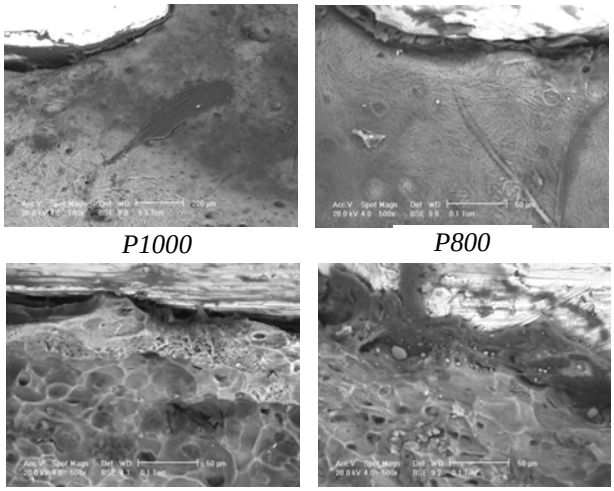

Fig. 1: ESEM images regarding new born bone tissue round Ti6Al4V alloy type implant

At a P1000 implant roughness of Ti6Al4V alloy type, we notice, at great dimensions peri-implant hiatus level (15 µm), the presence of a rich vascular plexus. New born bone tissue has large and remote Havers channels. At P800 roughness, the hiatus is 10 µm, at the peri-implant level being observed the presence of uncalcified fibrous tissue, with 20-25 µm growth. In the image we could see the vascular axes of some collateral Havers channels. At a P600 roughness, the peri-implanted hiatus has small dimensions, usually 5 µm, and the

vascular plexus missing. We can also notice the fibrous tissue absence. The new born bone tissue has a re-molding appearance. P320 surface roughness was the decisive element of new-bone maximum adherence for this implant (2 μm).

At the P1000 side roughness of Co-Cr-Mo type alloy implant the hiatus is 20 μm, observing at the peri-implant level the calcified fibrous tissue presence here and there, with 60 μm thickness. At P800 roughness we notice a 10 μm peri-implant hiatus.

The fibrous tissue is in a late mineralization process while new born bone tissue has large Havers channels. P600 surface roughness is, probably, an important factor for new-bone adherence determination. The peri-implantar fibrous calus is dense and easily mineralized. After we identified the P320 surface roughness, we observed a high adherence to the implant (5 μm). The proteic matrix, well represented (60 μm), presents a high calcification level, while the new-born bone presents a completely functional remodelling (high density Havers channels with low diameter).

The 316L alloy with P1000 roughness has a peri-implantar hiatus with very high dimensions (50 μm). We notice the absence of the plexal vascularization while the fibrous tissue is well represented. In case of P800 roughness, we observe the same structural features, the only difference being an up to 40 μm peri-implantar space reduction. Only at P600 roughness we notice the peri-implantar vascularization presence with the “try to osteointegrate” look, imagisticaly similarly to a first stage of this process. The peri-implantar hiatus is still 20 μm. At 250X magnitude, we identified the P320 roughness. The peri-implantar hiatus has medium dimensions (10 μm), the vascular plexus being low developed. The fibrous tissue, doesn’t present osification signs altrough has a low tickness (10 μm).

DISCUSSION & CONCLUSIONS:

No matter the used alloy type we notice the implants biointegration and, microscopically a direct proportionality between the implant surface roughness and the peri-implantar tissue transformation into mature bone speed (inflamatory tissue with neo-formation vascular plexus, fibrous tissue, and new born bone tissue).

The maximum adhesion of the bone tissue has been observed at P320 roughness (the bigest one) for the pure Ti implant, the hiatus being minim (1-2 μm). The observed and described imagistic elements permit a first evaluation of the metallic implant chemical composition influence on the biointegration complex process, its quality decreasing from Ti to Ti6Al4V alloy, CoCrMo alloy type and 316L type austenitic stainless steel.

We didn’t observe peri-implantar ostheolysis processes for none of the four used materials type which proves the presence of an favourable interaction between implants and the biological structure (bone tissue).

REFERENCES: [1] Matsuo M. Nakamura T. Kishi Y. Takahashi K. (1999) *Microvascular changes after placement of titanium implants: scanning electron microscopy observations of machined and titanium plasma-sprayed implants in dogs*, Journal of Periodontology. 70(11):1330-8; [2] Sanz A. Oyarzun A. Farias D. Diaz I. (2001) *Experimental study of bone response to a new surface treatment of endosseous titanium implants*, Implant Dentistry. 10(2):126-31; [3] Simmons CA. Valiquette N. Pilliar RM. (1999) *Osseointegration of sintered porous-surfaced and plasma spray-coated implants - An animal model study of early postimplantation healing response and mechanical stability*, Journal of Biomedical Materials Research. 47(2):127-38; [4] De Benedittis A. Mattioli-Belmonte M. Krajewski A. Fini M. Ravaglioli A. Giardino R. Biagini G. (1999) *In vitro and in vivo assessment of bone-implant interface: a comparative study*, International Journal of Artificial Organs. 22(7):516-21; [5] Hallgren C. Sawase T. Ortengren U. Wennerberg A. (2001) *Histomorphometric and mechanical evaluation of the bone-tissue response on implants prepared with different orientation of surface topography*, Clinical Implant Dentistry & Related Research. 3(4):194-203.

European Cells and Materials Vol. 9. Suppl. 1, 2005 (pages 29-30) ISSN 1473-2262

Experimental Researches Concerning Metabolic Chemical Phenomenon At the Bone Tissue-Metallic Implant Interface

Miculescu, F.[1], Bunea, D.[1], Ciocan, L.T.[2], Miculescu, M.[1], Antoniac, I[1]

[1] *Politehnica University of Bucharest, Bucharest, Romania*

[2] *Medicine and Pharmacy University of Bucharest, Bucharest, Romania*

INTRODUCTION: The aim of this paper is to analyze, from the chemical point of view the interaction between metallic implants and peri-implant bone tissue.

METHODS: We have studied four types of biomaterials frequently used in dentistry: 99,99% purity titanium, Ti6Al4V type titanium alloy, 316L type austenitic stainless steel and CoCrMo type alloy. Equal dimensions and surfaces prepared samples were implanted trans-cortically in the same organism body, tibia (rabbit), two by two, bilaterally.

Two months from the implant process, biological samples were taken (the two tibias with metallic implant) by sacrificing the subject. These samples were put under qualitative and quantitative imagistic investigations, by linear EDAX analysis being identified and quantified, at the interface specific elements both for the implant alloy and for new born peri-implant bone tissue. Linear EDAX analyses results were materialised into several graphics of element distribution.

RESULTS: By surface EDAX analysis, we identified Ti sample as being made up of pure titanium. At linear EDAX analysis made at new born bone tissue interface, we identified titanium atomic migration from the implant surface. The peri-implant organic matrix is densely mineralized as we can see in figure 2.

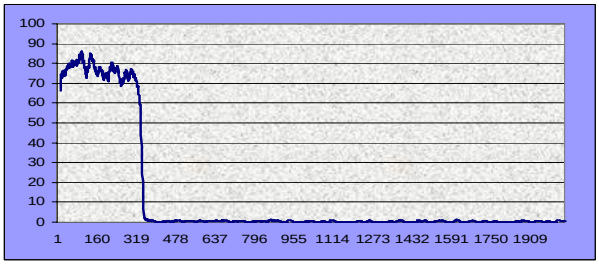

Fig. 1: Titanium distribution variation at the interface between sample and new born bone tissue

By EDAX analyze at the surface the sample proved to be made up of Ti6Al4V type alloy. From its level, in the peri-implant tissue, we may notice a high diffusion of vanadium and a lower one of aluminium and titanium, the last one being less stable from the new born bone tissue diffusion compared to the pure titanium implant.

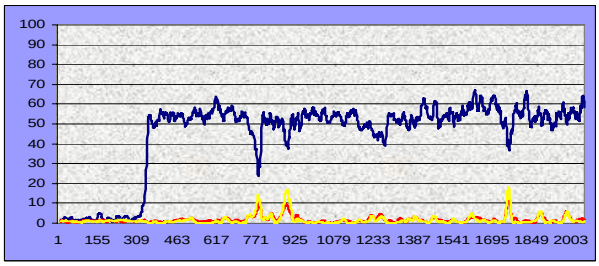

Fig. 2: Carbon (__) distribution variation compared to Ca (__) and P(__)

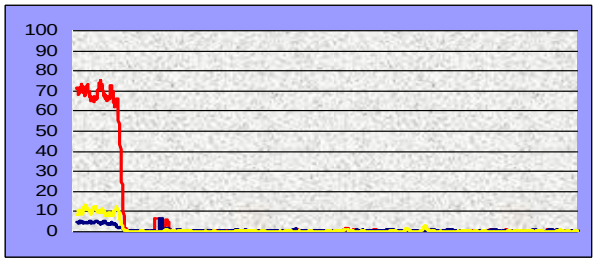

Fig. 3: Concentration variation of sample basic chemical composition elements (Ti__, Al__, V__) in the tissue

The quantitative analysis of organic matrix mineralization level shows a low mineralization by elements diminution (P, Ca) and organic components quantitative growth (C).

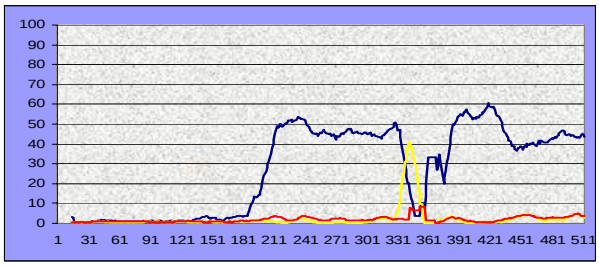

Fig. 4: Mineral and organic elements distribution at sample made from Ti6AL4V interface, C(__),Ca(__) & P(__)

After identifying the EDAX composition of 316L alloy sample, we discovered that from the alloy elements, iron has a higher migration, nickel a medium one, and chromium a lower one, the last

one being the most stable of them in the chosen environment.

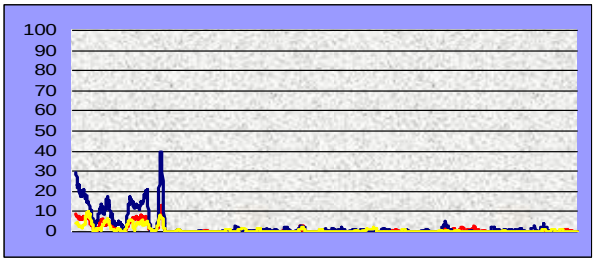

Fig. 5: Linear distribution in tissue of samples basic elements (Fe__, Ni__, Cr__)

The weaker organic matrix has the lowest mineralization level from all the four samples, as we can see in figure 6.

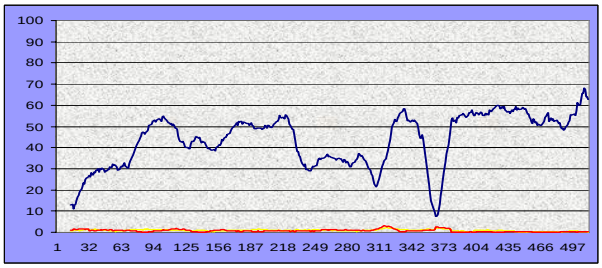

Fig. 6: Linear distribution of mineral and organic elements at sample 3 interface (stainless steel), C(__),Ca(__) şi P(__)

By analysing chemical composition of the implant surface, we identified that the 4th sample is made up of Co-Cr-Mo. By analysing chemical stability of biomaterial from which is made up sample 4th, in biological environment, we notice a high migration of molybdenum and a lower migration of cobalt and chromium. Peri - implant organic matrix is better developed and much more mineralized that Fe-Ni-Cr alloy implant.

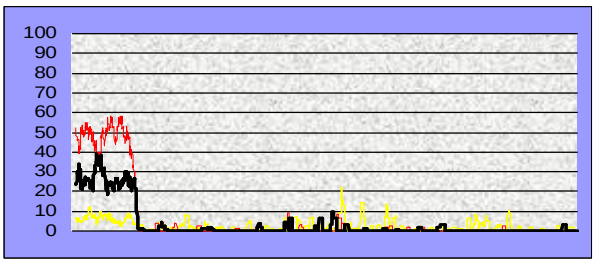

Fig. 7: Tissue diffusion of Co-Cr-Mo sample chemical composition basic elements(Co__,Cr__, Mo__)

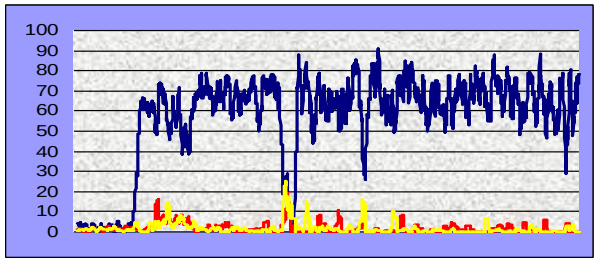

Fig. 8: Chemical elements distribution of sample 2 (CoCrMo) mineral and organic interface (C__, Ca__,P__)

DISCUSSION & CONCLUSIONS: No matter the metallic biomaterial the implant is made up of we observed its elements migration. The most chemically stable in the biological environment was pure titanium implant. Stainless steel implant caused a mainly iron diffusion and secondary a nickel one, chromium being much more stable. Developing and mineralization level of peri-implantation organic matrix was in deep correlation to the interface biochemical changes. New born bone tissue was densely mineralized in pure Ti implant case, lower mineralized in Ti6Al4V implant case, weaker mineralized to Co-Cr-Mo implant and the lowest mineralized for stainless steel implant.

REFERENCES: [1] Jinno T. Goldberg VM. Davy D. Stevenson S. (1998) *Osseointegration of surface-blasted implants made of titanium alloy and cobalt-chromium alloy in a rabbit intramedullary model*, Journal of Biomedical Materials Research. 42(1):20-9; [2] Masuda T. Yliheikkila PK. Felton DA. Cooper LF. (1998) *Generalizations regarding the process and phenomenon of osseointegration. Part I. In vivo studies,* International Journal of Oral & Maxillofacial Implants. 13(1):17-29; [3] De Lange G., De Putter C. (1993) *Structure of the bone interface to dental implants in vivo,* Journal of Oral Implantology. 19(2):123-35; discussion 136-7; [3] Guglielmotti MB. Renou S. Cabrini RL. (1999) *Evaluation of bone tissue on metallic implants by energy-dispersive x-ray analysis: an experimental study,* Implant Dentistry. 8(3):303-9; [4] Budd TW. Nagahara K. Bielat KL. Meenaghan MA. Schaaf NG. (1992) *Visualization and initial characterization of the titanium boundary of the bone-implant interface of osseointegrated implants*, International Journal of Oral & Maxillofacial Implants. 7(2):151-60.

European Cells and Materials Vol. 9. Suppl. 1, 2005 (pages 31-32) ISSN 1473-2262

Quantitative evaluation of dentin permeability and adhesive restorations microleakage

N. PRADELLE-PLASSE a,b,c F. WENGER b, P. COLONa,b

a Département d'Odontologie Conservatrice et Endodontie, UFR d'Odontologie, Université Denis Diderot Paris 7, Paris.

b Laboratoire de Biomatériaux, UFR d'Odontologie, Université Denis Diderot Paris 7, Paris.

c Laboratoire LGPM, Ecole Centrale Paris, Chatenay Malabry

INTRODUCTION: Many different techniques may be used to evaluate microleakage : air pressure, bacterial studies, radioisotopes studies, neutron activation studies, scanning electron microscopy, chemical tracers, dye penetration studies, the most common method, and electrochemical studies. The advantages of the last one are non- destructive techniques and the obtention of quantitative values. Actually, they often use direct current techniques such as the potential membrane method, the conductimetric method, the conductance, and the potentiometric method. Their main defects are a limited sensitivity and a polarization risk. Methods using alternating current as electrochemical impedance spectroscopy method presents some advantages compared to the method using direct current : a great sensitivity (ionic conduction), no disturbing of the charge distribution inside the dentin sample by the use of low values of alternative potential (40 mV), and immediate results.

The purpose of this in presentation was to presente a quantitative methodology and his applications : the impedance method.

METHODS:

Samples :

Disks of dentin of 1.2 or 2 mm included in resin cylinder exposing a surface area of 28.26 mm² (6 mm diameter) (Figure 1)

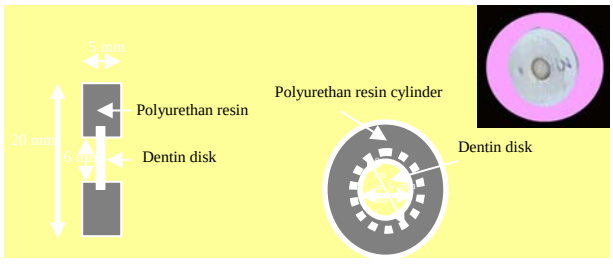

Figure 1 : Sample

Electrochemical cell

The system is a "like" permeation cell. The Plexiglas cell presented two compartments (50 cm^3) connected with stems and screws. A 250 mm² titanium-platinum gauze electrode was placed into each compartment. The sample was placed in the cell between two silicone rubber "O" rings (with a hole of 10 mm) preventing any lateral leakage. The cell was filled with an electrolyte solution of KCl 10^{-1} M at 20 +/- 1 °C (Figure 2).

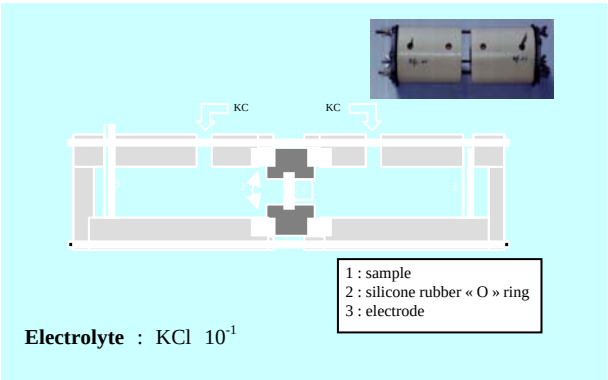

Figure 2 : Electrochemical cell

Electrochemical setting and electrochemical method

The electrodes were connected to a potentiostat (Solartron 1287) that was used for application of an alternating potential difference of 10 mV across the assembled cell over a frequency range from 1 Hz to 65 kHz (Figure 3). It also measured the current flow through the cell, which, together with the measured input potential difference, was fed to the Frequency Response Analyser (FRA, Solartron 1255[c]), which was microcomputer-controlled (Software ZPlot 2[d]). At every frequency, the FRA measured the amplitudes and phases of these two signals (potential and current), and the data were converted into complex impedance values Z, defined by real (resistive) R and imaginary (reactive) G parts : $Z = R - jG$ (with $j^2 = -1$)

The resistance of the solution Re was obtained by measuring the impedance at the same frequency, with the same polyurethane resin cylinder without the dentin disk (Rd = 0). From these impedance data, the Rd value specific to each specimen was derived.

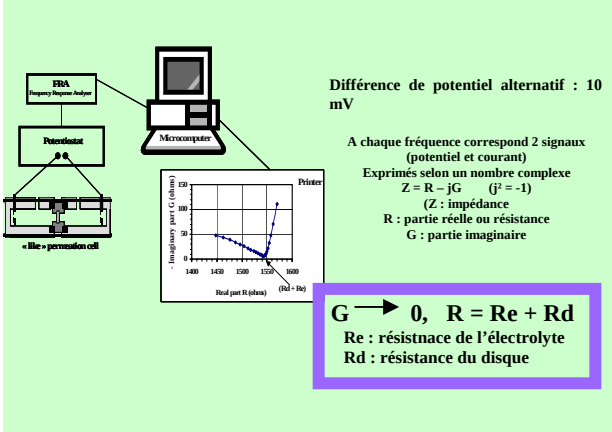

Figure 3 : Electrochemical setting and electrochemical method

APPLICATIONS and RESULTS

1 / Evaluation of dentin permeability (figure 4)

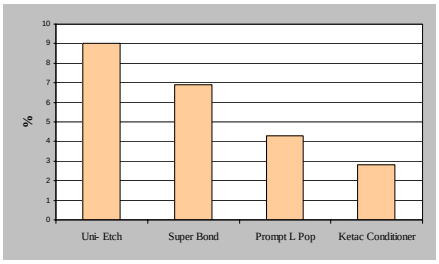

2 / Evaluation of microleakage of adhesive restorations (figure 5)

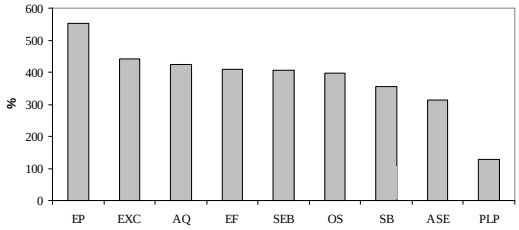

3 / Influence of thermocycling on the microleakage of composite resin restorations (figure 6)

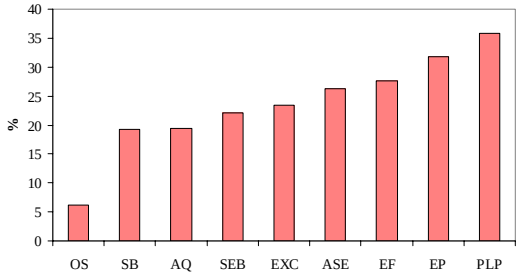

4 / Influence of water storage on microleakage (figure 7)

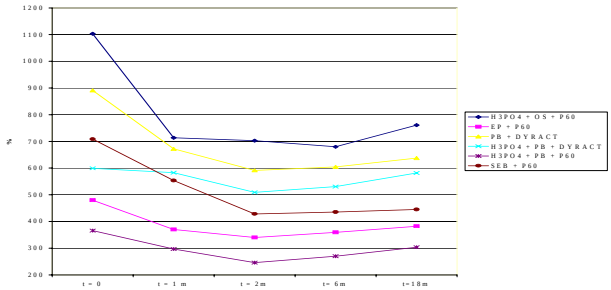

DISCUSSION – CONCLUSIONS

This table resume the advantages and limits of this methodology (Table 1) :

Parameters	Impedance method
Reproductible	X
Defect localisation	NO
Quantitative	X
Easy	X
Time evaluation	X
Modelling	X
Evaluation of permeability and microleakage	X
Non destructive	X
Weak cost	NO
Multitude of interfaces	NO
Sample geometry in relation with clinical considerations	NO

REFERENCES

Levinkind M, Vandernoot TJ and Elliott JC. Evaluation of smear layers on serial sections of human dentin by means of electrochemical impedance measurements. J Dent Res 1992, 71(3) : 426-433.

Pradelle –Plasse N, Colon P, Wenger F, Picard B. Quantitative evaluation of self-etching primers action on dentin permeability : a correlation between impedance measurements and acidity. Am J Dent 2004, 17 : 131-136.

Pradelle-Plasse N, Wenger F, Colon P. Effect of conditioners on dentin permeability using an impedance method. J Dent 2002, 30(5-6) : 251-257.

Pradelle-Plasse N, Wenger F, Picard B, Colon P. Evaluation of microleakage of composite resin restorations by an electrochemical technique: the impedance methodology. Dent Mater 2004, 20(5) : 425-434.

European Cells and Materials Vol. 9. Suppl. 1, 2005 (pages 33-34) ISSN 1473-2262

Contribution of the dilatometric studies on the polymerization's kinetics of the dental composite resins

C Villat [1,3], N Pradelle-Plasse [2,3] , B Picard [2,3] & P Colon[2,3]

[1] *Université Claude Bernard Lyon 1, UFR d'Odontologie, Rue Guillaume Paradin, 69372 – LYON, Fr*

[2] *Université Denis Diderot Paris 7, UFR d'Odontologie, 5 Rue Garancière, 75006- PARIS, Fr*

[3] *Laboratoire de Biomatériaux, Université Denis Diderot Paris 7, UFR d'Odontologie, 5 Rue Garancière, 75006- PARIS, Fr*

INTRODUCTION: Leakage involved by the polymerization shrinkage is a major drawback of composite restorations. However, the only value of the final polymerization shrinkage is not able to explain all laboratory results. A recent study using a dilatometer has described the velocity of the polymerization shrinkage of resin composites[1]. The aim of this study was to characterize the different elements of the curves of polymerization contraction of two dental composite resins regarding the light curing unit (LCU).

METHODS: Polymerization shrinkage as a function of time was investigated with a mercury dilatometer[2,3] (fig.1). To complete the study, temperature rise was registered on samples of 8 mm diameter and 2 mm thick.

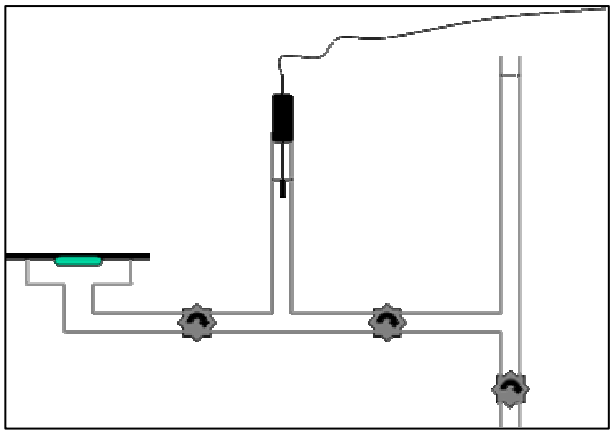

Fig. 1: Schematic representation of mercury-filled dilatometer

Two dental microhybrid composite resins (CR) (Z100®, Tetric Ceram®) were used with one conventional halogen LCU (Elipar® Highlight) and two light emitting diodes LCU (Elipar® Freelight 1, and Apollo GC-e Light®). The light curing modes used were 20 s, 40 s, and 40 s progressive.

RESULTS: The analysis of the polymerization curves during the two first minutes of the setting reveals four characteristic elements (fig. 2) : the dilatation peak at the beginning of the curing procedure (table 1), the angle formed by the initial slope of shrinkage with the vertical axis, the angle formed by the secondary slope of shrinkage with the vertical axis, and the intersection point between the two slopes of shrinkage (table 2). The stastistical analysis used was the ANOVA multi range test and the Fisher's test.

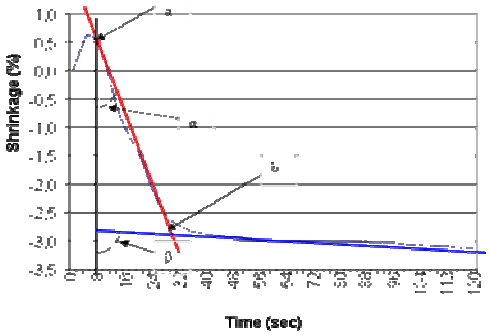

Fig. 2: Example of shrinkage curve (point a : dilatation peak at the beginning of the curing procedure ; angle α : angle formed by the initial slope of shrinkage with the vertical axis ; angle β : angle formed by the secondary slope of shrinkage with the vertical axis ; point b : intersection point between the two slopes of shrinkage)

CR	LCU	20 s	40 s	40 s prog
Z100®	EHL	0,11	0,09	0
	EFL1	0,04	0,04	0,02
	AGCL	0,09	0,03	0
Tétric Ceram®	EHL	0,63	0,54	0,10
	EFL1	0,09	0,19	0
	AGCL	0,17	0,18	0,06

Table 1. Mean values of the dilatation peak (%) (point a).

Table 2. Mean values of the angles formed by initial slope of shrinkage and the vertical axis (angle α), formed by the secondary slope of shrinkage and the vertical axis (angle β),) and the intersection point between the two slopes of shrinkage (point b).

LCU	Mode of polymerization	Z100®			Tétric Ceram®		
		Angle α (SD)	Angle β (SD)	Intersecti (SD)	Angle α (SD)	Angle β (SD)	Intersecti (SD)
EHL	20 s	23,18 (4,25)	89,43 (0,20)	16,00 (2,16)	29,83 (2,67)	88,93 (0,55)	25,25 (2,50)
	40 s	22,25 (0,60)	88,69 (0,84)	16,50 (2,38)	30,92 (2,17)	88,96 (0,75)	24,50 (1,00)
	40 s prog	22,42 (3,52)	87,75 (1,16)	28,25 (0,50)	44,42 (4,55)	87,99 (0,97	35,50 (2,52)
EFL1	20 s	27,19 (2,37)	89,23 (0,74)	17,25 (2,63)	43,55 (2,72)	88,03 (0,27)	27,50 (1,92)
	40 s	26,81 (5,86)	88,90 (0,74)	19,25 (3,20)	42,00 (3,51)	87,16 (0,74)	26,25 (1,71)
	40 s prog	23,62 (3,79)	88,41 (0,55)	26,25 (1,89)	42,89 (5,02)	86,86 (0,64)	35,25 (1,26)
AGCL	20 s	26,13 (3,26)	88,93 (0,40)	18,25 (2,75)	44,49 (3,46)	87,30 (0,44)	28,25 (0,96)
	40 s	27,57 (2,19)	89,00 (0,76)	20,00 (1,41)	44,64 (2,74)	87,16 (0,64)	32,00 (1,83)
	40 s prog	27,85 (1,45)	88,60 (0,52)	28,50 (1,73)	43,94 (3,34	87,49 (0,84)	41,00 (2,16)

DISCUSSION & CONCLUSIONS: "Soft-start polymerization modes seem to have an influence on different characteristics of the contraction curve. Those types of polymerization mode delay the gel point[4-6] and modify the angle between the initial contraction slope with the vertical axis for the halogen curing light. The gel point occurs in the 5 first seconds following the start of the polymerization[1] and is delay with "soft-start" curing modes. According to the curve, the maximum of the stress occur during the 20-30 first seconds of the setting during the initial contraction slope. However, no statistical differences have been shown between the standard modes and the "soft-start" modes for the LED-Light Curing Units as it was observed in the mechanical studies[7-10]. The type and the proportion of the photoinitiators may have an incidence on the results according to mechanical studies[11].

This study establishes other characteristics attributed both to the composite resins and/or to the light curing units that could have an interest in the understanding of stress distribution during setting.

REFERENCES: [1]Alvarez-Gayosso C, Barceló-Santana F, Guerrero-Ibarra J, Sáez-Espínola G, and Canseco-Martínez MA. Calculation of contraction rates due to shrinkage in light-cured composites (2004) *Dental Mater* **20**:228-35. [2]Bausch JR, De Lange K, Davidson CL, Peters A, De Gee AJ (1982) Clinical significance of polymerization shrinkage of composite resins *J Prosthet Dent* **48**:59-67. [3]Watts DC, Cash AJ. (1991) Determination of polymerization shrinkage kinetics in visible-light-cured materials : methods development. *Dental Mater* **7**:281-7.[4]Sakaguchi RL, Berge HX (1998) Reduced light energy density decreases post-gel contraction while maintaining degree of conversion in composites *J Dent* **26**:695-700. [5]Mehl A, Hickel R and Kunzelmann K-H (1997) Physical properties and gap formation of light-cured composites with and without "softstart-polymerization" *J Dent* **25**:321-30. [6]Feilzer AJ, Dooren LH, De Gee AJ, Davidson CL. Influence of light intensity on polymerization shrinkage and integrity of restoration-cavity interface. *European Journal of Oral Sciences*. 1995 ; **103**:322-326. [7]Hofmann N, Hugo B, Klaiber B. Effect of irradiation type (LED or QTH) on photoactivated composite shrinkage strain kinetics, temperature rise, and hardness (2002) *Eur J Oral Sci* **110**:471-9. [8]Jandt KD, Mills RW, Blackwell GB and Ashworth SH. Depth of cure and compressive strength of dental composites cured with blue light emitting diodes (LEDs) (2000) *Dental Mater* **16**:41-7. [9]Kurachi C, Tuboy AP, Magalhães DV and Bagnato VS. Hardness evaluation of a dental composite polymerized with experimental LED-based devices (2001) *Dental Mater* **17**:309-15. [10]Mills RW, Uhl A, Blackwell GB and Jandt KD. High power light emitting diode (LED) arrays versus halogen light polymerization of oral biomaterials : Barcol hardness, compressive strength and radiometric properties (2002) *Biomaterials* **23**:2955-63. [11]Uhl A, Mills RW, Jandt KD. Photoinitiator dependent composite depth of cure and Knoop hardness with halogen and LED light curing units (2003) *Biomaterials* **24**:1787-95.

Corrosion and biocompatibility of dental alloys

C. Manaranche[1], H. Hornberger[1]

[1] Metalor Technologies Neuchâtel, Switzerland.

INTRODUCTION: All materials are more or less subject to corrosion by their environment. For dental materials such as ceramics, polymers, cements and alloys, various elements can be released like mineral, metallic or organic compounds and may induce adverse biological reactions. In the literature, several studies [1-8] exist about the cytotoxicity of metallic ions. However, depending on the test method used (cells, toxicity assessment, time of exposure, etc), the results vary and finally, the cytotoxic effect of the metal ions are contrarely discussed.
The objective of this study was to find correlations between corrosion and biocompatibility of precious metals and to interpret the results by comparison with ion concentrations found in daily food and necessary for daily need.
And finally, the maximal quantity released by the precious dental alloy was compared to metal ions contained in food and compared to concentrations of trace elements necessary for the body.

METHODS: In a first step different categories of alloys (see Table 1) have been tested according to static immersion test of the ISO 10271 Standard [1]. The metallic ions released in this very corrosive solution, were analysed and the ions most released were determined.
In a second step, the concentration level of cytotoxicity was determined by testing various concentrations of pure metals according to ISO standard 10993/5 in indirect contact. This test was carried out by a certified institute (BIOMATECH-Chasse sur Rhône), who are specialised for biological tests. The study was restricted to the metals most released from precious alloys, such as Gallium, Copper, Zinc and Indium. First, an extract of the test materials was obtained by immersion for 48 hours in the cell medium (Sigma Aldrich M2279) at 37°C. Then the extract was put into contact with fibroblasts of mice (L929) for 48 hours. A red stain permitted to know the cellular density after the test. The material was considered as cytotoxic, if there was 25% of cellular reduction or more.
Additionally, some of the dental alloys were tested according to this method. The composition of the extract after test was analysed by ICP (Induced Coupled Plasma) in order to determine the nature and quantity of ions released.
Finally, literature research was carried out, where the need of metal ions as trace elements is described as indispensable for being in good health [9-10]. The concentrations of daily need and daily intake by food were compared with the maximised release of dental alloys. The maximised values were obtained by immersion into a very corrosive solution for seven days according to the ISO standard 10271 (pH= 2.3, [NaCl] = 5.83 g, [Lactic acid] = 9 g/l). The surfaces for crowns were estimated as followed: 2.1 cm^2 for a molar crown and 1.3 cm^2 for an anterior crown.

RESULTS & DISCUSSION: Pd-base and Au-Pt-Pd bonding precious alloys (see Fig 1) released few metallic elements (<10 $\mu g/cm^2$.week). On the contrary, NiCr alloys which contained less than 18 wt% chromium released a high amount of nickel ions (<1000 $\mu g/cm^2$.week). For other precious alloys, zinc and copper ions were mainly released but in acceptable quantity (<100 $\mu g/cm^2$.week). These metals are added in dental alloys to increase the hardness.
The concentrations of gallium, copper, zinc and indium which induced 25 % of cell death is given in Fig 2. Indium seemed most cytotoxic as 1.3 ppm was already sufficient, followed by zinc with 4.8 ppm, copper with 8 ppm and gallium with 17 ppm. Literature confirms that zinc appears more toxic than copper [2-6]. However, for indium and gallium, the studies in literature are contrarily discussed [1;4;8].
The metallic ion release of two non-cytotoxic dental alloys (see Fig 3) showed that the concentrations are very below the cytotoxic concentrations which were found for the pure metals.
Discussing the results it has to be carefully considered that the correlation of metallic ion release and their effect on biocompatibility is not linear. Other studies have found that antagonist effects are possible, for example the cytotoxic effect of a combination of several ions released in one solution is not simply an added effect, the combination can be less toxic than the addition of single effects [8]. Therefore, even it is not possible to predict the cytotoxicity with the help of a data base of corrosion values, it is it possible to explain bad cytotoxic result by the correlated ion release during corrosion.

The need of zinc and copper were reported as 7 to 10 mg/day and 1 to 1.5 mg/day respectively for an adult (See Fig 4). The quantity of metallic ions released by the surface of a full dental crown is very low: 0.08- 0.13 mg/day for copper and 0.33-0.53 mg/day for zinc related to the calculated area.

CONCLUSION: Zinc and copper were found to be the two metal ions most released by precious dental alloys tested. However, the quantities released do not induce cytotoxic effects and are far lower than the concentrations found in food.

Table 1: Atomic composition (°/°°) of main elements containing in tested dental alloys

Alloys	Category	Au	Pt	Pd	Ag	Cu
Conventional (CONV)	Au-Ag-Cu	250-605	0-75	0-60	115-505	145-315
	Ag-Pd-Cu	0-65	0	180-615	240-630	0-230
Bonding (CM)	Pd-base	10-35	0	700-750	0-65	0-110
	Au-Pt-Pd	650-780	65-95	90-160	0-40	0-6
	Au-Pd-Ag	300-620	0	280-505	0-225	0-90
	Au-Pt	800-850	110-120	0	0	0
Universal (UNIV)	Au-Ag	420-505	0-100	0-145	200-375	0
Alloys	**Category**	**Cr**	**Co**	**Ni**	**Mo**	**Be**
Non-precious (NP)	CoCr	305	550	0	30	0
	NiCr	205	350	340-680	50	0-105

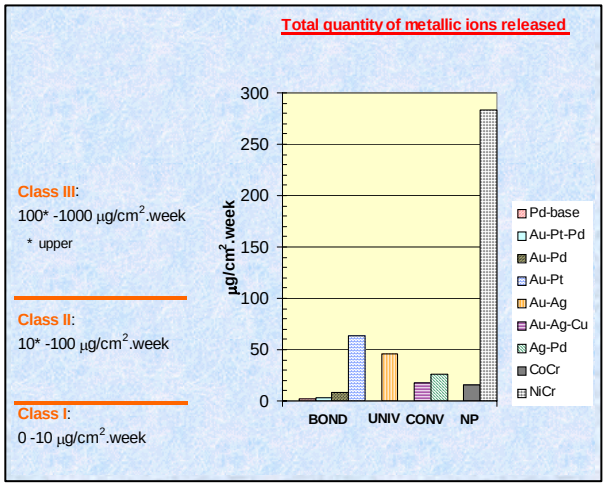

Fig. 1: Total quantity of metallic ions released by different dental alloys categories

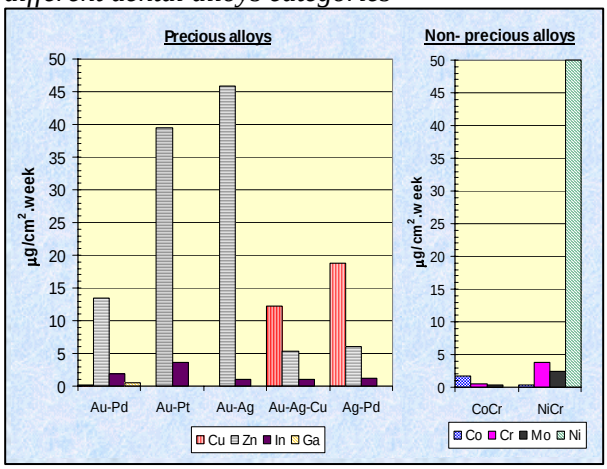

Fig 2: Main metallic ions released by different dental alloys categories

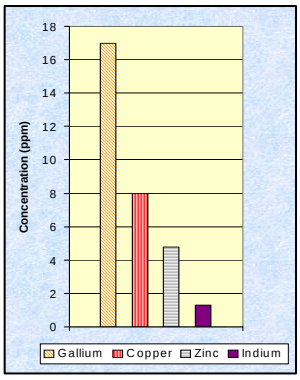

Fig 3: Metallic concentrations induced cytotoxic effects (25 % reduction of cellular density)

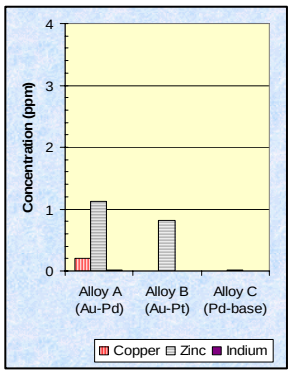

Fig 4: Examples of metallic release by two dental alloys non-cytotoxic in cell media

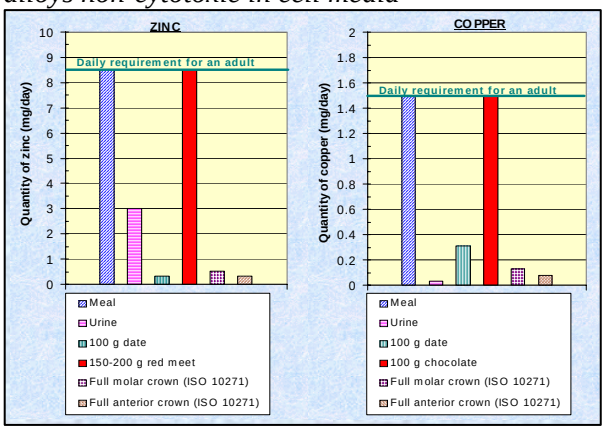

Fig 5: Zinc and copper: present in food, released by dental crown (maximised quantity)

REFERENCES: [1] A. Schedle, P. Samorapoompichit, X. H. Rausch-Fan, A. Franz, W. Füreder. Response of L-929 Fibroblasts, Human Gingival Fibroblasts, and Human Tissue Mast Cells to Various Metal Cations, J. Dent. Res. 74(8): 1513-1520, August, 1995.[2] G. Schmalz, H. Langer, H. Schweikl, Cytotoxicity of Dental Alloy Extracts and Corresponding Metal Salt Solution, J. Dent. Res. 77 (10): 1772-1778, October, 1998. [3] J. C. Wataha, C. T. Hanks, R. G. Craig, In vitro synergic, antagonistic and duration of exposure effects of metal cations on eukaryotic cells, J. of Biomed. Mat. Res., 26: 1297-1309, 1992.[4] J. C. Wataha, C. T. Hanks, R. G. Craig, In vitro effects of metal cations on eukaryotic cell metabolism, J. of Biomed. Mat. Res., 25: 1133-1149, 1991[5] J. C. Wataha, C. T. Hanks, Z. Sun, Effect of cell line on in vitro metal ion cytotoxicity, Dent. Mater., 10: 156-161, 1994.[6] J. C. Wataha, C. T. Hanks, Z. Sun, In vitro reaction of macrophages to metal ions from dental biomaterials, Dent. Mater., 11: 239-245, 1995.[7] A. Yamamoto, R. Honma, M. Sumita, Cytotoxicity evaluation of 43 metal salts using murine fibroblasts and osteoblastic cells, J. Biomed. Mater. Res., 39, 331-340, 1998.[8] J. C. Wataha, C. T. Malcolm, C. T. Hanks, Correlation between cytotoxicity and the elements released by dental casting alloys, Int. J. Prosthodont., 8: 9-14, 1995. [9] Guidelines for water quality-2nd Ed. Vol1, Recommendations, Geneva, WHO p57: 1993. [10] Guidelines for water quality-2nd Ed. Addendum to Vol1, Health criteria and other supporting information, Geneva, WHO, 31-46: 1998.

European Cells and Materials Vol. 9. Suppl. 1, 2005 (pages 37-38) ISSN 1473-2262

Computer Assisted Mechanical Tests for Metal-Ceramics Dental Systems

Patrascu, I., Ciocan L.T., Galbinasu B., Iordache B.

Dental Technology and Dental Materials Department, Faculty of Dental Medicine, University of Medicine and Pharmacy "Carol Davila", Bucharest, Romania

INTRODUCTION

The importance of metal-ceramics bond strength in obtaining long term clinical success of metal-ceramics fixed prosthesis was the subject of numerously international studies. In present, due to continuously development of new alloys and plating ceramics materials it is necessary to evaluate them comparatively from bond resistance level point of view.

AIM OF THE STUDY

Inspired by the metallurgical trial tests, we tried to imagine and realise a micromechanical computer assisted system and a suitable method for testing and evaluate the resistance level between the two components of the metal-ceramic crowns, which can be applied for comparative analyses of the numerous systems existing on the market.

MATERIAL AND METHODS

Figure 1: CAM_T – Computer Assisted Mechanical Testing System

Using a electro-tension translator it can be determined the precisely value of the detachment stress. This translator makes it possible to record in real time the diagram stress applied/time of exposure. Actually, the diagram, is a image of the sample behavior until the detachment of the two materials takes place. Knowing the value of the registered parameter, the value of the force Fr can be determined precisely respectively the detachment force σ_r or τ_r. In this work we will not describe the components of the system, because technical data are part of the documentation needed to patent this invention.

One of the most important tests used in testing the metal-ceramic bond are those imagined by Mc Lean and Sced. The feature characteristic for this method is the fact that by adequate preparing of the sample is obtained a favorable situation for the detachment of the ceramic material, because the interface detachment stress has a lower value in comparison with the compression resistance of ceramic material. On the other hand, the surface has volute of 45 degree that offer favorable conditions for detaching.

The elements presented above are put in evidence with the McLean's test. For this test were prepared samples, with specific characteristics for testing with this system. There were done three tests of detachment using metallic alloys with different qualities and the same type of ceramics IPS CLASSIC (IVOCLAR).

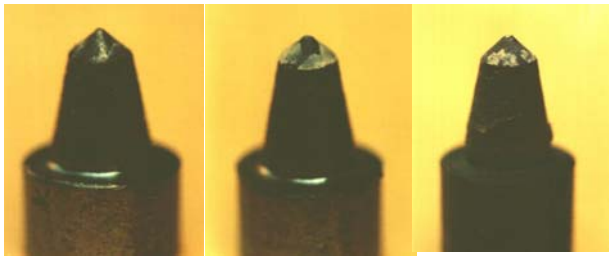

Figure 2: Samples: I, II and III

The data regarding testing conditions are: a) Oxidation- Raising temperature 10 min. to 1020oC- maintaining 3 min.- cooling 7 min. b) Firing opaquer IVOCLAR- Raising temperature to 980oC- maintaining 1 min.- cooling 7 min. c) Firing IVOCLAR ceramics mass- Raising temperature to 930oC- maintaining 1 min.- cooling 7 min.

RESULTS

For the detachment forces of 412 N (for sample I) 561 N (for sample II) and 496 N (for sample III) are corresponding values of the tensions. The surface of the samples tested was S=8.95mm.

Has been obtainned the two components of the samples: the part obtained from the investigated

alloy having a coned shaped surface f and the extraction socket. The same components has been obtainned together with sinterized ceramic material on the conical surface.

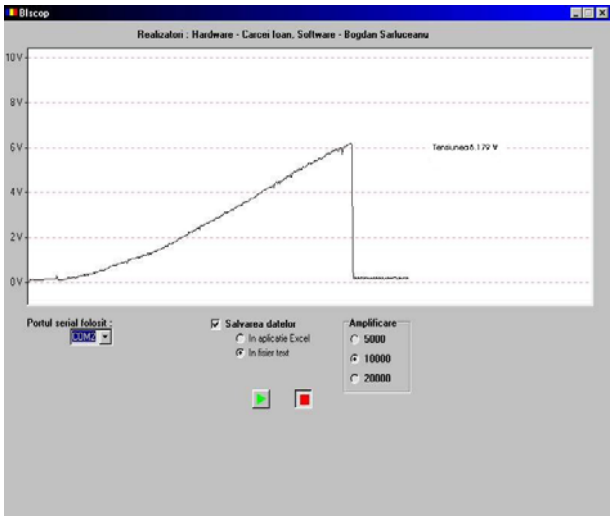

Figure 3:Tension-time diagram for sample II

CONCLUSIONS

According to the tests performed and the results obtained it can be said:

About the technical system CAM$_T$ system: CAM$_T$ system meet the requirements imposed by the researches in the field of dental materials, the values of the detachment tension obtained with McLean and Sced's test are close to that presented by the previous studies; Electronic system of CAM$_T$ system allows recording, processing and storing data of the real time tests; Using a dedicated software with a PC (at least Pentium II) it can be followed the evolution of the experimental testing, drawing the diagram and some other characteristics specific to the test realized.

About the tests type McLean and Sced: The compression modulus of the ceramics was adopted correctly for obtaining the detachment; The analyses of the results for II test and I confirm the considerations from the documentary study according to which the sandblasting of the metallic surface increases the adherence.

The best adherence can be observed in case of the NEY QII alloy proved by the analysis of the fracture on the volute surfaces of the samples I and II- the sample II presents the optimal type of fracture (O'Bien)- the cohesive fracture through porcelain

REFERENCES: [1] Cambell S., Sirakian A., Pelletier , Hordano, R. - *Effects of Firing Cycle and Surface Finishing on Distortion of Metal Ceramic Castings*; The Journal of Prosthetic Dentistry, vol. 74, noiembrie, 1995;

[2] Cuncil of Dental Materials, *Instruments and Equipments - Report on Base Metal Alloys for Crown and Bridge Application: benefits and risks*, J. Am Dent Assoc, 33:1391, 1946;

[3] Dorsch P. - *Thermal Compatibility of Materials for Porcelain Fused to Metal (PFM) Restorations*, Caramic forum International, Ber Dt Keram Ges, 59:1, 1982;

[4] O'Brien W. J. - Dental Materials, Properties and their Selection, Quintessence Publ., Chicago, 1989;

[5] Johnson W., Mellor, P.B. - *Engineering Plasticity,* John Wiley & Sons, ISBN 0 - 470 - 20012 - X, 1983.

[6] McLean, John - T*he Science and Art of Dental Ceramics*, Quintessence Publ. Co., Chicago, vol II.

European Cells and Materials Vol. 9. Suppl. 1, 2005 (pages 39-40) ISSN 1473-2262

EFFECTS OF VARIOUS HYGIENIC TREATMENTS OF ORTHODONTIC ALLOYS ON *IN VITRO* MUTANS STREPTOCOCCI ADHERENCE.

A-L Bertrand[1], J-J Morrier[1], G Benay[1], L Ponsonnet[2], O Barsotti[1]

[1] Faculté d' Odontologie – EA 637, Rue Guillaume Paradin 69372 Lyon Cedex 08, France.
[2] CEGELY - Ecole centrale de Lyon, rue 36 avenue Guy de Collongue, BP 163, 69131 Ecully cedex, France

INTRODUCTION: It has been reported that orthodontic treatments increase the carious risk and the concentration of cariogenic micro-organisms (mutans streptococci) in dental plaque and saliva. Nevertheless, little is known about the relationships between fixed orthodontic materials and oral colonisation by mutans streptococci (MS). The plaque retaining capacities of orthodontic wires have never been studied. The first objective of this investigation was to evaluate and to compare the adherence of MS to alloys currently used in confection of orthodontic wires: stainless steel, a Nickel – Titanium alloy (NiTi) and a Titanium-Molybdene alloy (Ti-Mo). For each alloy, bacterial adherence was studied, after a salivary coating, according to 3 different hygienic treatments in order to investigate the effect of these regimens on bacterial adherence: disinfection or steam autoclaving commonly used in dental office and sterilisation by gamma X rays, a common industrial sterilisation process.
Numerous studies have shown the influence of the physico-chemical properties of bacterial and substrata surfaces on microbial adhesion process. Therefore the second objective of this work was to investigate the surface properties of bacterial strains and orthodontic alloys

MATERIAL AND METHODS: Four bacterial strains were used for this study: 2 reference strains: *S. mutans* ATCC25175[1] and *S. sobrinus* ATCC33478, and 2 fresh isolate strains of *S. mutans* and *S. sobrinus*. All strains were grown on Columbia agar supplemented with 5% defibrinated sheep blood in a CO_2 enriched atmosphere (Generbox CO_2).
Metal samples (Table 1) consisted of discs or (S = 1cm²; Ra < 0.15µm). Specimens were divided into 3 groups with different hygienic treatments:
Disinfection (D): (1 h) with 5% Lysetol®.SA. (S&M France,)
Steam autoclave sterilization (S.A.): 121°C during 30 minutes.
Gamma X ray sterilization (G.R.): (2500 Gy) according to standard condition (NF EN 552).

Table 1: Tested metal alloys

NiTi (AMF-France)				
Ni %	Ti %	Fe %	Cu %	O %
55,5	45,5	0,02	0,002	0,10
Stainless steel AISI 304 (Goodfellow - France)				
Fe %	Cr %	Ni %	Mn%	C %
67 - 75	17 - 20	8 - 11	< 2	traces
TiMo (TIMET. SA France)				
Ti %	Mo %	Al %	Nb %	Si %
77	15	3	3	2

Bacterial adherence tests and bacterial numeration on saliva-coated metal samples were carried out as described by Sardin et al. (2004). For each bacterial strain, each alloy and according to each hygienic regimen, the experiment was carried out three times. The average number of adherent cells per mm² was calculated. Results of bacterial adherence were compared using ANOVA and Fisher's t test (PLSD) at a significance level of p=0.05.

Surface properties of metal samples and bacteria were evaluated by the sessile drop method. Three probe liquids of different polarity were used for contact angle measurements: distilled water, diiodomethane and formamide. Contact angle measurements. were carried out using a GBX Scientific Instrument[2], (i) on saliva coated substrata and bare substrata as described by Sardin et al (2004) and (ii) on bacterial lawn as described by Bussher et al (1984)(BOS). For each liquid, and for each sample (n=3 samples), three drops were examined. The total SFE (γ_S^{tot}), its polar (γ_S^{AB}) (acidic (γ_S^{+}) and basic (γ_S^{-}) components) and non-polar (γ_S^{LW}) components were determined from contact angle measurements according to van Oss approach (BOS et coll).

[1] American Type Culture Collection, Rockville MD, USA

[2] GBX, Romans sur Isère, France

RESULTS:

Figure 1 : Means of adherent bacteria on tested alloys per mm^2 according to the different hygienic treatments

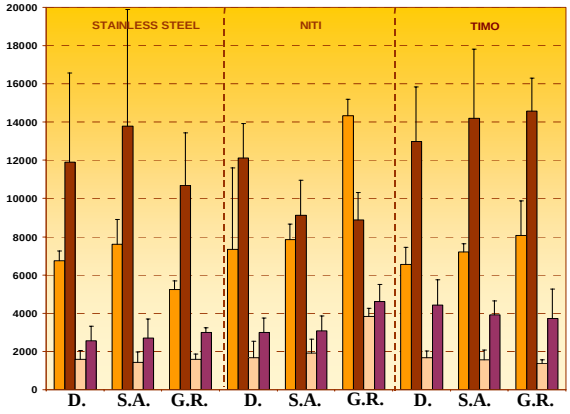

Figure 1 shows the mean values of adherent bacteria on saliva-coated substrata according to the different hygienic treatments.

Surface properties of alloys: In the absence of a salivary coating the γ_S^{tot} of alloy samples was ranged from 31.9mJ/m^2 to 46.9mJ/m^2 with a strong dispersive component. No significant difference was observed between the different alloys according to the nature of hygienic treatment. The electron-donor character of alloy samples was weak (0.1mJ/m^2 to 11.5mJ/m^2) with the exception of steam autoclaving Ti-Mo samples (21.9mJ/m^2).
With a salivary coating, the γ_S^{tot} of alloy samples was ranged from 29.2mJ/m^2 to 40.9mJ/m^2 with the exception of disinfected and autoclaved Ni-Ti samples: γ_S^{tot} values were respectively 59.9mJ/m^2 and 63.2mJ/m^2. These surfaces demonstrated a less hydrophobic character. All saliva-coated specimens demonstrated a strong increase in basic (ie. electron-donor character) properties with lowest values observed on Ni-Ti and Stainless-steel specimens (≅17mJ/m^2)

Surface properties of bacterial strains: The cell surface of all mutans streptococci strains exhibited moderate hydrophobicity: mean values of total SFE (γ_S^{tot}) were ranged from 38.7mJ/m^2 to 47mJ/m^2. All bacterial strains exhibited a low polar component and a strong electron donor (ie basic) character (34 mJ/m^2 - 48.4. mJ/m^2). Therefore γ_S^{tot} of *S. sobrinus* ATCC38478 was slightly higher (47 mJ/m^2) and its electron donor component was lowest (34mJ/m^2).

DISCUSSION & CONCLUSIONS: The results presented in this study indicate that saliva coating modified total SFE values (γ_S^{tot}) with a strong increase of the basic character (γ_S^-) as reported by numerous investigations. Since bacterial surfaces demonstrated important basic character these results indicate that acid-base interactions need to be taken into account when one is evaluating bacterial adherence on orthodontic materials. The number of adherent bacteria was significantly higher on Ni-Ti discs treated by gamma X rays sterilization with *S. mutans* reference strain and *S. sobrinus* strains ($p < 0.05$). No significant difference was observed between bacterial adherence on stainless steel, Ni-Ti and Mo-Ti discs treated by disinfection or steam autoclaving. Thus stainless steel, Ni-Ti and Mo-Ti samples, disinfected or steam autoclaved, could have the same effect on the formation of a cariogenic biofilm. The adherence of fresh oral isolates was greater than that observed for the reference strains. The number of adherent *S. mutans* cells was significantly higher than the number of adherent *S. sobrinus* cells ($p<0.05$). These results confirm that bacterial adherence is strain dependant and that it is necessary to use several bacterial species and strains when one is evaluating bacterial adherence on dental materials.
Crotty et al (1996) showed that steam autoclaved sterilization didn't modify the mechanical properties of the NiTi alloys and Pernier et al (2002) didn't find significant modification of the surface quality of the NiTi alloy, after steam autoclaving. According to these results, sterilization of Ni-TI, orthodontic materials by steam autoclaving could be recommended in dental office.

REFERENCES. R. BOS, H.C. Van der Mei and H.J. Busscher (1999) *FEMS Microbiol. Rev.* **23**: 179-230.
S. SARDIN, J.J. Morrier., G. Benay and O. Barsotti (2004) *J Oral Rehabil*..**31**: 140-148.
O.P. CROTTY, E.H. Davies and S.P. Jones (1996) *Br J Orthod*.. **23 (1)**: 37-41.
C. PERNIER, B. Grosgogeat., L. Ponsonnet, G. Benay and M. Lissac, Effect of sterilization on the surface topography of orthodontic wires. *1° Pan European Federation of IADR Scientific Meeting. Cardiff, Wales UK.* 2002.
ACKNOWLEDGEMENTS: We thank F. Gourbière for the statistical analysis.

European Cells and Materials Vol. 9. Suppl. 1, 2005 (pages 41-42) ISSN 1473-2262

Influence of accelerator and initiator concentration on resin matrix colour of Spectrum® composite resin.

JP Salomon[1], A Raskin[1] , J Déjou[1] & M Degrange[2]

[1]*UFR d'Odontologie de Marseille, Université de la Méditerranée. Laboratoire IMEB ET 30 27 Bd Jean Moulin. 13385 Marseille Cedex . Fr*

[2] *Faculté d'Odontologie de ParisV, Université René Descartes. Groupe de recherche en Biomatériaux. 1 Rue Maurice Arnoux. 92100 Montrouge*

INTRODUCTION: The aim of this study was to evaluate the influence of camphoroquinone (CQ) and DMABEE (4-N,N-dimethylaminobenzoic acid ethyl ester) concentration on colorimetric parameters of resin matrix of a composite resin (Spectrum®, Dentsply).

METHODS: Five concentration (0.2, 0.4, 0.6, 0.8, 1,0 W%) of CQ and DMABEE (eq) have been mixed with resin matrix before light curing. Ten samples of each group (1mm thick, 5mm diameter) were light cured between two Mylar strips , under 2 glass slides with an halogen VIP (Bisco) curing unit, standard mode (600 mW/cm^2, 30 s). Measurements were carried out 24 hours after the end of the curing, the samples being stored at 37°C in dry air. Colorimetric parameters were obtained with a BYK Gardner (45°-0°) spectrocolorimeter with the C/2° illuminating. Measurements were realized on a white and a black background. Parameters were obtained in the L*a*b* the L*C*h° reference marks. Besides, two indexes, Wb (White Berger) and YlD1925 (Yellow) were calculated.

Statistical analysis: Kruskal-Wallis non parametric analysis of variance was carried out to evaluate the influence of the CQ concentration (5 modalities). Bonferroni-Dunn *a posteriori* tests were used in order to localize the differences pointed out by the Kruskal-Wallis test. Spearman rank correlation was carried out to point out the relationship between colorimetric parameters and CQ concentration.

RESULTS:

Results are summarized in Table 1 and Figure 1 and 2 .

Table 1 : Influence of CQ concentration (%) on colorimetric parameters

CQ%	L*w m	L*w sd	a*w m	a*w sd	b*w m	b*w sd	C*w m	C*w sd	h°w m	h°w sd	WB w m	WB w sd	Yl w m	Yl w sd
0.2	82.48	0.83^{d}	-4.75	0.14^{d}	8.968	0.25^{e}	10.20	0.21^{a}	117.85	0.40^{e}	34.70	51.73^{e}	15.01	0.43^{a}
0.4	81.22	81.05^{c}	-5.46	0.16^{c}	12.60	0.203^{d}	13.51	0.23^{b}	113.07	0.60^{d}	21.76	61.54^{d}	21.37	0.38^{b}
0.6	80.57	60.80^{bc}	-5.18	0.13^{b}	14.54	0.165^{c}	15.51	0.42^{d}	109.68	0.52^{c}	14.34	81.01^{c}	25.73	0.77^{c}
0.8	79.86	30.83^{b}	-5.15	0.08^{b}	17.23	0.105^{b}	17.77	0.15^{d}	106.84	0.22^{b}	5.397	0.70^{b}	30.34	0.39^{d}
1	78.28	0.83^{a}	-5.67	0.83^{a}	24.8	0.834^{a}	25.47	0.83^{e}	103,0	0.83^{a}	-15.9	0.834^{a}	44.04	0.83^{e}
p =	0.0001		0.0001		0.0001		0.0001		0.0001		0.0001		0.0001	

For each column. groups with the same superscript letter did not significantly differ

Figure 1 : Influence of CQ concentration (%) on L, a*, b* (white background)*

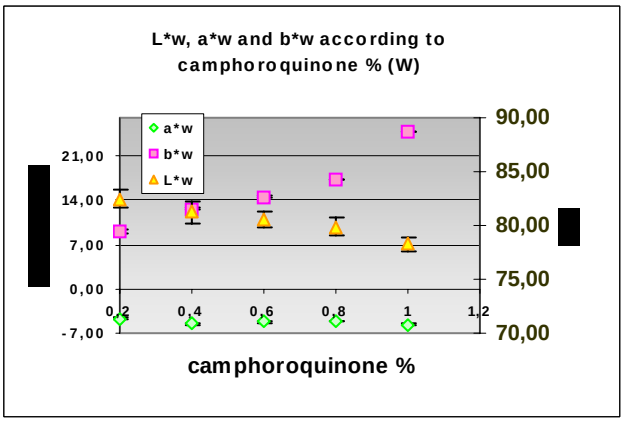

Figure 2 : Influence of CQ concentration (%) on WB and Yl (white background)

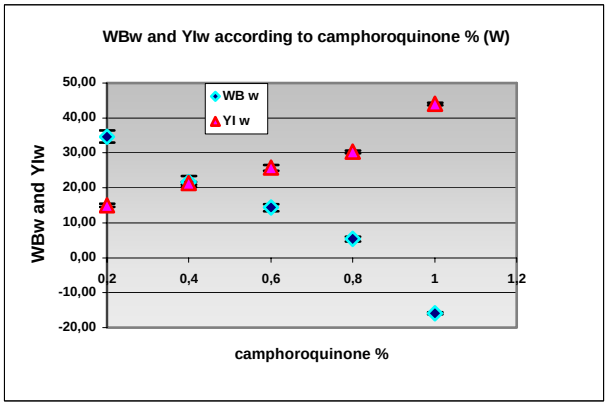

Whatever the parameter evaluated, there were differences between the five CQ concentrations. Linear relationship could be pointed out (p = 0.0001) between CQ concentration and L*, a*, b*, h°, C*, WB and Yl.

DISCUSSION & CONCLUSIONS: Initiator and co-initiator concentration have been shown to influence the polymerisation kinetic, conversion rate and polymerisation stress of composite resins. This study showed that modifying CQ concentration can lead to deeply modify colour of one composite resin (Spectrum®, Dentsply).

REFERENCES:

Asmussen E, Peutzfeldt A. 2002**,** Influence of composition on rate of polymerization contraction of light-curing resin composites.
Acta Odontol Scand. Jun;60(3):146-50

Braga RR, Ferracane JL. 2002**,** Contraction stress related to degree of conversion and reaction kinetics.
J Dent Res. Feb;81(2):114-8.

European Cells and Materials Vol. 9. Suppl. 1, 2005 (pages 43-44) ISSN 1473-2262

Influence of finishing/polishing procedures on surface roughness of a microhybrid composite resin

A Raskin , JP Salomon & J Déjou

UFR d'Odontologie de Marseille, Université de la Méditerranée. Laboratoire IMEB ERT 30

27 Bd Jean Moulin. 13385 Marseille Cedex . Fr

INTRODUCTION: The aim of this study was: (1) to compare the efficiency on samples of Miris® microhybrid composite resin of 18 finishing/polishing procedures involving diamond finishing burs with different grit sizes (45 µm, 30 µm, 15 µm grit size) and/or 12 and 30 bladed tungsten carbide and (2) to evaluate the effect of Brushine® (Diatech) silicone carbide polishing powder impregnated brushes after finishing/polishing with the 18 procedures.

METHODS: 360 rectangular shaped samples of Miris® (Coltène Whaledent) (5mm width, 8mm length, 1mm thick) were used in this study. The samples were light-cured, under a Mylar strip covered by a glass slide, with a LED unit (Freelight Elipar 2, 3M-ESPE) in a standard curing mode (1140 mW/cm^2 – 20 s). Immediately after curing the samples were subjected to the following procedures (*Table 1*):

Table 1. Sequences of the finishing/polishing procedures compared in the study

With carbide multi-blades burs		12 blades 15µm + 12 blades 25µm + 12 blades 45µm + 12 blades 15µm + 12 blades+ 30 blades 25µm + 12 blades + 30 blades 45µm + 12 blades + 30 blades 15µm + 30 blades 25µm + 30 blades 45µm + 30 blades 12 blades + 30 blades
Without carbide multi-blades burs	With 15µm burs	45µm + 15µm 45µm + 25µm + 15µm 25µm + 15µm 15µm
	Without 15µm burs	45µm + 25µm 25µm 45µm

After every step the samples were thoroughly rinsed with a spray of air and water.

Measurements were carried out 24 hours after the end of the polishing steps (the samples being stored at 37°C in dry air**)** with a surface profilometer- SURFTEST SV 400 MITUTOYO: cut-off value 0.25mm, diamond stylus with a radius tip of 5µm, stylus traveling speed 0.1mm/second, length of profile : 1.5 mm

Two roughness parameters were calculated: Ra and Rt. For each sample, five different measurements were realized.

Statistical analysis: Mean Ra and Rt were calculated for each sample and were used as criteria for the statistical evaluation of results.

Kruskal-Wallis non parametric analysis of variance was carried out to evaluate the influence of the finishing/polishing procedure (18 modalities). Bonferroni-Dunn *a posteriori* tests were used in order to localize the differences pointed out by the Kruskal-Wallis test.

Mann and Withney non parametric test was carried out to compare the surface roughness with or without Brushine® use. Signification level was p=0.05.

RESULTS: Among the 18 finishing/polishing procedures, 3 groups have been differentiated (*Table 2 and 3*). Procedures involving tungsten carbide 12 and/or 30 bladed burs led to the best results, whatever the sequence used (with or without diamond burs). The worst results were obtained with the groups involving only diamond burs and particularly when 15 µm grit size burs were not used in the procedures.

When evaluating the effect of Brushine® polishing brushes, only the worst Ra and Rt could have been improved (mainly, those obtained without the carbide multi-blades burs).

Table 2. Influence of finishing/polishing procedure and Brushine® use on surface roughness (Ra, µm) of Miris® composite resin samples.

		Ra (µm)	With Brushine m(sd)		No Brushine m(sd)		p =
With carbide multi-blades burs		12 blades	0.18 (0.03)	a	0.17 (0.03)	a	NS
		15µm + 12 blades	0.18 (0.02)	a	0.22 (0.04)	a	0.003
		25µm + 12 blades	0.20 (0.04)	a	0.21 (0.03)	a	NS
		45µm + 12 blades	0.23 (0.06)	a	0.23 (0.06)	a	NS
		15µm + 12 blades+ 30 blades	0.18 (0.04)	a	0.18 (0.04)	a	NS
		25µm + 12 blades + 30 blades	0.11 (0.01)	a	0.18 (0.03)	a	0.0001
		45µm + 12 blades + 30 blades	0.19 (0.04)	a	0.20 (0.07)	a	NS
		15µm + 30 blades	0.20 (0.04)	a	0.19 (0.04)	a	NS
		25µm + 30 blades	0.19 (0.04)	a	0.21 (0.03)	a	NS
		45µm + 30 blades	0.16 (0.05)	a	0.23 (0.03)	a	0.001
		12 blades + 30 blades	0.19 (0.05)	a	0.26 (0.04)	ab	0.001
Without carbide multi-blades burs	With 15µm burs	45µm + 15µm	0.70 (0.06)	b	0.35 (0.04)	b	0.0001
		45µm + 25µm + 15µm	0.71 (0.05)	bc	0.42 (0.06)	b	0.0001
		25µm + 15µm	0.64 (0.10)	b	0.41 (0.08)	b	0.0001
		15µm	0.61 (0.04)	b	0.40 (0.06)	b	0.0001
	Without 15µm burs	45µm + 25µm	0.94 (0.10)	c	0.57 (0.10)	c	0.0001
		25µm	1.01 (0.08)	c	0.60 (0.10)	c	0.0001
		45µm	4.09 (0.84)	d	2.71 (0.32)	d	0.0001
		p =	0.0001		0.0001		

For each colums, groups with the same superscript letter did not significantly differ

Table 3. Influence of finishing/polishing procedure and Brushine® use on surface roughness (Rt, µm) of Miris® composite resin samples.

		Rt (µm)	With Brushine m(sd)		No Brushine m(sd)		p =
With carbide multi-blades burs		12 blades	1.34 (0.19)	a	1.05 (0.21)	a	0.005
		15µm + 12 blades	1.21 (0.18)	a	1.47 (0.30)	a	0.03
		25µm + 12 blades	1.36 (0.23)	a	1.34 (0.22)	a	NS
		45µm + 12 blades	1.78 (0.81)	a	1.34 (0.25)	a	NS
		15µm + 12 blades+ 30 blades	1.16 (0.20)	a	1.13 (0.20)	a	NS
		25µm + 12 blades + 30 blades	0.79 (0.08)	a	1.21 (0.14)	a	0.0001
		45µm + 12 blades + 30 blades	1.47 (0.49)	a	1.27 (0.45)	a	NS
		15µm + 30 blades	1.24 (0.22)	a	1.14 (0.14)	a	NS
		25µm + 30 blades	1.20 (0.14)	a	1.24 (0.24)	a	NS
		45µm + 30 blades	1.09 (0.33)	a	1.32 (0.16)	a	NS
		12 blades + 30 blades	1.17 (0.28)	a	1.48 (0.19)	a	0.01
Without carbide multi-blades burs	With 15µm burs	45µm + 15µm	4.81 (0.32)	b	2.30 (0.35)	b	0.0001
		45µm + 25µm + 15µm	4.95 (0.45)	b	2.75 (0.42)	b	0.0001
		25µm + 15µm	4.70 (0.90)	b	2.70 (0.73)	b	0.0001
		15µm	4.60 (0.52)	b	2.65 (0.70)	b	0.0001
	Without 15µm burs	45µm + 25µm	6.35 (0.68)	c	3.50 (0.72)	c	0.0001
		25µm	7.54 (0.40)	c	3.93 (0.74)	c	0.0001
		45µm	23.90 (1.90)	d	16.61 (2.70)	d	0.0001
		p =	0.0001		0.0001		

For each colums, groups with the same superscript letter did not significantly differ

DISCUSSION & CONCLUSIONS: Whatever the sequence carried on, all procedures involving tungsten carbide 12 or 30 bladed burs led to excellent surface roughness. One could conclude that the simpler procedure should be chosen. Nevertheless, finishing/polishing procedures of composite resin restorations often include a reshaping step. This step is most of the time realized with diamond 45 or 30 µm grit size burs. Consequently, it seems that a procedure involving one diamond bur (45 or 30 µm) followed by one tungsten carbide 12 or 30 bladed is a simple, fast and efficient procedure.In these conditions Brushine® should not be used to improve surface roughness. However the gloss of most of the 360 samples seemed to have been improved when using Brushine® polishing brushes. This could mean that gloss and roughness are note totally correlated.

ACKNOWLEDGEMENTS: Diamond Diatech burs, tungsten carbide Diatech burs, Brushine® polishing brushes and Miris® composite resin have been kindly provided by Coltene Whaledent

European Cells and Materials Vol. 9. Suppl. 1, 2005 (pages 45-47) ISSN 1473-2262

Titanium alloys orthodontics wires : electrochemical study in fluoride dental rinses

N.Schiff*[1], B.Grosgogeat [1], M.Lissac [1] & F.Dalard [2]
[1] Department of Biomaterials , School of dentistry, University of Lyon, France
[2] National Polytechnic Institute of Grenoble, CNRS, Saint Martin d'Hères, France

INTRODUCTION: The various technics of orthodontic treatments call for titanium alloys-based orthodontic wires. The main physical properties of NiTi, TMA and CuNiTi wires are the elasticity and the memory of form.
Throughout all the treatment, practitioners recommend a detailed attention with oral hygiene and prescribe fluoride mouthwashes.
The aim of our study is to compare the electrochemical behaviour of various pre quoted wires in 2 commercially available mouthwashes: Elmex® and Meridol®.

MATERIALS & METHODS: The various materials were provided by Ormodent (Montreuil, France). Their composition (wt%) is as follows : TMA: Ti 75.5, Mo 14, Sn 5.5; NiTi: Ni 55, Ti 45; CuNiTi: Cu 5.5, Ni 48, Ti 46.5. Three samples of each type of material were prepared to constitute the working electrode tip, turning at 100 rpm.
The study environments are fluoride dental rinses. The 1st test solution is ELMEX® (Gaba, France), containing 100 ppm of amine Fluoride and 150 ppm of sodium fluoride. Its pH is 4,3. The 2nd test solution is MERIDOL® (Gaba, France), containing 125 ppm of amine fluoride and 125 ppm of tin fluoride. Its pH is 4,2.
The electrochemical assembly is a cell (Roucaire, Courtabeuf, France) where the solutions are maintained at 37° C with a thermostated bath (Bioblock, Illkirsh, France). A calomel saturated electrode, a platinum counter-electrode and a working electrode (where the tip with the material is screwed) are connected to a potentiostat EGG PAR 273A, itself connected to a computer treating the obtained curves via specific software.
Thus, we could determine the corrosion potentials (E corr), the corrosion intensity (i corr), the corrosion speeds (v corr), and the resistance of polarization (Rp) of the various materials into the mouthwashes.
After chrono-amperometry, a SEM study enabled us the analysis of the samples surfaces in order to correlate the electrochemical results on the resistance to corrosion.

RESULTS & DISCUSSION: The corrosion potential of the different alloys was measured in the two test solutions 24 hours later. The values obtained are shown in table 1.

E corr (mV/SCE)	TMA	NiTi	CuNiTi
Elmex®	-200	-90	-150
Meridol®	-350	-350	-150

Table 1 : corrosion potentials (mV/SCE) of the samples in dental rinses after 24 h

In Elmex® (Fig.1), the TMA corrosion potential stabilized at -200 mV/SCE :
the regular decrease of the curve suggest a reduction of the resistance to corrosion of this material. For NiTi, the corrosion potential stabilizing at -90mV/SCE suggests a moderate corrosion to resistance.
The regular drop in CuNiTi corrosion potential, reaching -150mV/SCE, also suggests a moderate resistance to corrosion.
In Meridol® (Fig.2), the TMA corrosion potential is low, reaching -350m/VSCE. Kaneko et al [1] showed similar results in fluoride solutions.
For NiTi, the corrosion potential reached -350mV/SCE, suggesting insufficient resistance to corrosion.
The same conclusions are reported by other authors [1,2] in fluoride solutions. The CuNiTi corrosion potential was stable at approximately -150mV/SCE.

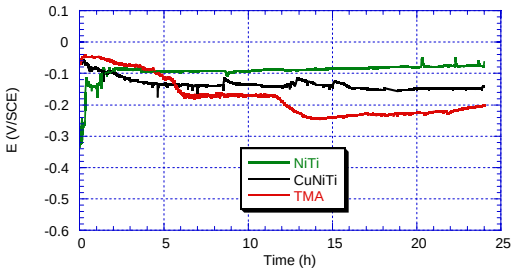

Fig. 1. Corrosion potential evolution during time in Elmex®solution for materials.

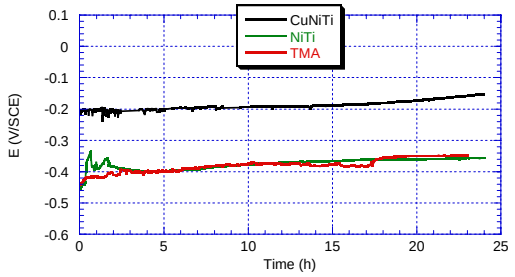

Fig. 2. Corrosion potential evolution during time in Meridol®solution for materials.

According to these first results, we can conclude that TMA & NiTi corrode more easily in Meridol® than in Elmex®. In order to assess the resistance to corrosion of the materials and the stability of the solutions, cyclic voltammograms were plotted for the different alloys in the two mouthwashes. The polarisation curves were plotted in the potential range of -800mV/SCE to +1200mV/SCE at a scanning rate of 0.2mV/s. The obtained values of corrosion current density (i corr), corrosion rate (v corr) and polarisation resistance (Rp) of the different materials in the two test solutions are shown in table 2 and 3.

i_{corr} (10^{-6} A.cm^{-2}) v_{corr} (µm/year)	TMA	NiTi	CuNiTi
Elmex®	3.5 ±0.1, 31±1.5	1.5±0.05 , 13±0.5	2.5 ±0.2, 22±1
Meridol®	8 ±0.3, 72±3	8 ±0.3, 70±3	2.5 ±0.2, 22±1

Table 2 : corrosion current densities (10^{-6} A.cm^{-2}) and corrosion rates (µm/year) of the samples in dental rinses

Rp (kohm.cm²)	TMA	NiTi	CuNiTi
Elmex®	150 ±15	300 ±30	200 ±25
Meridol®	50 ±5	45 ±5	180 ±15

Table 3 : Polarization resistance (kohm.cm²) of the samples in dental rinses

In Elmex® solution (Fig.3), the obtained curves and values for the different materials were quite similar.
All the materials presented a moderated corrosion resistance.
The materials were classified according to oxidation current at -500 mV/SCE and TMA was the most degraded material. These results were confirmed by the study of Kaneko et al. in fluoride solution.

In Meridol® solution (Fig.4), similar curves were observed for TMA and NiTi. The polarization resistance values were very low and resistance to corrosion currents doubled. The corrosion rate values were also very high for these materials, suggesting a very low resistance to corrosion. For CuNiTi, the obtained values showed a moderated resistance to corrosion, like in Elmex® mouthwash.
The materials were classified according to oxidation at 500 mV/SCE and TMA was also the most degraded material.

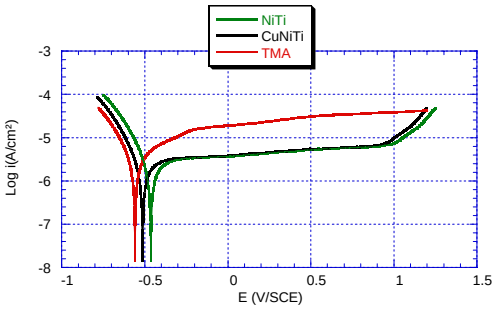

Fig. 3. Polarization curves in Elmex®solution for different materials.

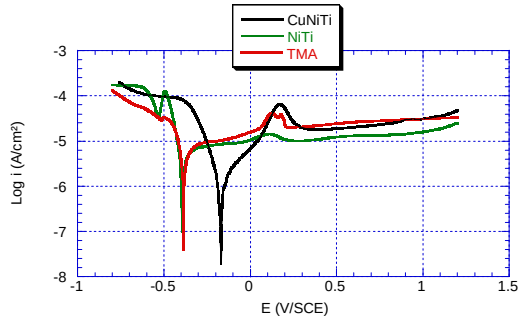

Fig. 4. Polarization curves in Meridol®solution for different materials.

While fluoride are an undeniable therapeutic asset in the prevention of dental caries, it should be recognised that they might interfere with the electrochemical properties of orthodontic wires with possible clinical repercussions : corrosion of NiTi orthodontic wire in the buccal cavity results in the release of toxic, allergy-provoking nickel ions into the organism [4]. Meridol® mouthwash was particularly aggressive for NiTi as well as for the TMA, which distinguishes it from Elmex®. Furthermore, the oxidation peaks obtained in this solution for TMA and CuNiTi alloys (Fig.4) seem to indicate that some species (additives) in the solution must be subject to oxidation reduction phenomena, thereby modifying the stability of the electrolyte, with repercussions on the corrosion of the materials.

Concerning surface analysis, specimens of NiTi in the mouthwashes were analyzed and compared: in the case of NiTi in Elmex®, the SEM photomicrograph (Fig.5) doesn't show any corrosion, in the case of NiTi in Meridol® the SEM photomicrograph (Fig.6), shows a slight localized corrosion [5].

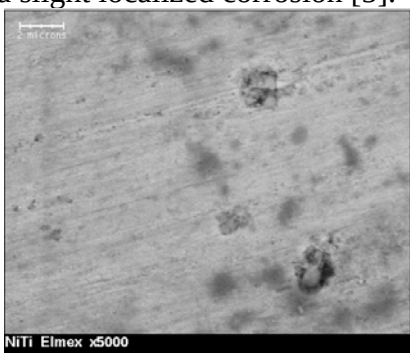

Fig. 5. SEM photomicrograph x 5000 of NiTi after oxidation in Elmex®solution

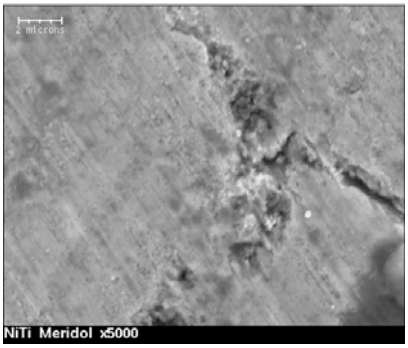

Fig. 6. SEM photomicrograph x 5000 of NiTi after oxidation in Meridol®solution

CONCLUSION: The results of this study show that Meridol®, fluorided dental rinse, can have a negative influence on the resistance to corrosion of some orthodontic wires such as NiTi and TMA.
That's why we advise the practitioners, whose patients are treated with these two materials, to prescribe Elmex® mouthwash than Meridol®.

AKNOWLEDGEMENTS:
We thank Gaba and Ormodent France for their participation in this study.

REFERENCES: [1] K. Kaneko , K. Yokoyama , K. Moriyama , K. Asaoka , J. Sakai , M. Nagumo (2003) *Delayed fracture of beta titanium wire in fluoride aqueous solutions*, Biomaterials., **24**: 2113-2120. [2] I. Watanabe , E. Watanabe (2003) *Surface changes* induced *by fluoride prophylactic agents on titanium-based orthodontic wires*, Am. J. Orthod. Dentofac .Orthop., **123**: 653-656. [3] N. Horasawa , H. Nakajima , JL. Ferracane , S. Takahashi , T. Okabe (1996) *Cyclic voltammetry of dental amagalms*, Dent. Mater., **12**: 154-160. [4] N. Staffolani , F. Damiani , C. Lilli , M. Guerra , N.J. Staffolani , S. Belcastro , P. Locci (1999) *Ion release from orthodontic appliances*, J. Dent., **27**: 449-454. [5] P. Neumann , C. Bourauel , A. Jäger (2002) *Corrosion and permanent fracture resistance of coated and conventional orthodontic wires*, J. Mater. Sci: Mater. Med., **13**: 141-147.

European Cells and Materials Vol. 9. Suppl. 1, 2005 (pages 48-49) ISSN 1473-2262

Synchrotron and non synchrotron X-ray microtomography three-dimensional representation of bone ingrowth in calcium phosphate biomaterials.

P Weiss[1], D Le Nihouannen[1], C Rau[2], P Pilet[1,3], E Aguado[4], O Gauthier[4], A Jean[1] and G Daculsi[1].

[1] *Laboratoire de Recherche sur les Matériaux d'Intérêt Biologique INSERM 99-03, Faculté de Chirurgie Dentaire, 1 place Alexis Ricordeau, 44042 Nantes Cedex 01, France*

[2] *European Synchrotron Research Facility (ESRF), BP 220, 38043 Grenoble cedex, France*

[3] Centre Régional de microscopie, Faculté de Chirurgie Dentaire, 1 place Alexis Ricordeau, 44042 Nantes Cedex 01, France.

4 Service de chirurgie, Ecole Nationale vétérinaire de Nantes, Route de Gachet, Nantes

INTRODUCTION: Numerous types of bone and dental surgery require bone substitutes. In recent years, our group has developed a new type of Injectable Bone Substitute (IBS), consisting of a mixture of BCP ceramic granules and a cellulosic polymer derivative. The resulting composite provides a sterile, ready-to-use, injectable material. Injectable CaP biomaterials should associate efficient bone colonization and implantation with non-invasive surgical techniques.

Typically the spatial resolution of conventional medical CT-scanners is in the range of 1-2.5 mm, which corresponds to 1-10 cubic mm voxel (volume element) size. Computerized X-Ray Micro Tomography gives possibilities to improve the spatial resolution by mm to µm. The purpose of the present study was to compare the 3-dimensional (3D) representation of bone ingrowth after implantation of injectable bone substitute suspension implanted in a rabbit model, using Synchrotron X-Ray Micro Tomography (SµT) and Laboratory Desktop Micro Tomography (LDµT). 2D imaging performed with Scanning Electron Microscopy (SEM) is used as the reference method.

METHODS: Injectable bone substitute (IBS): A CaP aqueous suspension was developed to obtain an injectable biomaterial associating a biphasic CaP ceramic mineral phase (MBCP®, Biomatlante, Vigneux, France) sieved in two different ranges (BCP granules 40 to 80, or 80 to 200 µm in diameter) with a 3% aqueous solution of a cellulosic polymer (hydroxypropyl-methylcelullose) in a 50/50 (w/w) ratio. The CaP fillers used were composed of BCP ceramic (60% HA and 40% β-tricalcium phosphate). The IBS was sterile, ready-to-use and injectable (CNRS Patent WO 95/21634; (MBCP Gel®)Biomatlante, Vigneux, France).

In vivo study: These materials were implanted for 3 weeks into critical-sized bone defects at the distal end of rabbit femura. Implantations were performed on New Zealand white rabbits, as detailed in previous studies, in aseptic conditions and under general anesthesia. The samples were embedded in methylmethacrylate with glycol. For each sample, rods (0.6 mm x 0.6 mm x 10 mm) were cut perpendicularly to the drilling axis of the implantation site, using an Isomet™ diamond saw (Buehler LTD, Germany).

Synchrotron X-Ray Micro Tomography (SµT): The experiment was carried out at the European Synchrotron Radiation Facility (ESRF) [1] at the Micro-Fluorescence, Imaging and Diffraction beamline ID22. The sample was set at a distance of 65 m from the undulator source with a horizontal rotation axis. The distance between the sample and the detector was 8 mm. In the CCD-based high-resolution X-ray image detectors commonly used in microtomography, a visible-light image is generated by a fluorescent screen and then projected by a microscope optic onto a CCD camera. The shadow projections of the object were recorded with a high-resolution CCD-based camera system. The scintillator was a lutetium aluminum garnet (LAG) single crystal with a 12 µm-thick europium-doped luminescent layer. An optical microscope (magnification: x 10) projected the scintillation-light image onto a 2,048-by-2,048-pixel CCD camera with a 14-bit real dynamic range. For this configuration, the effective pixel size was 1.4 µm which corresponds to the resolution of the chosen scintillation screen. After darkfield correction and flatfield normalization of the projections, the tomograms were reconstructed using the filtered backprojection technique. 3D histomorphometric analysis was performed in voxels with Imaris™ (Bitplane AG, Zurich, Switzerland) software.

Laboratory Desktop Micro Tomography (LDµT): We use a compact desktop system (SkyScan-1072) with a laboratory X-Ray source. It consists of the

combination of an x-ray shadow microscopic system and a computer with tomographic reconstruction software.
The system "SkyScan 1072" allows reaching a spatial resolution of 5 µm corresponding to near $1x10^{-7}$ cubic mm voxel size.
The X-ray shadow projections digitized as 1024x1024 pixels with 4096 brightness gradations (12 bit) for cooled camera or 256 gradations (8 bit) for analog camera. The reconstructed cross-sections have a 1024x1024 (or 2048x2048, 512x512, 256x256…) pixels (float point) format. Typical cycle of data collection for reconstruction contains of shadow image acquisitions from 200 to 400 views over 180 or 360 degrees of object rotation.

Table 1. Experimental characteristics for the both methods of this study

	(SµT)	**(LDµT)**
Source size	Beam 800X30µm	Cone from 5µm to 22 mm
Camera CCD	2048X2048	1024 X 1024
Pixel size	0.7	1.8 µm
Resolution	1.4µm	5µm
exposure time	0.5 s	6.5 s
angular range	180 °	360 °
Projections	625	400

RESULTS:

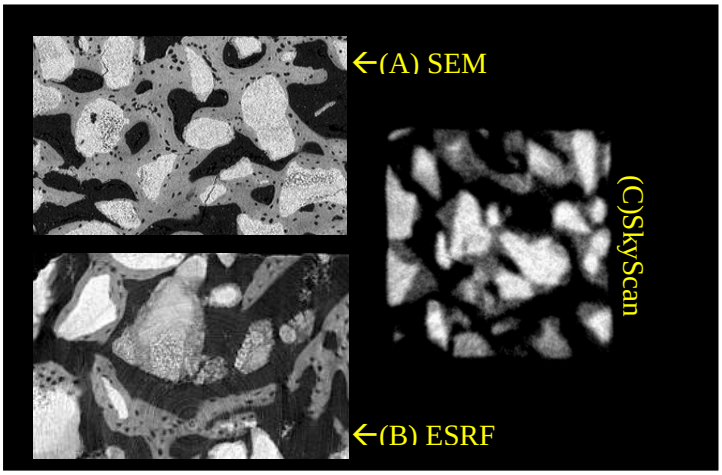

Fig. 1: Scanning electron microscopy (SEM, X 50) picture (A), synchrotron (B) and Skyscan (C) tomography reconstruction of bone ingrowth with IBS

The results show and can differentiate the mineral structures like bone and BCP ceramic with all the techniques used (Fig. 1). The SEM picture and the ESRF reconstructions are similar with the presence of osteocytic *lacunae* (osteoplasts). The desktop system (SkyScan-1072) don't show this small structure and the limits of the mineral contours are less accurate (blurred).
The 3 Dimensional (3D) representations of both implanted biomaterials (Fig. 2) are similar with the same representation of the 3 D structures, BCP ceramics (white), Trabecular Bone (grey), and soft tissue (black) with the two µscan methods.

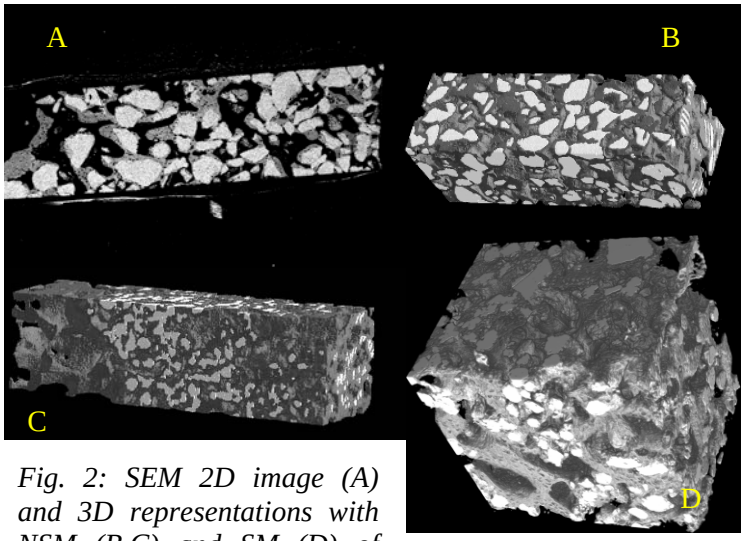

Fig. 2: SEM 2D image (A) and 3D representations with NSM (B,C) and SM (D) of bone ingrowth with IBS with BCP granules 80 to 200 µm (A,B) or 40 to 80 µm (CD) in diameter

DISCUSSION & CONCLUSIONS:

These systems allow making a non-destructive three-dimensional reconstruction of bone ingrowth within an injectable bone substitute with the same information on the structure. SM method allows visualisation of small structure getting near the µm, osteons, osteocytic *lacunae* but it's less easy to use than a compact desktop system. The NSM method shows good 3D results but the quantification of 2 mineral phases has to be improved because of the delimitation between these different grey levels (Fig. 1C)
This study shows the advantage and the limits of each technique for the qualitative representation and quantitative measurement of the different mineral phases into calcium phosphate implants.

REFERENCES: [1] P. Weiss, L. Obadia, D. Magne et al. (2003) Synchrotron X-ray microtomography (on a micron scale) provides three-dimensional imaging representation of bone ingrowth in calcium phosphate biomaterials, *Biomaterials*, **24**: 4591-601.

European Cells and Materials Vol. 9. Suppl. 1, 2005 (pages 50-51) ISSN 1473-2262

Comparison of the Knoop microhardness of various composite materials according to 3 types of luminous irradiation

E. Castany[1], J-C Chazel[1], F.Duret[1] & B. Pelissier[1]
[1] *UFR d'Odontologie de Montpellier I*
545, Avenue du Professeur Jean-Louis Viala. 34193 Montpellier, France

INTRODUCTION: Lamps LED of 1st generation had a power seldom exceeding 250mW and were to use many LED; the 2nd generation of LED uses only one LED in general and is higher than 500mW. It seemed to us interesting to analyze and compare polymerization (Tests on the surface and in-depth to 2 mm) several composite materials of restoration of various colours and viscosities by using 3 types of luminous irradiation.

MATERIEL AND METHODS: Samples (Fig. 1) in the form of pastilles of 5mm of diameter and 2mm thickness of various composites of the Dentsply Detrey company, of colours A2 and A4 and different viscosities were insolated with 3 types or modes of luminous irradiation during 10 seconds. Measurements of immediate microhardness were taken surfaces some and in-depth with a microdurometer Leica VMHT 30 with a load of 500 mW during 10 seconds at various points according to the diameter of the sample (9 points of measurement every 500 microns); 5 pastilles were carried out for each material, each colour and each lamp used.

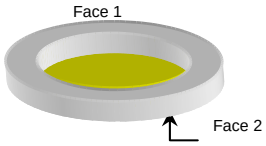

Fig 1: sample : pastille of 5mm of diameter and 2mm thickness of various composites.
Face 1 : measurement in-surface Knoop microhardness
Face 2 : measurement in-depth Knoop microhardness

Lamps used :
- a plasma lamp (A) Apolo 95E®, job number : A.601.500, of average power: 1256 mW/cm2 (diameter of tip: 7.5 mm) (Fig.2) ;
- a halogenous lamp (H): Demetron 501®, job number: 53101533, of average power: 443 mW/cm2 (diameter of tip: 11.1 mm) (Fig.3) ;
- a lamp L.E.D. (L.E.D.) : MiniL.E.D.®, job number: ML-B1.3-330-2444, of average power: 1331 mW/cm2 (diameter of tip: 7.5 mm) (Fig.4).

Fig 2: A plasma lamp Apolo 95E®

Fig 3: A Halogen lamp Demetron 501®

Fig 4: A lamp L.E.D MiniLED®

Composites used :
THP spectrum® A2, number of batch: 0301281 (scratch date: 01/2006); THP spectrum® A4, number of batch: 0203203 (scratch date: 03/2005); Dyract AP®A2, number of batch: 0305000286 (scratch date: 03/2005); Dyract AP® A4, number of batch: 03030002625 (scratch date: 03/2005); Dyract flow® A2, number of batch: 030801 (scratch date: 05/2007); Dyract flow® A4, number of batch: 030306 (scratch date: 02/2005); Esthet X® A2, number of batch: 0306247 (scratch date: 06/2006); Esthet X® A4, number of batch: 030118 (scratch date: 01/2006); Esthet X® flow A2, number of batch: 030821 (scratch date: 08/2006); Esthet X® flow A2, number of batch: 030122 (scratch date: 01/2006).

RESULTS & CONCLUSION: The averages of measurements of hardness show significant differences between the 3 types of lamps according to the composite used, its colour, its viscosity and the analyzed side. With the MiniLED® lamp, we obtain the best results surfaces some except for Dyract flow" where this lamp is preceded by the halogenous lamp

Demetron 501® and the lamp plasma Apollo 95E® (Fig.5).
In-depth, for the composites with low viscosity, the order is as follows: MiniLED® > Demetron® > Apollo 95E® (Fig.6).
For the composites with strong viscosity, the order is different: Apollo 95E® > MiniLED® > Demetron®. The differences obtained can be explained by the composition of the various composites materials studied but also by the irradiations of different light intensities according to lamps used in this study and being able to release from heat, which is not the case for lamps LED of 2nd generation.

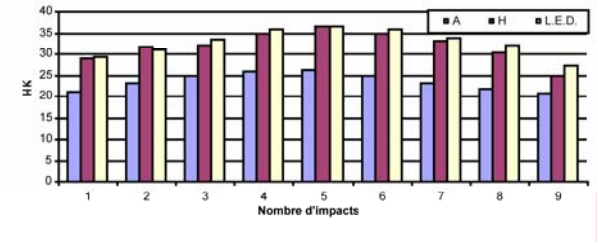

Fig 5: In-surface Knoop microhardness of THP spectrum® A2 Dentsply

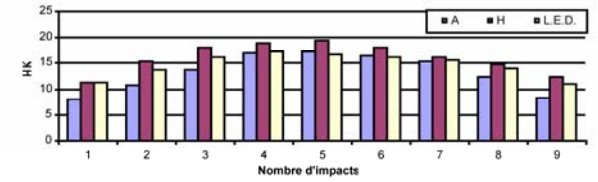

Fig 6: In-surface Knoop microhardness of Diract Flow® A2 Dentsply

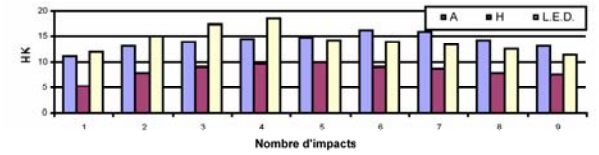

Fig 7: In-depth Knoop microhardness of Esthet X® flow A4 Dentsply

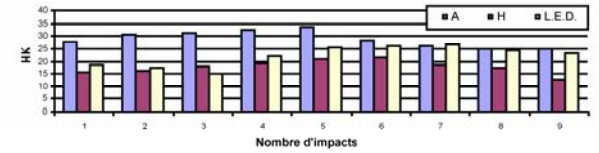

Fig 8: In-depth Knoop microhardness of Esthet X® A4 Dentsply

REFERENCES :

[1] J-L. Ferracane (1985) *Correlation betwween hardness and degree of conversion during the setting reaction of unfilled dental restorative resins.* J. Dent. Res. 1:11-14.

[2] F. Stahl, SH. Ashworth, D. Jandt, RW. Milis (2000) *Light-emitting diode (LED) polymerisation of dental composites : flexural properties and polymerisation potential.* Biomater. 21:1379-1385.

[3] B. Pelissier, J-C. Chazel, E. Castany, F. Duret, (2003) *Lampes à photopolymériser.* Encycl. Méd. Chir. Stomat./Odont. 22-020-A-05: 11p

[4] D. Dietschi, N. Marret, I. Krejci (2003) *Comparative deffinciency of plasma and halogen light sources on composite microhardness in different curing conditions.* Dental Materials, 19 : 493-500

European Cells and Materials Vol. 9. Suppl. 1, 2005 (pages 52-53) ISSN 1473-2262

Effect of four dentin desensitizer on the shear bond strength of three bonding systems.

N Lehmann *, M Degrange *
* *Unité De Recherche Biomatériaux et Interfaces.*
Faculté de Chirurgie Dentaire, 1 Rue Maurice Arnoux, 92000 MONTROUGE
Université Renée Descartes, Paris 5, France.

INTRODUCTION: Dentin sensitivity is a common problem that affects between 10 and 20 % of population [1]. Various theories have explained the mechanism of dentin sensitivity. Currently, the hydrodynamic theory is widely accepted. It is a displacement of tubular contents such as fluids that might produce a deformation of nerve fibers wrapped around the odontoblast cells [2].Thus, products that occlude dentin tubules to any extent can significantly reduce fluid filtration across the dentin and lover by this way the pain [3].

Among dentist-applied treatments, topical methods are widely used because they are convenient and have an immediate effect. Applying desensitizer solutions and dentifrices containing ferric, aluminium and potassium oxalates is the first treatment of choice [3]. Nevertheless their effect is not permanent. The durability of these topical treatments is influenced by several factors. The most common problem is the dissolution of the desensitizer material by saliva and oral fluids [3, 4].

To obtain a long-lasting effect, adhesive restorative procedures can be used when a desensitizer treatment has failed[5]. Pashley demonstrated that sealing dentinal tubules with polymeric resins reduces sensitivity. However, there is concern regarding the effect of pretreatment with a desensitizer on the bond strength between dentin and resin composite [6].

The aim of this study was to assess the influence of a dentin pre-treatment with 4 desensitizer agents on the shear bond strength of 3 dentin bonding systems (DBSs).

METHODS: The materials used in this study are listed in table 1.

Tooth preparation

For this study 150 non carious human third molars were used within two months after extraction. The teeth were stored in 1 % chloramine T solution at 4°C.

The occlusal enamel was removed with #80 SiC under water. The teeth were embedded in an acrylic resin. After polymerisation, dentin surfaces were ground with #400 SiC and hand finished using a wet #800 SiC paper for 30 seconds to create a standardized smear layer. The teeth were then stored in distilled water before testing.

Bonding procedures

Teeth were randomly assigned to one of fifteen experimental groups (n=10).

Each desensitizing agent was coupled with each dentin bonding system. In three reference batches, the three DBS were directly applied on untreated dentin.

Both desensitizing agents and DBSs were used according to manufacturers instructions.

After the application of the DBS, a 3x5 mm composite cylinder (Z100) was bonded to all surfaces in two increments; each increment was light-cured for 40 seconds. The teeth were then stored in distilled water at 37 °C for 24 hours before testing.

Methods

The shear bond strengths were measured using an universal tensile machine (T30K, Lyod Instruments) at a crosshead speed of 0.5 mm/min.

An statistical analysis was carried out using Statview 5 (SAS Institute Inc; Cary, North Carolina, USA), subjecting the data to analysis of variance (ANOVA 2). Post hoc multiple comparisons were done using PLSD Fisher test , at the level $p \leq 0,05$.

Product	Manufacturer	Batch No.
MS Coat	Sun Medical	80845(Liq A) 80743(Liq B)
Viva Sens	Ivoclar Vivadent	F09832
Tubulicid	DentalTherapeutics AB	3103031132
Gluma	Heraeus Kulzer	040053
Optibond FL	Kerr	212652 (primer)
		301335 (bonding)
Clearfil SE Bond	Kurraray – Dexter	80543 (pimer)
Xeno III		80321 (bonding)
	Dentsply	0210000032 (liquid A)
Z100		0210000032 (liquid B)
	3M-ESPE	564321

Table 1: Materials used in this study.

RESULTS: The shear bond strength values to dentin are presented in figure 1.

The application of Gluma desensitizer significantly affected the shear bond strength (SBS) of both Optibond FL ($p<0,0001$) and Xeno 3 ($p=0,0009$).

MS Coat significantly decreased the SBS of Xeno 3 ($p<0,0001$).
The SBS of Clearfil SE Bond was not affected whatever the desensitizing pretreatment.
Tubulicid and Viva Sens do not alter the adherence of both Optibond FL, Clearfil SE Bond and Xeno 3.

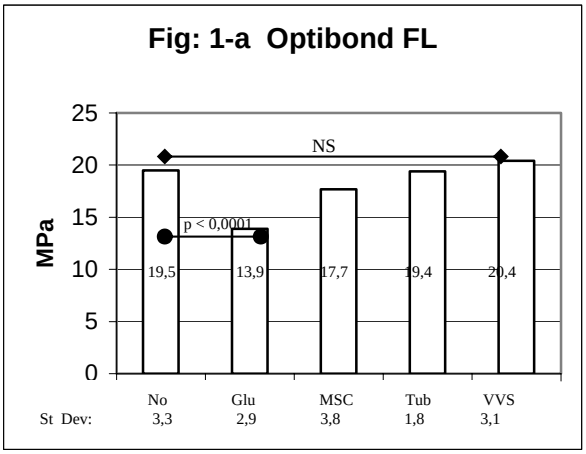

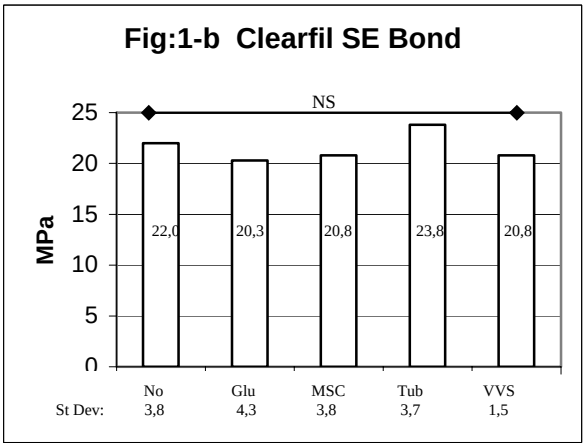

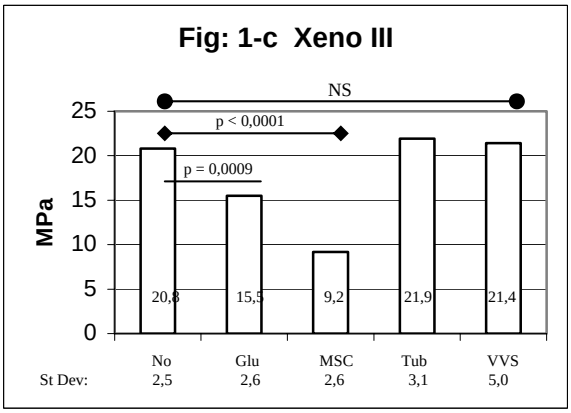

Shear bond strength values of Optibond FL (fig.1-a), Clearfil SE Bond (fig.1-b), Xeno III (fig. 1-c).

Legend: no: control; Glu: Gluma desensitizer; MSC: MS Coat; Tub: Tubulicid; VVS: Viva Sens.

DISCUSSION & CONCLUSIONS: The desensitizing pre-treatment used are classified into three types: MS Coat and Viva Sens materials are based on a hydrophilic polymer emulsion; Gluma desensitizer contains glutaraldehyde that reacts with proteins producing precipitation on the dentin surface. Tubulicid is based on calcium fluoride crystals formation on the dentin surface. The DBSs involved in this study belong to three different classes of adhesives: one 3-step etch and rinse system (Optibond FL), one 2-step self etching system (Clearfil SE Bond), and one 1-step "all-in one" system (Xeno III).
The results of this study show that DBS with phosphoric acid etching sustained rinsing is not the more compatible DBS with the overall pretreatments. The dentin superficial etching and the rinsing can restore the original chemical properties and the original morphology of the dentin surface. The organic pretreatments (Gluma, MS Coat) affected widely the dentin surface. The minimal effects of the Viva Sens on the DBS remain unclear because its principle and composition are similar to MS Coat.
Within the limits of the present data, in no case were Tubulicid and Viva Sens desensitizers agent observed to decrease SBS of the three DBS.
In the present study, Clearfil SE Bond is not affected by the different desensitizing agents. This reaction may explained by its chemical composition, in particular with MDP groupment contains.

REFERENCES: [1]Hefti AF, Stone C (2000) Power tooth brushes, gender and dentin hypersensitivity, *Clin Oral Invest* **4**: 91-97. [2]Brännström M, Aström A (1964) A study on the mechanism of pain elicited from the dentin, *J Dent Res* 1964; **43**: 219-227. [3]Jain P, Vargas MA, Denehy GE, Boyer DB (1997) Dentin desensitizing agents: SEM and X-ray microanalysis assessement, *Am J Dent* **10**: 21-26. [3] Pashley DH, Carvalho RM, Pereira JC, Villanueva R, Tay FR (2001), The use of oxalate to reduce dentin permeability under adhesive restorations, *Am J Dent* **14**: 89-94. [4] Ciucchi B, Bouillaguet S, Holz J, Pashley DH (1995), Dentinal fluid dynamics in human teeth in vivo, *J Endod* **21**: 191-194. [5] Mausner IK, Goldstein GR, Georgescu M (1996). Effect of two dentinal desensitizing agents on retention of complete cast coping using for cements, *J Prosth Dent* **75**: 129-134. [6] Pashley EL (1992). Denti permeability: Sealing the dentin in crown preparations, *Op Dent* **17**: 13-20.

European Cells and Materials Vol. 9. Suppl. 1, 2005 (pages 54-55) ISSN 1473-2262

Modeling of Titanium Melting by Finite Elements Analysis and Stress Evaluation by Neutron Diffraction

I. Lopez[1], P. Millet[1], P. Fogarassy[1], A. Lodini[1,2]
[1]LACM EA3304, Université de Reims Champagne-Ardenne URCA, FR
[2]Laboratoire Léon Brillouin, CEA-Saclay, 91191 Gif sur Yvette Cedex, France

INTRODUCTION: Commercially pure Titanium is, among other metals and alloys such as nickel-chromium or cobalt-chromium alloys, the most biocompatible metal. However, casting this alloy is particularly difficult for dental laboratories because expensive casting machines should be used, sometime with uncertain quality results. The centrifugation casting technique is of special interest if high enough centrifugal acceleration can be reached. In order to analyse the influence of different parameters, a finite elements analysis was performed, using Viewcast and MSC/NASTRAN. The standard sample (model MBS) usually employed to quantify the flow of alloys was used for analysis. The time of titanium solidification, under different condition (the temperature, the viscosity of material, the size and the shape of the sample and centrifugation acceleration) was analysed. Then we intend to evaluate by neutron diffraction the level of residual stress in titanium cast samples in order to validate this simulation experimentally.

METHODS: A numerical simulation casting model has been developed, using finite element analysis with the commercial software ViewCast in order to visualize the mould filling and solidification during the castings process. We observed the mould filling sequence and the subsequent solidification, as well as the locations where shrinkage porosities may occur. This simulation process is based on several steps meaning : the CAD (geometry of the part to be cast – Figure 1); fine or medium meshing; rheological data pure titanium; process conditions and process data definition.

All simulation was realized with progressive increase of centrifugal acceleration. The solidification time of titanium was analysed under different conditions such as the temperature and the viscosity (stop flow time).

In this paper, the residual stress introduced during the casting process is evaluated using a finite element analysis model and the validation is performed by neutron diffraction technique.

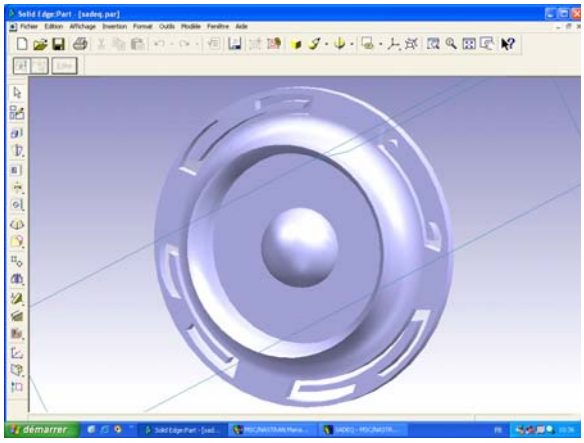

Figure 1 MBS geometry

In order to evaluate the residual stress, the thermal gradient in the analysed part should be calculated; this results from the instantaneous temperature distribution for a certain moment during the solidification.

The temperature field evolution results from complex phenomena interactions of the melted alloy flowing through the mould, accompanied by conduction and convection heat transfer to the mould walls. The resulting thermal field distribution was exported to FEMAP and the residual stress analysis was performed with MSC/NASTRAN. For the Residual stress evaluation by neutron diffraction: The samples were cast with the ERSCEM centrifugation machine.

The methodology used is the evaluation of residual stress by neutron diffraction in order to show the quality of cast samples. The conditions of measurements were: wavelength, $\lambda = 0.332$ nm; Ti {101}, $a = 0.295$ nm, $c = 0.4686$ nm and $2\theta = 95.85°$. Using the {101} diffraction peak of titanium sample, the state of

deformations and stress are obtained across the component, as can be seen from geometrical configuration of measurements.

RESULTS: By increasing the centrifugation (1G to 100G), the mould filling time was reduced considerably. For the Stop Flow Time, the results obtained in term of time of solidification with this new parameter are similar with previous parameter.

Table 1: Simulation according to the length of the cone of cast:

Model MBS	Without cone	Cone 5 mm	Cone 10 mm
Solidification time (s)	13	15	17

Figure 2 shows the localization of the sensitive areas (where the maximal shrinkage occurs), which means that the defects will be concentrated in the thickest areas (central thickening and casting stem) as well as in the entrance of a zone with a brutal contracting of the casting path.

Increases the centrifugation speed could also increases some defects risk.

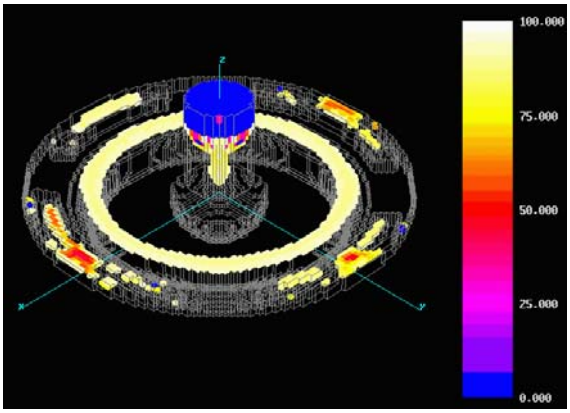

Figure 2 X-ray view of shrinkage.

The uneven cooling of the solidified titanium part, from different temperatures, down to room temperature (300 K) introduces residual stress in both radial (r) and tangential (θ) direction; the residual stress in axial direction (z) is negligible. The residual stresses in radial direction are mainly compressive, while in tangential direction residual stresses are mainly tensile.

The {101} peaks from titanium sample cast by centrifugation (ERSCEM) are Gaussian peaks. It appears that cristallinity of the samples studied is not textured and that the crystal grains are fine as expected for a dental material. The measured residual stresses are relatively low, ranging from about -120 to 80 MPa. The finite analysis (FEA) results are in very good agreement with measurements results being between -120 and 120 MPa.

DISCUSSION & CONCLUSIONS: The main purpose of this simulation was to analyze the model MBS filling of titanium in order to compare with that of conventional centrifugal casting. The finite elements simulation predict with this process a good cast since all the parts of the mould are filled correctly. The ViewCast software allowed locating the zones where shrinkage is most significant. High centrifugal force in the casting results in a high hydrostatic pressure in the molten titanium, improving the filling of fine detail of the casting (Suzuki *et al*., 1996). However, high centrifugal force could induce defects in the sample.

The numerical simulation was experimentally validated, predicted residual stress level being close to the experimental measurements.

REFERENCES: [1]P.T. Wieder (2000) On the strain-free lattice constants in residual stress evaluation by diffraction, *Journal of structural Geology,* **22**:1601-1607. [2]J.Lu (1996) *Handbook of Measurement of residual Stresses,* [Society for Experimental Mechanics, The Fairmont Press, Inc., Lilburn]. [3]G.S Schajer (1981) Application of Finite Element Calculations to Residual stress Measurements, *Journal of Enineering Materials and Technology,* **103**:157-163. [4]J.M Meyer, C Susz, L Reclaru (2002) Le point sur les alliages en 2002. In : *Journées du Collège Français de Biomatériaux* (19 ; Lille):7-36

ACKNOWLEDGEMENT: This paper has been carried out with financial support from the Commission of the European Communities, specific RTD programme "Competitive and Sustainable Growth", DENTICAST, Contract N° G1ST-CT-2002-50223. It does not necessarily reflect its views and in no way anticipates the Commission's future policy in this area.

European Cells and Materials Vol. 9. Suppl. 1, 2005 (pages 56-57) ISSN 1473-2262

Effets des différents conditionnements de surface sur l'adhésion du tenon Light-Post®

N Cheleux [1], M Degrange [2] & P. Sharrock[3]

[1] *Faculté de Chirurgie Dentaire, Toulouse, Fr*

[2] *Recherche biomatériaux et interfaces, Paris V, Fr*

[3] *Laboratoire de chimie bio-inorganique Médicale, UPS, Toulouse, Fr.*

INTRODUCTION: An alternative non metallic post and core have been introduced into dentistry. Quartz fiber posts are widely used and are intented to be adhesively luted into the root canal. This clinical act is part of the endodontic continuum, and allows for better stability and retention of the coronary restoration. This preserves longer lifetimes for natural teeth. Quartz fiber posts present favourable mechanical properties for strain shielding. Bonding to root dentin is delicate, but the weakest adhesion is found at the post-adhesive interface [1]. The aim of our study is to improve the adhesion strength by modifying the surfaces with various physico chemical treatments.

METHODS: The n°2 radio-opaque Light-post® (RTD, France) is composed of 60 % quartz fibres and 40% epoxy resin (in volume). 8 groups of 10 posts were made according to the selected surface treatment : G1 (control) : post(po) ; G2 : po + Prime&BondNT/SelfCureActivator (adh) ; G3 : po + chloroform 15sec + adh ; G4 : po + chloroform 1h + adh ; G5 : po + silane (sil) ; G6 : po + sandblasting (sand) ; G7 : po + sand + adh ; G8 : po + sand + sil + adh. Posts were cleaned in 70% ethanol and air dried. 50µ alumina particles were used for sandblasting. The post was dipped into chloroform either for 15 sec or for one hour and then wipped during one minute with a chloroform impregnated cloth. The silane and adhesive are used according to the supplier's guidelines (Dentsply). Filling material is Lumiglass® (RTD), a photopolymerized microhybrid composite. A Spectrum 800® lamp (Dentsply) is used for composite photopolymerization (40 sec at 600 mW/ cm²). Push-out tests were carried out with a specific teflon experimental model. 6 mm high and 9 mm wide cylindrical specimens were obtained (Fig.1). The push-out tests are realized with an MTS instrument equipped with Test Works software at a crosshead speed of 1mm/min and using a 5KN gage. The force required for extrusion was recorded throughout for each specimen, and the push-out strength (σ) was calculated using the following formula :

$$\sigma = F/\pi TD$$

where F=force, T=thickness of the specimen and D=diameter of the post. Mean push-out strength and standard deviation were calculated for each group. One way analysis of variance (ANOVA) was computed to determine statistically significant differences at 5%. Multiple paired comparisons by Fisher's protected least difference (PLSD) test were used to identify differences between pairs of groups.

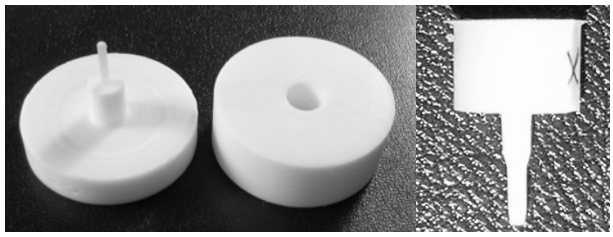

Fig. 1: Moule en téflon avec le tenon positionné (left) échantillon prêt pour le test (right).

RESULTS: Statistical analysis reveals significant differences between groups. The use of adhesive improves shear strength independently of the surface structure (G2vsG1 ; G7vsG6). Silane improve bonding in anycase. (G5vsG1 ; G8 vsG7). There is non difference between action of chloroform and sandblasting (G4=G7). The best values are obtained by combining sandblasting with silane treatment and adhesive (G8).

Table 1. Push-out strenght. The same letters indicate mean values with no significant differences.

Group (n=10)	Mean ± Standard deviation (MPa)	Coefficient of variation (%)
G1	18,5 ± 2,0 e	10,7
G2	23,5 ± 2,6 d	11,2
G3	23,2 ± 2,2 d	9,3
G4	28,5 ± 2,3 b	7,9

G5	23,7 ± 1,2 cd	5,1
G6	25,6 ± 2,8 c	10,8
G7	28,6 ± 1,9 b	6,8
G8	34,4 ± 2,3 a	6,6

DISCUSSION & CONCLUSIONS: Push-out tests are frequently used to evaluate the shear strength of adhesive-post assemblies [2]. The small standard deviations obtained for each group shows our experimental model is reliable and reproducible. Use of adhesive alone (G2) increases adhesion values by 27% with respect to the reference (G1). Similar results were previously published [3]. Chloroform is an organic solvent which can superficially dissolve the organic matrix of the post. A one hour dissolution time is required to observe a signification effect on the adhesion value. Shorter immersion times in chloroform do not seem to improve the surface for adhesion. Sandblasting with alumina micro crystals is a widespread physical treatment which cleans surfaces and creates surface roughness by plastic deformation and abrasion. Sandblasting (G6) results in a 38% increase in adhesion with respect to reference. Yet the highest adhesion values are observed in group 8 posts which combine the mostly physical effect of sandblasting with the chemical effect of the silane treatment. Silanes couple the adhesive and the post by bonding with specific functional groups both to the glass fibers and to the adhesive polymer. Similar results were very recently presented [4]. Post function would greatly benefit from specific surface preparations.

REFERENCES: [1] D. Dietschi, M. Romelli, A. Goretti (1997) *Int J Prosthodont* **10**(6) : 498-507. [2] L. Boschian Pest, G. Cavalli, P. Bertani, M.Gagliani (2002) *Dent Mater* **18** : 596-602. [3] S.O Hedlund, N.G Johansson, G. Sjögren (2003) *Brit Dent J* **195** : 155-158. [4] A. Sahafi, A. Peutzfeldt, E. Asmussen, K. Gotfredsen (2004) *Oper Dent* **29**(1) : 60-68.

ACKNOWLEDGEMENTS: we are pleased to thank RTD and Dentsply for material support.

European Cells and Materials Vol. 9. Suppl. 1, 2005 (pages 58-59) ISSN 1473-2262

Evaluation of microleakage at the CEJ of Class V cavities restored with four different adhesive systems

M. Bolla [(1)], E. Baltcheva [(2)], D. Fortin [(2)], P. Rompre [(2)], A. St-George [(2)]

[1] *Faculté de chirurgie dentaire, Université de Nice Sophia-Antipolis, France*

[2] *Faculté de médecine dentaire, Université de Montréal, Québec*

INTRODUCTION: Today, people get to keep their teeth longer because they have a better hygiene and the population is aging. On the other hand, teeth are exposed to a greater risk to develop sever cavities, such as Class V. In Class V cavities, half of the restoration covers enamel and the other half covers dentin [1]. Enamel possesses an important quantity of hydroxyapatite and its organic tissue is in smaller proportions. Acid etching eliminates about 10 µm of superficial enamel, leaving a rough surface with high surface energy [2]. Dentin is made of two different substrates: the intertubular dentin, which is not very mineralized, and the peritubular dentin, which is very mineralized. The presence of water in dentin decreases the surface energy and prevents adhesive agents from establishing a good mechanical retention[3]. Therefore, microleakage becomes a part of a Class V restoration. This in vitro study evaluated the microleakage of four different dentin-bonding systems, by quantifying the dye penetration at the tooth-restoration interface.

METHODS: Forty (40) human freshly extracted molars were selected for this study. Thirteen extra teeth were also prepared. The teeth were stored in 0,1 % thymol solution diluted in 0,4% saline. Class V cavities were prepared at the CEJ on the lingual and buccal surface of each toot. Dimensions of each preparation are 4 mm mesiodistal, 2 mm occlusal gingival measurement:, axial depth: 1,5 to 2 mm, with 90º cavosurface angles. The cavities were prepared using diamond burrs in a high-speed water-cooled hand piece. A bevel was made on the enamel part of each cavity, using a flame burr. The specimens were divided in four groups of 10 teeth each, according to the adhesive system used to restore the cavity.

Group 1: 3M Single Bond
Group 2: EXM-618 Self-etch adhesive 3M
Group 3: OptiBond Solo Plus (OBSP) Kerr
Group 4: OptiBond Solo Plus Self-etch primer

All the adhesives were used according to the recommendations of the manufacturers. All the preparations were restored with the resin composite Filtek A 110/ (3M) in one increment and the composite was light cured for 40 s. The restorations were then polished with finishing disks (3M). The roots of all teeth were cut off and closed with sticky wax. Two layers of nail polish were applied on all external teeth surfaces, leaving a 1 mm wide varnish-free margin around the restoration. All teeth were placed in the same basket and were thermocycled for 1000 cycles in water between 5 C and 55 C for 30 s in each bath and 15 s transfer between baths. After thermocycling, all teeth were immersed in a 0,5 % basic fuchsine solution for 24 hours at room temperature. After dying, teeth were rinsed with distilled water for 10 min. Each tooth was then cut in two pieces in a mesio-distal plan, leaving the restoration intact. Then, all pieces were embedded in a cold curing epoxy resin for 2 hours at 60 C. Then the blocs of resin were left at room temperature for 6 hours to obtain complete polymerization. Finally, two bucco-lingual sections were made through each restoration with a low speed saw from Isomet Buehler. The pieces were glued on glass slides and pictures of each piece were taken. Microleakage at the enamel and dentine margins was evaluated and scored using the following scale [4]

0: No dye penetration
1: Dye penetration extended for less than or up to 1/3 of preparation depth.
2: Dye penetration greater than 1/3 of preparation depth, but not extending to the axial all.
3: Dye penetration extending to the axial wall.
4: Dye penetration past the axial wall.

The median of the four scores of each experimental teeth was taken to make statistical tests. The results were analyzed with the Kruskal-Wallis test, the Mann-Whitney U test and a multiple comparison test was done, with a 5% level of significance.

RESULTS: None of the adhesive systems tested in this study was completely resistant to microleakage at the dentine margin. However, all the tested products demonstrated perfect sealing at

the enamel margin of the restoration. Table 1 shows the results for the Mann-Whitney U test.

Table 1: Mann – Whitney U test

Group	Rank Sum	Mann -Whitney U test
3M SB EXM-618 3M	84.500 125.500	29.500
3M SB OBSP Kerr	133.000 77.000	78.000
OBSP Kerr OBSP SE	109.000 101.000	54.000
OBSP SE EXM-618 SE	64.500 145.500	90.500

The best results at dentin margins were obtained with the OptiBond Solo Plus Self-etch from Kerr (Group 4). The second best sealing was achieved with the OptiBond Solo Plus from Kerr (Group 3). The EXM-618 Self-etch adhesive/3M demonstrated the worst adhesive capacity. Indeed, this group has the highest median 1.000 and the highest median maximum 3.500. The multiple comparison test shows that there is no significant difference in the results for two adhesive systems from the same label (the two 3M show no difference in their results. The same applies for the Kerr products). However, there is a significant difference between the OBSP Self-etch Kerr and the EXM-618 Self-etch/ 3M ($P = 0.001$). Group 1 (3M Single Bond) and group 3 (OBSP Kerr) showed a considerable difference in their adhesive performance as well.

DISCUSSION & CONCLUSIONS: This study demonstrated a significant difference between bonding to enamel and to dentin. There was no microleakage on enamel margins and variable microleakage on dentin margins. This difference can be explained by the composition of these two tissues, witch is very different. Dentin is a wet tissue and contains more water than enamel and this water interferes with the adhesive particles. These ones can penetrate the dentin only if they are hydrophilic. The formation of smear layer at the surface of the dentin, after the use of burrs, blocks dentinal tubules and prevents all direct contact of any material with the dentinal substrate. The bond obtained in this situation is insufficient and fragile, with much higher possibilities for microleakage. Concerning the dentin bonding, Kerr adhesives demonstrated a much better sealing than 3M adhesive systems. The main difference between the 3M products and the Kerr adhesives is that the Kerr ones are microfilled with 0.4 micron barium glass.

In order to obtain a good seal, the adhesive monomers have to penetrate into the collagen network. After etching, if this network is dehydrated, the collagen will collapse and will impede the penetration of monomers and the formation of a good hybrid layer. This led to the observation that dentin bond strengths of certain adhesives were increased if the adhesive was applied with the “wet bonding” technique. This technique implies that the dentin surface must be moist when applying the adhesive, in order to promote the diffusion of the polymerizable monomers. After the acid etching, water fills the spaces in the collagen network. Primers must bring enough monomers to fill these spaces in the network and take water’s place. To do so, the primer is combined to a solvent, such as acetone or ethanol, which help to remove water from the collagen network[16]. 3M adhesives, used in this study, contained water, while both Kerr adhesives did not. This extra water competes with the alcohol solvent, preventing its efficient penetration through the collagen network. Because Kerr adhesives do not contain water, their primers penetrate easily and in bigger proportion in the network, providing a better seal.

REFERENCES: [1] Santini A, Plasschaert A, Mitchell S. *Marginal leakage of filled dentin adhesives used with wet and dry bonding techniques*. Am J Dent 2000; 13: 93. [2] Roulet J-F, Degrange M. *Collages et adhésion : La révolution silencieuse*. 2001, Quintessence Int.[3] Jang Kt, Chung DH, Shin D, Garcia-Godoy F. *Effect of Eccentric Load Cycling on Microleakage of Class V Flowable and Packable Composite Resin Restorations*. Oper Dent 2001; 26: 603-608. [4]Amaral, CM, Hara AT, et al. *Microleakage of hydrophilic adhesive* systems in Class V composite restorations. Am J Dent February 2001, vol. 14, no. 1.

European Cells and Materials Vol. 9. Suppl. 1, 2005 (pages 60-61) ISSN 1473-2262

A PHYSICO-CHEMISTRY STUDY OF POST-SHRINKAGE IN DENTAL RESIN

D Truffier-Boutry[1-2], S Demoustier-Champagne[2], J Devaux[2], J-J Biebuyck[2], P Larbanois[3], M Mestdagh[4], G. Leloup[1]

[1] Ecole de Médecine Dentaire et de Stomatologie, Avenue Hippocrate 15, 1200 BRUXELLES, BE
[2] Unité de Chimie et de Physique des Polymères, Place Croix du Sud 1, 1348 LOUVAIN LA NEUVE, BE
[3]N.V. Mettler-Toledo S.A., Leuvensesteenweg 384, 1932 ZAVENTEM, BE
[4] Unité de Chimie des Interfaces, Place Croix du Sud 2/18, 1348 LOUVAIN LA NEUVE, BE

INTRODUCTION: Nowadays, dental resins find increasing use by practitioners. However, photopolymerisation of such resins causes three main problems: a limited "depth of cure"[1], the appearance of long-life free radicals[2] and the shrinkage phenomenon[3]. Reactional mechanism of photocured methacrylated resins is thus investigated to understand and to reduce these problems. Dentists have to fill layer by layer cavities with dental resins in order to reduce composite shrinkage. In this part of the study, shrinkage phenomenon will be analysed theoretically and experimentally (DSC, ADSC, DMA and TMA).

In a first step during the photopolymerisation (0 to 40s), a shrinkage due to a chemical reaction (polymerisation) is observed. Between 40s and 24hrs, a post-shrinkage is still observed but with no significant chemical reaction. In this work, the second step is studied.

METHODS:

Methacrylated resin studied is composed of Bisphenol A Glycidyl diMethAcrylate (Bis-GMA from Heraeus Kulzer, Dormagen, Germany), TriEthylene Glycol diMethAcrylate (TEGDMA from Aldrich) (7:3), and of an initiator system (1% in weight of camphorquinone and tertiary amine from Aldrich) and it is light cured. Samples are photopolymerized with a visible light device "Translux Energy" manufactured by Heraeus Kulzer (Dormagen, Germany) during 40 seconds with an intensity of 900 mW/cm^2 under "the conventional mode".

Thermo Mechanical Analyzer (TMA) from Mettler-Toledo: TMA measures mechanically the coefficient of thermal expansion of samples (shrinkage or dilatation). Samples are analyzed at room temperature (below the glass transition temperature) during 15 hours to follow the shrinkage phenomenon.

Electron Scanning Resonance (ESR):

The X-band (9.4616 GHz) ESR spectra were measured at room temperature, using a JEOL JES-RE 2X spectrometer equipped with an ES-UCX2 cylindrical cavity. The microwave irradiation power (0.5 mW), the magnetic field modulation amplitude (0.5 mT) and frequency (100 KHz) were set to avoid signal saturation and were kept constant. All data treatment were performed with the JEOL "Esprit 330; 01.521 version" software(23).

Density column:

Density variations between 0 and 24h are measured in a density column from Daventest Instruments at 23°C. The density-gradient of the column is prepared by mixing potassium bromide and water to reach a density range between 1.00 and 1.41, range of photocured samples densities. To deduce the shrinkage percent from the density, a pycnometer was used to measure the density of the uncured resin.

Grindo Sonic MK5 "Industrial" from J.W. Lemmens:

Dynamic elastic modulus is measured by the technique of excitation by impulsion. Samples are photocured in a mold, which has an appropriated geometry (24cm*2cm*2cm).

Table 1: Young Modulus, density and shrinkage percent of the organic matrix with time after the photopolymerization.

time after photopolymerization (h)	Young Modulus (Gpa)	density	shrinkage (%)
0	2,22	1,203	8,02
24	3,27	1,220	9,44
48	3,31	1,222	9,67

RESULTS: A shrinkage phenomenon of about 0,3% occurs during the first 24 hours after the photocuring of a sample (Figure 1) despite the conversion degree does not change. The glass transition temperatures (Tg) are measured at 0 h

and at 24 h by DMA showing clearly that Tg increases significantly during post-polymerisation (from 55°C to 80°C) (Figure 2). Densitiy and Young Modulus increase during this period and samples become more rigid at Tambient<Tg.

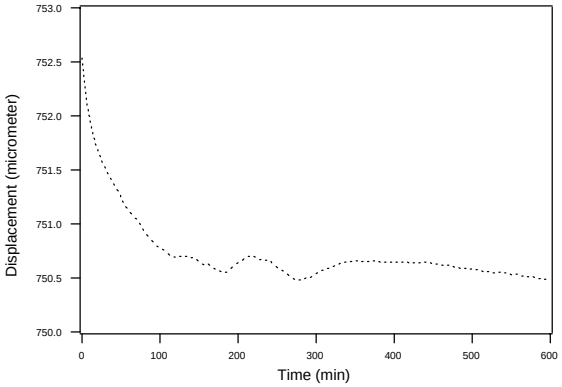

Figure 1: Post-shrinkage measurement versus Time (10 hours).

DISCUSSION & CONCLUSIONS: Post-polymerization is often attributed to a chemical phenomenon, which should occur just after the polymerization. But the DC[1] does not increase significantly after the irradiation period as the initiation step is stopped, propagation and termination step should be also hindered due to the gelation and the vitrification of the organic matrix, which behaves like a thermoset. The fact that shrinkage occurs at T<Tg proves that a physical phenomenon takes place which can, in turn, be responsible for a secondary chemical phenomenon (post-polymerization). The proposed explanation is that, as photopolymerization of dental resins is very fast, a large excess of free volume is trapped in non-equilibrated samples. As they have no time to return to an equilibrium state, free volume should decrease below Tg and samples do physically shrink during the first 24 h. As a consequence, free radicals can come into "contact" and can undergo limited propagation but significant termination justifying the decrease in overall radical concentration and the increase of samples hardness.

Many studies turn on reducing the shrinkage by influencing the initiation step with different lamps, which are based on different polymerization cycle, and the so-called soft-start system is often proposed. Such methods should allow the material to relax before vitrification, thus should decrease the second step (post-polymerisation) shrinkage at the expense of the first step one. Future studies have to be done by playing on the initiation step, which should reduce the shrinkage phenomenon.

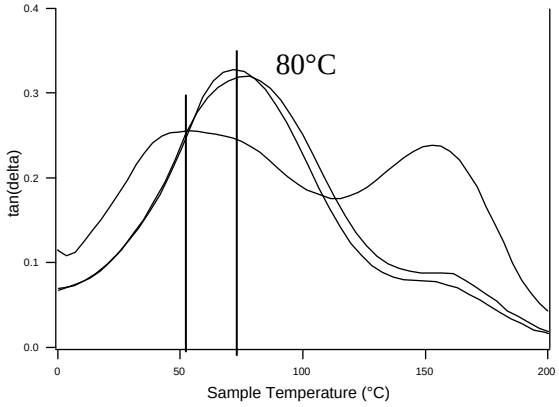

Figure 2: Tangent(δ) versus sample Temperature obtained by DMA.

REFERENCES: [1] Pianelli C., Devaux J., Bebelman S., Leloup G *J. Biomed. Mater. Res.* Ed 1999, 48, 675-681.[2] Truffier-Boutry D., Gallez X., Demoustier-Champagne S., Devaux J., Mestdagh M., Champagne B., Leloup G. *J. of Polym. Sci. : Part A.* Ed 2003, 41, 1691-1699. [3] Truffier-Boutry D., Demoustier-Champagne S., Devaux J., Biebuyck J.J., Mestdagh M., Larbanois P., Leloup G. To be submitted.

European Cells and Materials Vol. 9. Suppl. 1, 2005 (pages 62-63) ISSN 1473-2262

Electrochemical behaviour of Au-Pt based ceramo-metallic alloys in correlation with cations release, crystallographical and physical analysis

C Susz [1], L Reclaru [2], R Cerny [3], K Lacroute [2] & J Boesch [1]

[1] *Qualident, Route des Acacias 45, CH 1227 Genève*

[2] *PX Tech, Boulevard des Eplatures 46, CH 2304 La Chaux-de-Fonds*

[3] *Université de Genève, Lab. de cristallographie, Quai Ernest-Ansermet 24, CH 1211 Genève*

INTRODUCTION. The gold and platinum based ceramo-metallic alloys, developed some years ago, had a tendency to release a non negligible quantity of cations, such as Pt, Zn,…, despite their high content in precious metals (Au+Pt: 96 – 99 %, with Pt > 10 %).

The goal of this study is to establish a correlation between the measured corrosion resistance and cation release with the physical properties and crystallographic structures of the alloys.

MATERIALS & METHODS. A classical ceramo-metallic alloy, containing 77.6 % Au, 19.6 % Pt, 2.1% Zn, 0.6% Ta and 0.1 % Ir was tested in this study. All samples were cast by a standard dental technique and then annealed at 1000°C for 30min. The specific samples for corrosion, release and crystallographic measurements were annealed for 30 min at 1000°C and water quenched then heat treated for 30min at 1000°C (state a), at 670°C (state b), at 450°C (state c) and after simulation of baking of the ceramic (state d).

The corrosion potential E_c, and charge between E_c and 500 mV SCE were evaluated in Fusayama-Meyer artificial saliva at 37°C with a rotating electrode. The polarisation curves were registered from –1000 to 1000 mV SCE.
For measuring the ion release, the samples were plunged into artificial saliva at 37°C for one week. The concentrations of Au, Pt and Zn released into the solutions were then analysed by ICP-MS.
Electrical resistance and thermal expansion of the alloy were measured as a function of temperature at a rate of 8 °C/min. The ageing curves of samples homogenised at 1000 °C for 30mn were obtained by heat treatments for 30 min at temperature from 250 to 1000°C. The crystallographic study was performed with an Bruker D8 X-ray diffractometer using the CuKα_1 radiation.

RESULTS. The measurements of electrical resistance and of the mean coefficient of thermal expansion (Fig. 1) show that this alloy undergoes important structural changes upon heating. Fig.1 suggests three distinct stability regimes: (i) below 500°C, (ii) between 500 and 800 °C, and (iii) above 800 °C. The ageing curves in function of the ageing temperature (Fig. 2) are in agreement with the above observations.

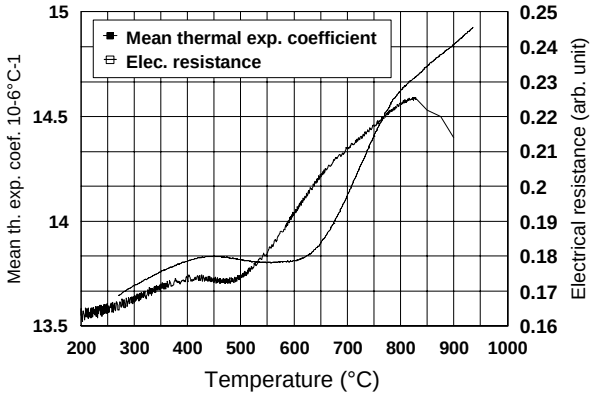

Fig.1 Electrical resistance and mean thermal expansion coefficient between 25°C and the temperature T.

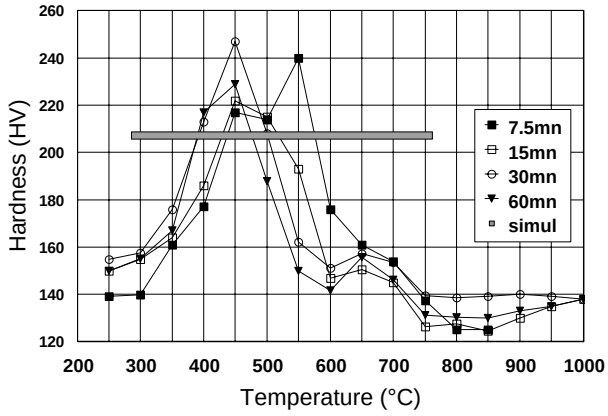

Fig. 2 Hardness in function of the ageing temperature T for times ranking from 7.5 min to 60 min, and after simulation of the baking of the ceramic (state d)

The results of the measurements of the corrosion resistance and cation release for the four states a-d are listed in Table I. The breakdown potentials E_b are all very low. The corrosion potentials E_0 vary from 75 to 295 mV SCE. They are significantly higher for states c and d stabilized at low temperature than for the states a and b.

The corrosion's effect, determined by the charge Q (that is the integrated current for potentials comprised between E_c and 500 mV SCE), varies in the same way. The rates of released cations, R_{Pt} and $R_{Zn,}$ are relatively important and dependant of the metallurgical state. They too are smaller for the states stabilized at low temperature (c and d). No significant release of gold (R_{Au}) was observed.

The results of crystallographic analysis are summarized for each state in Table II. By interpretation of wavelengths and intensities, and with the use of the Ebert's law on elementary cell dimension:

$$a\,(Au_{1-x}\,Pt_{x}) = 4.0789 - 0.1556 * x \quad (1)$$

we found, for each state, the coexistence of two or three phases: (Au-rich Pt) phases with a cell parameter of. 4.05 Å and (Pt-rich Au) phases with a cell of 3.92 Å.

It was confirmed by X-ray microanalysis that Zn and Ta are principally associated with the (Pt-rich Au) phase (Fig. 3).

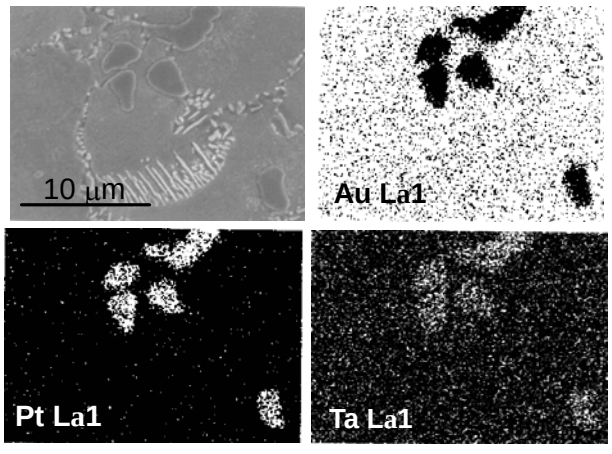

Fig. 3 MEB image und X-ray mappings for Au, Pt, and Ta for a characteristic zone of the specimen in the state d.

Table I. Results of the measurements of the resistance to corrosion and that of the release of cations Au, Pt and Zn.

state	E_c	E_b	Q	R_{Au}	R_{Pt}	R_{Zn}
	mV	mV	mC		mg/cm2	
a	75	880	2.8	<0.005	0.04	2.85
b	85	800	4.3	<0.005	0.03	9.85
c	200	800	0.4	<0.005	0.04	1.36
d	295	900	0.1	<0.005	0.04	0.38

Table II. Results of crystallographic analysis (elementary cell in Angstrom)

state	el. cell	%phases	compositions
a	4.0496	93	$Au_{80}Pt_{20}$(Zn)
	3.9284	7	$Pt_{97}Au_3$(Ta-Zn)
b	4.0572	88	$Au_{86}Pt_{14}$(Zn)
	3.9537	7	Pt_{100} (Ta-Zn)
	3.9230	5	$Pt_{96}Au_4$ (Ta-Zn)
c	4.0516	66	$Au_{82}Pt_{18}$(Zn)
	4.0749	26	$Au_{98}Pt_2$(Zn)
	3.9235	8	$Pt_{99}Au_1$ (Ta-Zn)
d	4.0533	94	$Au_{83}Pt_{17}$(Zn)
	3.9512	4	Pt_{100} (Ta-Zn)
	3.9227	2	$Pt_{99}Au_1$ (Ta-Zn)

CONCLUSIONS.

The alloy is always highly biphased. The second (Pt-rich Au-Ta-Zn) phase is responsible for the relatively bad comportment in corrosion resistance and Pt-Zn release.

That effect is corroborated by the good relationship between the charge Q and the total rate of cation release.

The metallurgical states stabilized at low temperature or after baking of the ceramic present a better comportment than the ones at higher temperatures.

REFERENCE. [1] Ebert H., Abart J., Voitländer J.; Z. für Physikalische Chemie, Neue Folge, **44** (1985), 223-229.

European Cells and Materials Vol. 9. Suppl. 1, 2005 (pages 64-65) ISSN 1473-2262

Corrosion Testing of Cobalt-Chromium Dental Alloys doped with Precious Metals

P.Y. Eschler[1], L. Reclaru[1], H. Lüthy[2], A. Blatter[1], C. Larue[1], C. Süsz[3], J. Bösch[3].
PX Tech[1], La Chaux-de-Fonds; University of Zürich[2]; Qualident[3], Geneva; Switzerland

INTRODUCTION

Non precious dental alloys (CoCr) compared to conventional gold alloys reveal generally an inferior corrosion resistance (pitting, crevice corrosion)[1]. A recent generation of cobalt-chromium alloys, doped with precious metals (Au, Pt, Ru) to improve the corrosion resistance, are now entering the market.
The goal of this study was to verify this hypothesis.

MATERIALS AND METHODS

The compositions of the tested commercial alloys and of a "classical" CoCr alloy are listed in Table I.

Chemical composition (wt %)					
Element	**CoCr**	**#1**	**#2**	**#3**	**#4**
Co	63.7	63.5	52.0	50.6	59.3
Cr	28.9	21.0	25.0	18.5	25.0
Mo	5.3		4.5	3.0	5.0
Ga		4.5	6.0		2.5
In			5.0		1.2
Au		2.0	2.0		2.0
Pt			2.0	15.0	
Ru				10.0	
Sn			1.0		
Mn	0.8	6.5	0.5	1.0	
Si			2.0	0.75	
W	0.1			0.5	4.0
Nb				0.5	
Al		2.5			
Fe	0.4				

Table I. Composition of the tested alloys (wt %).

Polarization test

The test samples had the form of discs of diameter 11 mm. They were metallographically polished with diamond paste (granulometry 1 µm).
Electrochemical measurements were conducted in artificial saliva of the Fusayama type (dearated with nitrogen, temperature 37°C, pH = 5) using the rotating electrode technique. The cathodic and anodic potentiodynamic polarisation curves were measured from - 1000 mV to + 1250 mV vs. SCE.

Pitting or crevice corrosion test of the four doped alloys (#1 - #4) and the conventional CoCr were examined according to the standard ASTM F 746-84 (reapproved 1994). The test samples were machined into the form of cylinders of diameter 5 mm and height 10.8 mm and they were polished with 600-grit paper. The test surface was 40 mm^2. The de-aerated electrolyte (0.2 mg/l O_2) used for the test was a solution of 9 g/l NaCl in de-ionized water (18 MΩ.cm) at temperature 37°C.

RESULTS

Polarization test

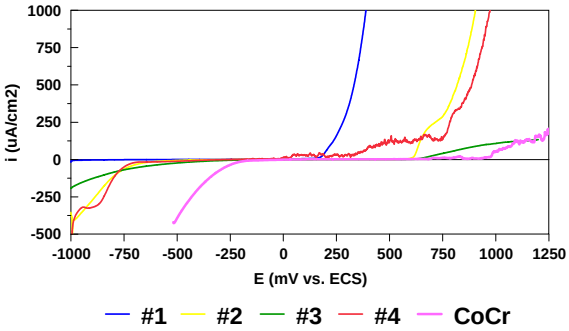

Fig. 1 Potentiodynamic polarization curves in linear system of alloys #1 to # 4 in comparison with a conventional CoCr alloy.

Pitting or crevice corrosion test

Code	**E_{corr}**	**i_{corr}**	**E(i=0)**	**R_p**	**Zone I**	**Zone II**
					$E_{i=0}$→300	300→700
	mV	nA/cm^2	mV	kOhm	mC	mC
CoCr	-135	50.13	-352.00	2120.00	0.37	6.35
#1	-2	17.00	-450.00	297.70	9.02	86.05
#2	41.7	4.11	-246.00	582.00	2.73	53.72
#3	62	18.23	30.00	1636.00	1.21	4.95
#4	-336	41.52	-254.00	321.00	35.67	164.10

Table II. Summary of electrochemical parameters for CoCr-Au,Pt, Ru alloys (artificial saliva, 37°C).

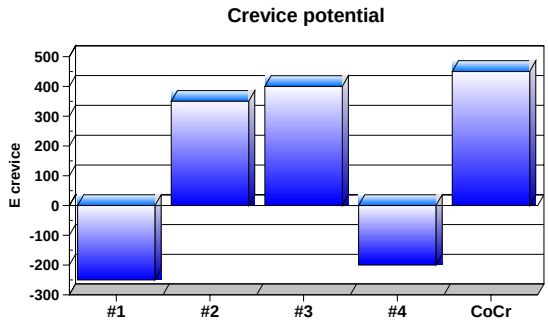

Fig. 2. Pitting or crevice potential of alloys #1 to # 4 in comparison with a conventional CoCr alloy.

The potentiodynamic curves displayed in Fig. 1 and the electrochemical parameters (Table II) reveal important differences in the behaviour of the studied alloys (#1 - #4) as compared to the conventional CoCr alloy. The worst behaviour was formed with the alloys containing only gold (#1 and #4), confirming the results of Kappert and Schuster[2].

As evidence in Fig. 2, the gold doped alloys (#1 and #4) also exhibit a substantially lower resistance to crevice or pitting corrosion than the conventional CoCr alloy.

In contrast, the crevice or pitting potentials of alloys doped with platinum group metals (#2 and #3) are comparable to that the conventional CoCr alloy.

CONCLUSIONS

According to these results, the classical CoCr alloy exhibit the best corrosion resistance in an oral type environment, followed by alloys #2 and #3 (addition platinum group metals, Pt and Ru). The worst behaviour was shown by samples #1 and #4, i.e. the alloys with the addition of only gold).

From the point of view resistance corrosion behaviour, CoCr dental alloys doped with precious metals are not an improvement.

REFERENCES

1. L. Reclaru; J.-M. Meyer, Effects of fluorides on titanium and other dental alloys in dentistry; *Biomaterials* **19** (1998), 85-92.

2. H.F. Kappert, M. Schuster; *Dental Labor* **43** (3) (2000), 352 – 354.

European Cells and Materials Vol. 9. Suppl. 1, 2005 (pages 66-67) ISSN 1473-2262

Volume contraction in photocured dental resins : the shrinkage - conversion relationship revisited

M Dewaele[1-2], D Truffier-Boutry[1-2], G Leloup[1], J Devaux[2]

1 Ecole de Médecine Dentaire et de Stomatologie, Avenue Hippocrate 15 B-1200 Bruxelles

2 Laboratoire de Chimie et de Physique des Hauts Polymères, Place Croix du Sud 1 B-1348 Louvain-la-Neuve

INTRODUCTION: The volume shrinkage undergone by methacrylate-based resins upon polymerization arises mainly from the chemical reaction itself. Before polymerization, monomer molecules are about 4 Angströms apart and linked by secondary cohesion forces – the so-called van der Waals forces. During the polymerization, the latter are replaced by covalent links about 1,5 Angströms length. In many studies, the contraction is related to the degree of conversion (extent of transformation of monomers in polymers). More precisely, the contraction should be linearly linked to the actual number of vinyl double bonds converted in single ones. Nowadays, literature still refers to the publication of Loshaeck (1953). In this study, it has been determined that for every mole of C=C being converted in C-C, there is an associated volume shrinkage of 23,0 cm^3. In the present study, we revisit these results and we attempt to accurately determine the volume contraction and to link it to the number of actual vinyl double bonds converted with the recent characterization techniques and the precision they offer.

METHODS: To determine the volume contraction associated with the number of double bonds converted, we analyzed a range of Bis-GMA/TEGDMA mixtures. Eight different mixtures from Bis-GMA/TEGDMA were prepared consisting of 0, 20, 30, 40, 50, 60, 70 and 80 % weight TEGDMA. In each mixture1% of an initiator/activator (camphorquinone/ amine) system was added.

Because of favorable stereochemistry, long-chain flexible TEGDMA exhibits relatively high degree of conversion of the methacrylate double bonds. Aromatic Bis-GMA is much more rigid. The degree of conversion in these different mixtures increases with content of TEGDMA. However, due to molar mass difference between TEGDMA and Bis-GMA, the initial number of C=C moles in these different mixtures is different. Thus, the degree of conversion does not allow a direct correlation with the contraction. In this work, the volume shrinkage is related to the molar concentration of converted C=C (in mole/cm^3) in each blend.

Three samples per resin mixture were prepared, polymerized and analyzed

The volume contraction is obtained by comparing unpolymerized to polymerized specific masses. The former is calculated by pycnometry, the latest using a density column.

The shrinkage was calculated by the following equation:

$$Volume\ contraction\ (\%) = 100 * (d\ polymerized - d\ unpolymerized)/d\ polymerized$$

The degree of conversion (DC) was measured in Raman spectrophotometry by intensity ratio (R) of the vibration bands of residual unpolymerized methacrylate C=C stretching mode at 1640 cm^{-1} to the aromatic C=C stretching mode at 1610 cm^{-1} used as internal standard. The DC of the analyzed resins was calculated by the following equation:

$$DC\ (\%) = 100 * (1 - (R\ polymerized/R\ unpolymerized))$$

The number of moles of C=C converted/g was obtained with the following equation:

$$Moles\ C{=}C\ poly/g = DC * (moles\ C{=}C\ init./g),$$

where the initial number of mole of C=C bonds per gram (moles C=C init./g) was obtained from the molar mass of the monomers. The molar conversion per cm^3 was finally obtained using the actual specific mass (d poly) of the polymerized resin.

$$Moles\ C{=}C\ poly/cm^3 = d\ poly * (moles\ C{=}C\ poly/g)$$

RESULTS:

Volumetric Contraction:

Table 1 shows the specific mass of the uncured composite resin (d unpolymerized), the specific mass of the cured composite resin (d polymerized) and the resultant shrinkage calculated as previously explained. The values of the

contraction percentage has to be considered as « free » volumetric shrinkage measurements.

Table 1: *Investigated resin mixtures and specific mass of the uncured and cured resins (d unpolymerized and d polymerized), and the resultant shrinkage.*

samples		d unpoly.	d poly.	contraction %
Bis-GMA 100	1	1,174	1,223	4,02
	2		1,219	3,74
	3		1,200	2,17
B/T 80/20	1	1,153	1,225	5,93
	2		1,227	6,09
	3		1,215	5,13
B/T 70/30	1	1,142	1,235	7,52
	2		1,231	7,25
	3		1,217	6,18
B/T 60/40	1	1,130	1,236	8,58
	2		1,220	7,40
	3		1,221	7,48
B/T 50/50	1	1,121	1,236	9,37
	2		1,233	9,15
	3		1,227	8,67
B/T 40/60	1	1,113	1,238	10,03
	2		1,234	9,77
	3		1,215	8,38
B/T 30/70	1	1,104	1,239	10,86
	2		1,235	10,60
	3		1,208	8,57
B/T 20/80	1	1,096	1,242	11,77
	2		1,231	11,03

Number of double bonds converted*:*

The values of degree of conversion (*table 2*) in mole% correspond to the average of three measurements in three different points for each investigated sample.

Table 2: *Average values of degree of conversion (DC) for each sample*

	DC sample 1	DC sample 2	DC sample 3
BISGMA 100	38,21	34,46	36,08
B/T 80/20	56,19	57,29	57,25
B/T 70/30	65,12	63,95	60,71
B/T 60/40	66,22	60,33	63,25
B/T 50/50	63,64	69,08	62,95
B/T 40/60	75,37	68,28	59,70
B/T 30/70	72,98	69,13	64,45
B/T 20/80	73,62	72,36	

Rate of contraction related to number of actual vinyl double bonds converted:

As shown in *figure1***,** an univocal relationship has been found between the volume contraction and the actual number of vinyl double bonds converted. The contraction increases linearly with the number of double bonds converted. In the present study, a contraction of 20 cm^3 per mole of double bonds converted was deduced from the 27 measurements.

In 1953, Loshaeck reported a volume contraction of about 23 cm^3/mole of C=C converted.

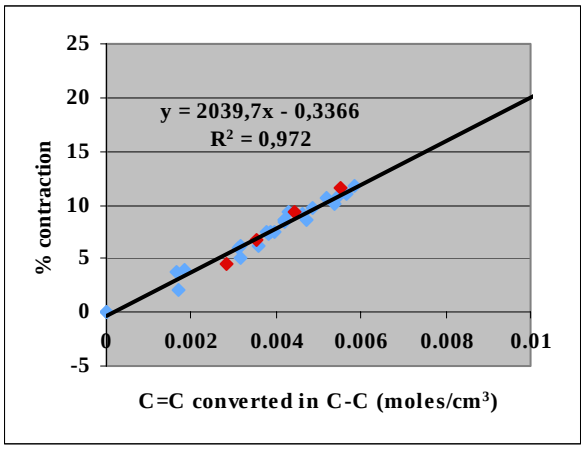

Fig. 1: *Evolution of the contraction related to the number of moles of C=C converted per cm^3 sample.*

(For each of the eight mixtures 3 samples were analyzed. Except for the mixture B/T 20/80, where we have only two values because of a fluorescence phenomenon. Additional values for Bis-GMA 100%, Bis-GMA/ TEGDMA 75/25; 50/50 and 25/75, arise from a pilot study.)

CONCLUSIONS: From the above results, a reduction of the polymerization shrinkage due to the chemical reaction may obviously be expected from the addition of molecules allowing to decrease the number of double bonds converted per unit of volume of resin matrix while maintaining the degree of conversion (of Bis-GMA and TEGDMA) and thus the mechanical properties.

REFERENCES: [1] S. Loshaeck and T.G. Fox (1953) *J. Am Chem Soc* **75**: 3544-3550.

Comparative study of fluoride release by two compomers with or without post-polymerization, in water and in artificial saliva (SAGF medium)

O Romieu [1], B LEVALLOIS [2]& JY GAL [3]

[1] *Univ. Montpellier I, UFR d'Odontologie, 545 Av. du Pr. Viala, BP 4305,34193 Montpellier, FR.*
[2] *Univ. Montpellier I, UFR d'Odontologie, 545 Av. du Pr. Viala, BP 4305,34193 Montpellier, FR.*
[3] *Univ. Montpellier II, Laboratoire Hydrosciences UMR 5569, FR.*

INTRODUCTION: For many years, there has been a need for restorative materials including caries-preventive elements. It is quite clear that fluoride is the most effective agent in caries prevention. Polyacid-modified composite resins (compomers) are fluoride containing and releasing materials [4]. The aim of this study is to investigate if thermal post-polymerization of compomers, well-known for increasing the conversion rate of composite resins [2-3], influence fluoride release.

METHODS: We realized two experiments, the first one was a pilot study to determine the influence of three parameters (product, medium of release and polymerization mode), the second one restart with one product and one medium to refine polymerization's result.

In the first experiment, 24 samples of Dyract AP® (Dentsply De Trey GmbH, Konstanz, Germany) and 24 samples of Compoglass F® (Vivadent, Schaan, Liechtenstein) were photo-polymerized with an halogen lamp (3M® Curing light 2500) according to manufacturer's recommendations. Disk-shaped samples 5 millimeters in diameter and 4 millimeters thick were prepared. 12 samples of each product have been post-polymerized in an oven (Prolabo®, 20-220C° double control) at 120°C during 10 minutes and the 12 others have been preserved at room temperature (25C°). Half of the post-polymerized samples and half of the preserved at room temperature samples of each product have been immersed in deionized water and other half in an artificial saliva: the SAGF medium [1]. All experiments were carried out at 25C°. The amounts of fluoride released were measured with a potentiometer equipped with an ISE 25F (Radiometer®) fluoride ion selective electrode, a reference XR 100 calomel electrode (Radiometer®) and a PHM 210 millivoltmeter (Radiometer®). The media were renewed after 1, 2 and 7Days. A pH acetate buffer (tafic) was added to the trial solutions before measurements.

In the second experiment, protocols to prepare the samples and to analyze trial solutions are identicals. The experimental protocol is simplified to increase statistic power. We decided to use Dyract AP® in water because results were more stable. 40 samples were prepared and divided in two groups, first group was only photo-polymerized and immersed in deionized water, second was photo-polymerized, post-polymerized and immersed in deionized water. Solutions were renewed and analyzed at day 3, 13, 20 and 27.

Table 1: distribution of samples (1st experiment).

Dyract AP® in water photo-polymerized	6
Dyract AP® in SAGF photo-polymerized	6
Dyract AP® in water post-polymerized	6
Dyract AP® in SAGF post-polymerized	6
Compoglass F® in water photo-polymerized	6
Compoglass F® in SAGF photo-polymerized	6
Compoglass F® in water post-polymerized	6
Compoglass F® in SAGF post-polymerized	6
Total	**48**

All tests were performed by non-parametric tests of Mann-Whitney-Wilcoxon or Kruskal-Wallis.

Table 2: distribution of samples (2nd experiment).

Dyract AP® in water photo-polymerized	20
Dyract AP® in water post-polymerized	20
Total	**40**

RESULTS: The first experiment can be analyzed in three ways: effect of polymerization, effect of medium and effect of product. Significant differences are signaled by red arrows in figures.

First experiment:

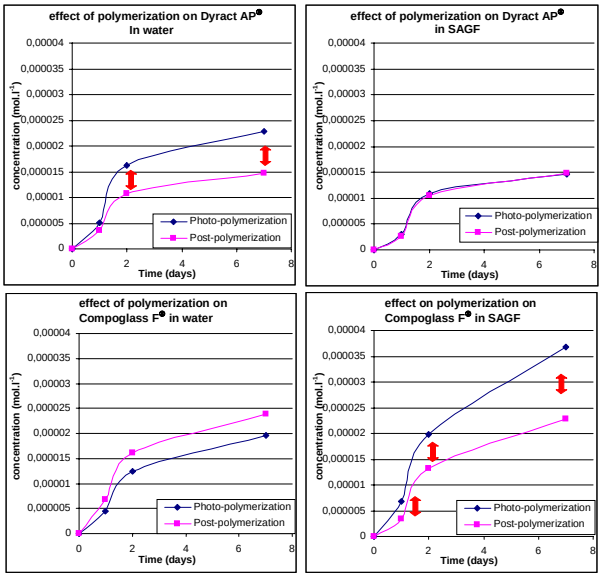

Fig. 1: Effect of polymerization.

For the Dyract AP® in water, samples with photo-polymerization only release significantly more on the second and seventh day (1st day :p_1=0,359, 2nd day : p_2=0,008, 7th day : p_7=0,003).

For the Dyract AP® in SAGF, we could not find any significant difference at any time of the experiment (p_1=0,244, p_2=0,319, p_7=0,653).

For the Compoglass F® in water, we could not observe any significant difference at any time of the experiment (p_1=0,183, p_2=0,214, p_7=0,282).

For the Compoglass F® in SAGF, samples with photo-polymerization release significantly more at the three times of the experiment (p_1=0,0002, p_2=0,029, p_7=0,003).

Second experiment:

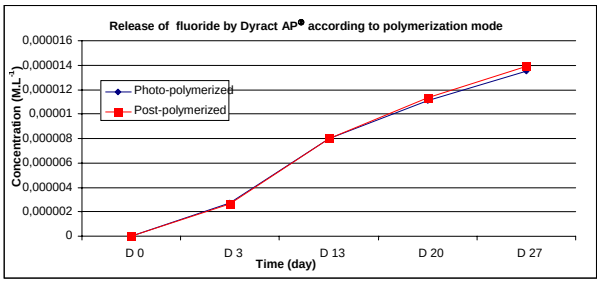

Fig. 2: Release of fluoride by Dyract AP® according to polymerization mode.

In the second experiment, the two groups of 20 samples of Dyract AP® in water had a very similar behavior. We could not show any significant difference at any time of the experiment. (3rd day: p=0.7344, 13th day: p=0.7251, 20th: p=0.6359 and 27th: p=0.4953).

DISCUSSION & CONCLUSIONS: The first experiment demonstrates an effect of the heat treatment after standard photo-polymerization on fluoride release on theses two compomers. We could not demonstrate it in all the conditions probably because of the small numbers of sample in each group (6). The effect underlined in this experiment is at very short time (7 days).

In the second experiment we had no effect of the heat treatment after standard photo-polymerization probably because we renewed releasing medium less often and we had continued the experiment for 27 days.

We can suppose that this difference between the two experiments is due to the profile of compomer's fluoride release. Compomers constantly release fluoride after an initial fluoride "burst". This greater amount of fluoride release during the first days may be the best moment to demonstrate a difference due to polymer matrix conversion.

We can also suppose that the matrix continues its maturation with the water penetration and the initial differences due to heat treatment may be shade by acid base reaction after some days.

The frequency of medium renewal can also influence the pattern of fluoride release. This has been demonstrated in previous experiments and when the medium is changed more often, release is proportionally higher than when the medium is not changed [1].

Dyract AP® in SAGF had lower release than in water which confirms previous results in our laboratory [1]. It has been suggested that it is due to CaF_2 precipitate on the surface of the material like Levallois & Coll. observed on glass-ionomers cements with a scanning electron microscope. We hope we could determine in the future if the same type of precipitate can be observed at the surface of polyacid-modified composite resins.

We want to continue these experiments by establishing if thermal post-polymerization of compomers modify their mechanic properties. We also want to study the effect of polishing the surface of the samples on fluoride release.

REFERENCES: [1] B. Levallois, Y. Fovet, L. Lapeyre, JY. Gal (1998) In vitro fluoride release from restorative materials in water versus artificial saliva medium (SAGF). Dent Mater 14(6):441-447. [2] YH. Bagis, FA. Rueggeberg (1997) Effect of post-cure temperature and heat duration on monomer conversion of photo-activated dental resin composite. Dent Mater 13(4):228-32. [3] JL. Ferracane, JR. Condon (1992) Post-cure heat treatments for composites: properties and fractography. Dent Mater 8:290-295. [4] L. Forsten (1999) Fluoride release and uptake by glass-

ionomers and related materials and its clinical effect. Biomaterials 19(6):503-508.

ACKNOWLEDGEMENTS: To Dr B Levallois for supervising this work. To Pr. JY Gal for welcoming me in his laboratory. To Pr. P Dujols for statistic analysis. And for all, their constant availability and help.

European Cells and Materials Vol. 9. Suppl. 1, 2005 (pages 71-72) ISSN 1473-2262

Implantation of aluminosilicate/calcium phosphate materials Influence on bone formation in rabbit tibias

S.MARTIN[1], A.C.DERRIEN[2], H.OUDADESSE[2], D.CHAUVEL-LEBRET[1], G.CATHELINEAU[1]

[1] *Equipe Biomatériaux en Site osseux UMR-CNRS 6511 – Université de Rennes 1, 2 rue du Professeur Léon Bernard – Bâtiment 15, F-35000 RENNES*
[2] *Cristallochimie et biomatériaux - Laboratoire CSIM UMR-CNRS 6511 – Université de Rennes 1, Institut de Chimie de Rennes, Campus de Beaulieu, F-35042 RENNES*

INTRODUCTION:

Many types of bone substitutes exist to fill a bony defect. They must be compatible and bond with the host tissue without any formation of fibrous capsule. The direct apposition of bone to bioactive materials, including bioactive glasses and calcium phosphates, has already been demonstrated. **[1]**

The composite (GPS-HT) was obtained by mixing an aluminosilicate named GPS (characterized by an amorphous network) with HA (hydroxyapatite) and β-TCP (tri-calcium phosphate). These materials (GPS and GPS-HT) present a good compromise between mechanical properties and percentage of porosity, which could allow good resistance and biological fixation. A previous study on cytotoxicity *in vitro* showed viable cells on two samples (GPS and GPS-HT) after 72 hours.

This study focuses on the preliminary observation of samples of GPS and GPS-HT implanted in rabbit tibias for 1 month. The aim of this study is *i)* to observe bone bonding on materials without any fibrous capsule and *ii)* to show their absence of toxicity *in vivo*. **[2]**

MATERIALS AND METHODS

Material:

The GPS is an aluminosilicate characterized by a high molecular ratio Si/Al=21. First step of its synthesis consisted in mixing KOH with $K_2O,3SiO_2,21H_2O$. This solution was mixed with aluminosilicate powder (SiO_2, Al_2O_3).

The composite GPS-HT was synthesised by mixing GPS with calcium phosphate, TCP-HA (7,8wt% of HA and 5,2wt% of TCP) at room temperature. Then resulting samples GPS and GPS-HT, were heated at 500°C in order to reduce pH value around 7 and to increase the percentage of porosity of the samples.

These materials present a high level of open porosity (65% to 75%) and mechanical properties in the range of cancellous bone values (1-7 Mpa **[3-4]**). Each implant was 4mm length and 6mm diameter.

Animal experiments:

10 adult male New Zealand rabbits of the same age were distributed into three groups corresponding to three implantation periods (1 month, 3 months, 6 months). The animals were kept in individual cages with appropriate temperature, ventilation, and hygrometric conditions in compliance with laboratory welfare regulation.

Material implantation:

The rabbits were anaesthetised with intramuscularly injected Ketalar®. Local intra-skinned and subcutaneous anaesthesia was accomplished using Xylocaine®. A longitudinal incision was made in the metaphyseal zone. A 6mm diameter drill was used to bore the implantation sites. The GPS implants were inserted in the right tibias and the GPS-HT implants in the left tibias *(Fig 1)*. Muscles and skin were securely anchored.

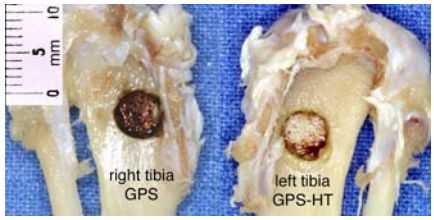

Figure 1: day 0

Bone sample removal and observation:

Four rabbits were euthanasied after one month. The tibias were dissected and removed. For each sample, radiographs and photographs were performed. The material cannot be demineralised, tibia segments containing material were excised and dehydrated in serial dilutions of ethanol, then embedded in polyester resin. Thin sections (70µm thick) were cut with a diamond disk, perpendicularly to the axis of the tibia. The sections were photographed, observed with a SEM (Scanning Electron Microscopy) and with light microscopy after staining with Masson trichroma, to observe type I collagen in bone and soft tissue around the implants.

RESULTS

Results only concern one-month implantation period, other results at 3 and 6 months will be presented in a next paper. Tibia's photographs show a bone healing on the implantation site, without any sign of necrosis on surface *(Fig 2)*

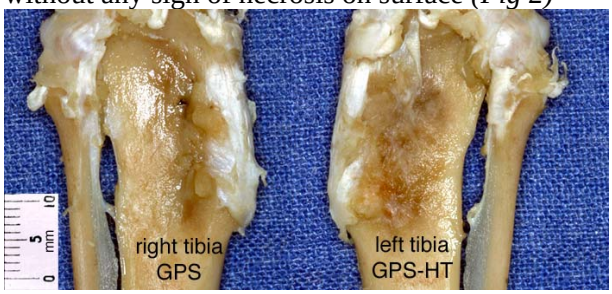

Figure 2: bone healing on the defect without any sign of necrosis. Day 30

Tibias radiographs show the material's opacity near bone cancellous. GPS is not regular on the periphery whereas GPS-HT has an entire white line periphery. We do not observe any dark zone around the implants *(Fig 3)*.

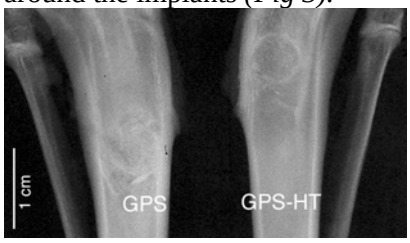

Figure 3: tibia's radio with white line periphery around implants

Light microscopy *(Fig 4)* and SEM *(Fig 5)* photographs show similar results with GPS and GPS-HT. There is bony union across the defect and the material is completely or partially covered by immature woven bone. We observe a bone growth from the inner side defect until the material surface. External pores of the material on the periphery are invaded by bone tissue. Sometimes we observe a bone strip from the cortical bone of the host to the material.

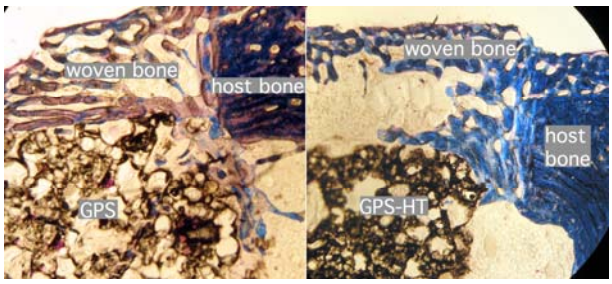

Figure 2: light microscopy, material with woven bone surrounded (X25)

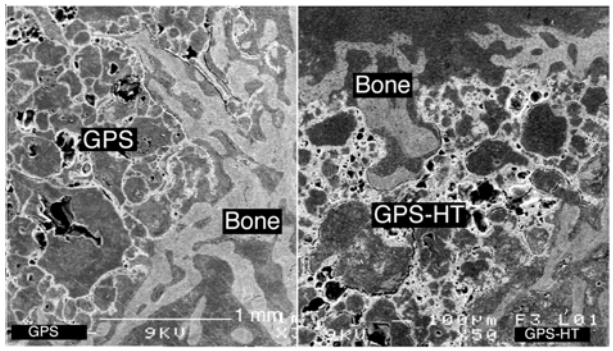

Figure 4: bone has intimate relationship with the implants without any sign of fibrosis between them (X20)

DISCUSSION AND CONCLUSION

Tested materials are biologically accepted by host bone, which has been already observed by cytotoxicity tests **[2]**. We do not notice any sign of necrosis, fibrosis or inflammation around the implant. Bone is observed in growth and healing on the surface of the implant, with penetration in external pores. These results after one-month implantation will be completed by two other periods of three and six months in order to observe bone healing and maturation.

There is no fibrous capsule; the bone is close to the implant; a hypothesis can be that chemical bridges exist to join bone and implant. As suggested this preliminary *in vivo* observation could be completed by *in vitro* study, which allows analyzing the interface between implant and bone **[3]**. Aluminium contented in material is well known as being toxic for the organism. A previous study focused on ICP (Induced Coupled Plasma) method sampling blood to determine aluminium level and dismissal in the body. The results were lower than the detection limit. Materials don't seem to be resorbed. We have to measure implant area by histomorphometric method to complete our hypothesis.

These first results allow us to keep on with studies about these materials in order to explain their good bioactivity.

BIBLIOGRAPHIE:

[1] Bioactive Materials Wanpeng Cao & Larry L. Hench *Ceramics International* 22 1996 493-507

[2] Physico-chemical properties of composites : Geopolymer (GPS) / Calcium phosphates and their influence on cytotoxicity *in vitro*, Derrien A.C., Chauvel-Lebret D.J., Oudadesse H., Pellen-Mussi P., Guigand M., Cathelineau G., *Bioceramic surfaces: behaviour in-vitro and in-vivo*, Volume edited by A. Ravaglioli and A. Krajewski ISTEC-CNR Editions. Faenza, December 2003. pp.348-355

[3] Novel bioactive materials with different mechanical properties T. Kokubo, H-M. Kim, M. Kawashita *Biomaterials 24* (2003) 2161-2175

[4] Les substituts osseux en 2001. D. Mainard, F. Gouin, D. Chauveaux, B. Loty. Eds Romillats 2001 7

In vitro evaluation of a simulated oral environment of different materials for Pit and Fissure sealing

Wladimir ARANDA / Frédéric COURSON / Michel DEGRANGE
Department of Biomaterials, Faculty of Dentistry (Montrouge), University René Descartes-Paris 5, 1 rue Maurice Arnoux, 92120 Montrouge, France

Introduction

Sealants are highly effective to prevent dental caries in occlusal pits and fissures of permanent teeth (ADA council 1997, Simonsen 2002, Feigal 2002). The preventive benefits of fissure sealants depend upon the material remaining intact and firmly adherent to the tooth. However, the parameters of the *in vitro* tests are generally far from clinical conditions. Previous studies have shown that the average oral temperature was between 30-35°C and the relative humidity ranged from 80% to 95% depending on location in the mouth and, that the dentin bond strength decreased when humidity increased (Yoshida 1983, Spierings et al 1984, Plasmans et al 1994, Miyazaki et al 1997, Nystrom et al 1998, Besnault & Attal 2001). The purpose of this *in vitro* study was to assess the penetration and the sealing ability of different pits and fissures materials in a simulated oral environment (temperature, relative humidity –RH).

The null hypotheses in this study were:

1. The influence of the different clinical conditions don't alter neither the penetration nor the sealing ability of the tested materials
2. The 4 tested biomaterials provide the same performances for both penetration and sealing.

Materials and Methods

Specimen preparation – Eighty extracted human molars, free of caries and extracted for orthodontic reasons, were included in this study. After extraction and root cleaning, the teeth were stored in a 1% chloramine solution at 4°C. The teeth were randomly divided into 8 groups. For this study, we used 4 sealing biomaterials of pits and fissures of permanent teeth: 2 light-cured hydrophobic resin-based sealants – Concise White Sealant –***CWS***-(3M/ESPE) and Ultraseal xt+-***USxt+-(***Bisco), 1 hydrophilic light-cured sealant - Embrace Wet Bond –***Emb***-(Gaba/Pulpdent) and 1 light-cured resin-modified glass ionomer cement - Fuji II LC –***FII LC***-(GC). For each material, 10 teeth were sealed in ambient conditions (20°C/30% relative humidity –RH) and 10 teeth in intra-oral conditions (30-35°C/95% RH). The humidity chamber was a device usually used in biology for cell cultures. The temperature/RH parameters measurements were made using a thermo-hygroscope (Testo 635, Gmbh & Co, Lehzkvitch, Germany). The sealing procedure was conducted 1 hour after the stabilization of the temperature/RH parameters. After occlusal sealing, the samples were directly thermocycled for 1800 cycles between 5°C and 55°C. The specimens were apically sealed and then coated with 2 layers of nail varish up to 1 mm from the sealing margins. The teeth were quenched in a 50% silver nitrate solution and stirred for 2 h in a dark room. The samples were then rinsed with water, cleaned before exposure to an intense light for 6 h, and immersed in a developer bath (Kodak, Chalon/Saône, France). After embedding with a self-curing acrylic resin (Plexil-Escil, Chassieu, France), a serie of 200 µm-thick axial sections were cut from each specimen with a water-cooled diamond disk at low-speed (Isomet, Buehler, Evanston, IL, USA). 3 to 6 sections were obtained per tooth according to the sample's dimensions.

Measurements – The collected sections were examined under a stereomicroscope (Olympus SZH10, Tokyo, Japan) at 40x magnification and the sections were assessed with a digital image analyzer and the program. For this study, 2 evaluations were realized: One evaluation for penetration and one evaluation for the microleakage. The penetration of the material into pits and fissures was expressed as a percentage of the total length of the fissure. The microleakage was observed by the silver nitrate penetration at the enamel-sealant interface and recorded in mm after the imaging system was calibrated to a millimetre ruler.

Statistical analysis – The influence of the two studied parameters (environmental conditions, material) was assessed by a Kruskal-Wallis and Mann-Whitney tests for the penetration and by a 2-way ANOVA for the microleakage.

Results

As shown in table 1, whatever the material or the environmental conditions, the filling rate

was high. The analysis demonstrated a difference depending on the material used ($p = 0.0007$) but not on the environmental conditions ($p = 0.20$). Fuji IILC showed a significant lower penetration rate than the other materials tested.

As regards with the sealing ability, an "environmental conditions effect" was statistically disclosed ($p < 0.0001$) but not a "material" effect ($p = 0.75$).

	Sealant penetration		Dye penetration	
	Ambient cond.	35°C/ 95% RH	Ambient cond.	35°C/ 95% RH
CWS	98.7 (2.3)	97.7 (3.1)	6.3 (12)	100
USxt+	93 (5.8)	92.3 (8.4)	12.6 (24.8)	94.3 (14.3)
Emb	95.1 (3.8)	99,4 (1,4)	26.6 (30.8)	67.6 (18.9)
FII LC	85.5 (12.6)	86.7 ((14.5)	30.8 (36.3)	63.9 (36.3)

Table 1: Sealant penetration and dye penetration (expressed in % +/- SD) according to environmental conditions

Discussion and conclusions

In this *in vitro* study, for the two evaluated parameters (penetration and microleakage), the materials showed different behaviors depending on the various environmental conditions.

As far as the penetration of pits and fissures of the permanent teeth is concerned, the environmental conditions did not influence the results whereas a statistically difference between the materials was observed. The resin-modified glass-ionomer cement showed a lower penetration rate for both the ambient and environmental conditions. Regarding the three resin-based sealants, the filling rate of fissures was high whatever the environmental conditions (between 92.3% and 99.4%).

Resin penetration is the consequence of two mechanisms: the wetting ability of the material on the enamel substrate and the capillary pressure. The etching solution (phosphoric acid for the sealants and polyacrylic acid for the glass-ionomer cement) and the different compositions of the materials could explain these differences.

For the microleakage, the results were strictly different. The environmental conditions have been of most importance; The simulated oral environment showed statistically significantly more microleakage whatever the material used. The hydrophilic character of Fuji II LC and Embrace did not increase the imperviouness of the sealing of pits and fissures. The claim of using rubber dam was probably attractive for the clinical perspective but was often difficult to use with young children.

The two null hypotheses were partially rejected. The simulated oral conditions influence the microleakage but not the penetration. Fuji II LC shows a lower penetrationability compared with the resin-based pit and fissure sealants.

References

ADA Council on Access, Prevention, and Interprofessional Relations; ADA council on Scientific Affairs. Dental Sealants (1997) J Am Dent Assoc **128**: 485-8.

Besnault C, Attal JP (2001) Influence of a simulated oral environment on dentin bond terngth of two adhesive systems. Am J Dent **14**: 367-72.

Feigal RJ (2002) The use of pit and fissure sealants. Pediatr Dent **24**: 415-22.

Miyazaki M, Rikuta A, Iwasaki K (1997) Influence of environmental conditions on bond strength of a resin-modified glass-ionomer. Am J Dent **10**: 287-90.

Nystrom GP, Holtan JR, Phelps RA, Becker WS, Anderson TB (1998) Temperature and humidity effects on bond strength of a dentnal adhesive. Oper Dent **23**: 138-43.

Plasmans PJJM, Creugers NHJ, Hermsen RJ, Vrijhoef MMA (1994) Intraoral humidity during operative procedures. J Dent **22**: 89-91. Sealant penetration and dye penetration (expressed in % +/- SD) according to environmental conditions

Simonsen RJ (1991) Retention and effectiveness of dental sealants after 15 years. J Am Dent Assoc **122**: 535-9.

Simonsen RJ (2002) Pit and fissure sealant: review of the literature. Pediatr Dent **24**: 393-414.

Spierings TAM, Peters MCRB, Plasschaert AJM (1984) Surface temperature of oral tissues: a review. Jour Biol Buccale **12**: 91-9.

Yoshida Y (1983) The effect of environmental temperature and humidity on the adhesion of composite resins to the etched enamel surface. Jpn J Conserv Dent **26**: 412-26.

European Cells and Materials Vol. 9. Suppl. 1, 2005 (pages 75-76) ISSN 1473-2262

Root canal posts for the restoration of root filled teeth

C. Borg, M. Muller-Bolla, L. Lupi-Pegurier, M. Bolla
Université de Nice Sophia Antipolis, Faculté de Chirurgie Dentaire, 24 Avenue des Diables Bleus 06357 Nice Cedex 04

INTRODUCTION: The restoration of root filled teeth remains a major concern in dentistry[1]. Endodontic therapy is primarily performed on teeth with clinical crowns previously damaged by caries, previous restorative failure, or fractures[2]. Moreover decay and trauma may often induce an extensive loss of tooth structure. When a large amount of the clinical crown has been lost to damage, it is often impossible to achieve sufficient anchorage of a restoration in the remaining dentin. Thus, endodontically treated teeth with important tooth structure loss have to be restored with a root canal post and a core as foundation for the final restoration. The coronal prosthetic core can be built thanks to the presence of the post. However, the post and core systems do not strengthen the root, but rather serve to improve retention of the final restoration[3].
Once it has been decided to use a post system in restoring endodontically treated teeth, countless post designs and techniques are available[4].
Some authors recommend the use of cast post and core systems as a foundation for the reconstruction of endodontically treated teeth whereas some others prefer using non-metallic posts. To date, there is only one meta-analysis in this area that takes into account both in-vitro and in-vivo studies on anterior single-rooted teeth. We attempted to track down all clinical studies irrespective of tooth type (anterior and posterior teeth). This review compares the failure rates of different types of post and core systems currently used so that clinicians can be better informed.

MATERIALS AND METHODS: The primary objective of this study was to compare the clinical failure rate of different types of posts used for the restoration of endodontically treated teeth. Differences in the failure rate for the different post and core categories has been evaluated regarding:

- The tooth type and its location.
- The prosthetic status of the tooth.
- The presence of ferrule effect according to the margins of crown.
- The type of alloy in the case of metallic posts.
- The presence of diaphragm if cast posts are used.

Randomised or quasi-randomised clinical trials (with a minimum duration of 6 months) such as parallel group design and split-mouth design were considered for this literature review.
The type of participants was chosen as follow: patients with permanent teeth endodontically treated by a dental practitioner in hospital or private practice. For these teeth, a root canal post had been clearly indicated as the means of retention for the final restoration.
This review dealt with three categories of post:

- I: passive metallic custom-cast posts and cores.
- II: 2-element system comprising a commercial active or passive pre-shaped metallic post and a core built up from amalgam, glass-ionomer cement, resin-modified glass ionomer or composite resin.
- III: 2-element system comprising a commercial pre-shaped non-metallic post and a composite resin, a glass-ionomer cement or a resin-modified glass-ionomer core.

Studies using zinc phosphate, zinc polycarboxylate, glass ionomer and resin as luting cements for posts were included.
Studies where post and core systems have been used with different prosthetic status were included.
Studies where failures of endodontically treatment were considered were to be excluded.

The failure rate of different post and core systems has been assessed by clinical and radiographic examinations. Technical failures included: loss of retention, post fracture and root fracture.
The survival time for different types of post and core systems was assessed.

In order to find relevant studies meeting the inclusion criteria;
(1) Electronic searches of the Cochrane Oral Health Group's Trials Register, the Cochrane Central Register of Controlled Trials (CENTRAL) in The Cochrane Library, MEDLINE, EMBASE, SCIsearch, Ovid based on a predetermined keyword list have been done.
(2) Searches of reference lists from articles and reviews for additional relevant articles have been done.

(3) Dental conference proceedings have been looked trough and congress members have been contacted to track down any unpublished studies.
(4) Manufacturers, researchers and experts known to be involved in the field have been contacted in an effort to trace unpublished studies or published studies not found.
The search attempted to track down all relevant studies irrespective of language. Non-English papers have been translated.

Two persons independently examined the title, keywords and abstract of reports identified from electronic searching for evidence of three criteria:
(a) It is a randomised or quasi-randomised clinical trial.
(b) It involves the use of one post system compared to another or the use of one post system in different clinical situations.
(c) Failures are assessed only on endodontically treated permanent teeth after root canal post cementation.
If the report fulfilled these three criteria or if one or both reviewers were not able to assess this from the title, keywords or abstract then the full article has been obtained.
Screening of full-text articles, decision about eligibility and data extraction have been carried out independently by three reviewers. Any disagreement between the three reviewers has been resolved by discussion with a fourth reviewer.
When authors have published several articles concerning the same study, only the last was taken into account.
The authors have been contacted for additional information if necessary.

The methodological quality of included studies has been assessed using the criteria described in the Cochrane Reviewers' Handbook 4.1.5 (Clarke 2002) concerning allocation concealment. A quality assessment has been carried out for all studies fulfilling the inclusion criteria.

RESULTS: The keyword searching through the different databases highlighted a total of 3668 articles. Of these, 3628 were excluded regarding title or abstract. From the 40 collected studies, 27 were excluded from further analysis:

- 12 articles did not fulfil our inclusion criteria.
- 15 others were about the following of one group of participants.

The 13 articles left (to be included in the meta-analysis) were:

- Controlled clinical trials: 9 articles
- Randomised clinical trials: 4 studies

The comparison of the failure rate between cast posts and fibre posts did not show any significative difference, neither did the comparison of the failure rate between cast posts and metallic prefabricated posts.
The results showed higher failure rate on anterior teeth regardless to the post type (cast posts or fibre posts). The failure rate was also higher when the tooth was part of a partial denture (fixed or removable).
No significative difference was shown regarding the tooth location.

REFERENCES: [1]A.S. Fernandes, G.S. Dessai (2001). Factors affecting the fracture resistance of post-core reconstructed teeth: a review. *The International Journal of Prosthodontics*, 14(4):355-363. [2]M. Abou-Rass (1992). Post and core restoration of endodontically treated teeth. *Prosthodontics and Endododontics*, pp 99-107. [3]M. Ferrari, A. Vichi, F. Garcia-Godoy (2000). Clinical evaluation of fibre-reinforced epoxy resin posts and cast post and cores. *American Journal of Dentistry*, 13:15b-18b. [3] B. Akkayan, B. Caniklioglu (1998). Resistance to fracture of crowned teeth restored with different post systems. *The European Journal of Prosthodontics and Restorative Dentistry*, 6(1):13-18.